

The dynamic role of Hsp40 chaperones in protein aggregation and proteotoxicity

Peter Mahan Douglas

A dissertation submitted to the faculty of the University of North Carolina at Chapel Hill
in partial fulfillment of the requirements for the degree of Doctor of Philosophy in the
Department of Cell and Developmental Biology

Chapel Hill
2009

Approved by
Advisor: Douglas Cyr
Reader: Vytas Bankaitis
Reader: Patrick Brennwald
Reader: Jean Cook
Reader: Mohanish Deshmukh
Reader: Nikolay Dokholyan

ABSTRACT

Peter Mahan Douglas: The dynamic role of Hsp40 chaperones in protein aggregation and proteotoxicity
(Under the direction of Douglas Cyr)

Protein homeostasis or proteostasis involves an intricate balance between the synthesis, folding, localization and degradation of each protein in the cell. Perturbations by age or chronic stress can compromise any one component of this integrated network and initiate a cascade of toxic misfolding events. Protein conformational disorders such as Alzheimer's disease, transmissible spongiform encephalopathies, and the polyglutamine-expansion diseases are characterized by the misfolding and subsequent conversion of disease-related proteins into β -sheet-rich conformers capable of assembling into highly ordered aggregates termed amyloid. For over a century, amyloid fibrils were believed to represent the toxic agent behind these diseases due to their overwhelming presence in postmortem brains of diseased individuals. However, recent evidence has begun to challenge the notion that amyloid formation is the toxic mechanism. Two observations described herein suggest that amyloid formation provides the cell a mechanism to buffer the formation of toxic protein species. First, my studies demonstrate that amyloid formation by the yeast prion protein, Rnq1, protects cells against proteotoxicity. Interestingly, the Hsp40 chaperone, Sis1, mediates the efficient conversion of nascent Rnq1 into amyloid-like, $[RNQ^+]$ prion assemblies. Inefficiencies in Sis1-mediated $[RNQ^+]$ assembly result in the toxic accumulation of soluble, low

molecular weight oligomers. Second, Sis1 activity relocates $[RNQ^+]$ prion assembly pathways from the cytosol to the nucleus, in which $[RNQ^+]$ assembly was more efficient and less toxic. Sis1 modulates the conformation of $[RNQ^+]$ prions which, in turn, act as environmental factors to promote toxicity of a huntingtin's protein exon-1 fragment with an expanded polyglutamine tract (Htt-103Q). Complex formation between $[RNQ^+]$ prions and Htt-103Q enabled nuclear $[RNQ^+]$ aggregates to attract Htt-103Q from the cytosol to the nucleus, which reduced the efficiency of nuclear Htt-103Q aggregation and exacerbated Htt-103Q toxicity. Thus, amyloid formation appears to represent a protective mechanism to ameliorate the toxic accumulation of small, soluble intermediates in the aggregation pathway. My studies also demonstrate that molecular chaperones directly and indirectly influence the cellular location of amyloidogenic proteins and therefore have a profoundly impact on proteotoxicity because the cytosol and nucleus have different capacities to package disease proteins into benign assemblies.

DEDICATIONS

For my loving wife, Lisa, and our daughter, Mia

ACKNOWLEDGEMENTS

My dissertation work represents the culmination of an extensive support network that extends from my family and co-workers to colleagues and collaborators. I would not have navigated my way through the intricacies of graduate school without the guidance of my dissertation advisor and mentor, Dr. Douglas Cyr. Under his guidance, he provided me with the freedom to embark on risky scientific endeavors yet helped me maintain my focus and conclude my graduate studies in a timely manner.

The members of the Cyr lab have played an integral role in my development as a researcher by providing both scientific and personal advice. I thank my dissertation committee members, Dr. Vytas Bankaitis, Dr. Patrick Brennwald, Dr. Jean Cook, Dr. Mohanish Deshmukh, and Dr. Nikolay Dokholyan, who sacrificed their time to provide critical feedback on my project. I am especially thankful to Dr. Vytas Bankaitis for his scientific and career advice throughout my graduate career as well as Dr. Patrick Brennwald for advice regarding yeast and for picking tetrads.

I thank Dr. Susan Lindquist and Sebastian Treusch at MIT for the fruitful collaboration established during the earlier stages of my graduate studies. Furthermore, I'd also like to thank Dr. Kerry Bloom for his assistance during the developmental stages of my second story.

Lastly, I would like to thank my family who helped me find my way as a scientist and provided any means of support at every juncture of my career. I thank my father, Dr. Michael Douglas, and sister, Sarah Douglas, for their critical reading of my manuscripts and continued support. Most importantly, I am so grateful for my loving wife, Lisa, who has supported me from the start of my scientific career and will continue to do so until the end.

TABLE OF CONTENTS

	Page
LIST OF FIGURES	viii
LIST OF ABBREVIATIONS.....	x
CHAPTER	1
1.1 Abstract.....	2
1.2 Introduction.....	3
1.3 Molecular chaperones antagonize aggregation of disease proteins	6
1.3.1 Chaperones prevent disease proteins from assembling into amyloid-like aggregations.....	7
1.3.2 Molecular chaperones solubilize protein aggregates	11
1.3.3 Chaperones participate in the degradation of proteotoxic substrates by the ubiquitin-proteasome system or chaperone-mediated autophagy	13
1.4 Chaperones promote aggregation of toxic proteins	15
1.4.1 Chaperone-mediated aggregation reduces proteotoxicity.....	16
1.4.2 Distinct signaling pathways facilitate protein detoxification via opposing mechanisms	20
1.5 Conclusions.....	21
1.6 References.....	23
2. Chaperone-mediated amyloid assembly protects against prion toxicity.....	35

2.1 Abstract.....	36
2.2 Introduction.....	37
2.3 Results.....	40
2.4 Discussion.....	58
2.5 Materials and methods	61
2.6 References.....	67
3. Hsp40 dependent localization of $[RNQ^+]$ prions to the nucleus reciprocally effects Rnq1 and Huntingtin toxicity.....	71
3.1 Abstract.....	72
3.2 Introduction.....	73
3.3 Results.....	78
3.4 Discussion.....	103
3.5 Materials and methods	107
3.6 References.....	113

LIST OF FIGURES

		Page
Figure 1.1	Schematic representation of the amyloid assembly pathway	4
Figure 1.2	Hsp70-Hsp40 hydrolytic cycle for the binding and refolding of non-native proteins	9
Figure 1.3	Roles for Sis1 in $[RNQ^+]$ prion assembly	19
Figure 2.1	Overexpression of Rnq1 is toxic to $[RNQ^+]$ cells	41
Figure 2.2	Factors influencing Rnq1 toxicity include the expression level and presence of a carboxy-terminal tag	43
Figure 2.3	Sis1 overexpression protects against Rnq1 toxicity	46
Figure 2.4	Sis1 binding to a conserved chaperone-binding motif in the non-prion-forming domain of Rnq1	48
Figure 2.5	Mutations in the chaperone-binding motif of Rnq1 reduce the efficiency of $[RNQ^+]$ amyloid assembly	49
Figure 2.6	Mutation of the chaperone-binding motif slows the rate of Rnq1 assembly into $[RNQ^+]$ prions	51
Figure 2.7	Depletion of Sis1 hinders assembly of nascent Rnq1-GFP into SDS-resistant $[RNQ^+]$ aggregates	53
Figure 2.8	Rnq1 L94A toxicity and assembly status in $[rnq^-]$ yeast	55
Figure 2.9	Analysis of the mobility of Rnq1 L94A in extracts from $[RNQ^+]$ and $[rnq^-]$ strains by gel-filtration chromatography	56
Figure 3.1	Suppression of Rnq1 toxicity by Sis1 correlates with nuclear accumulation $[RNQ^+]$ prions	79
Figure 3.2	Sis1 overexpression does not promote the nuclear accumulation of $[PSI^+]$ prions or a nucleocytoplasmic transport reporter protein	81

Figure 3.3	Identification of nuclear import factors that are required for Sis1-mediated concentration of Rnq1-GFP to the nucleus	82
Figure 3.4	Sis1 overexpression needs to precede Rnq1-GFP expression to observe the nuclear localization of $[RNQ^+]$ prions	84
Figure 3.5	Rnq1-GFP-NLS is less toxic than Rnq1-GFP	86
Figure 3.6	Rnq1-GFP-NLS assembles into SDS-resistant $[RNQ^+]$ prions with greater efficiency	87
Figure 3.7	Expression of Rnq1-GFP-NLS suppresses Rnq1 L94A toxicity and promotes the nuclear accumulation of Rnq1-mRFP	90
Figure 3.8	Elevation of Sis1 levels exacerbate growth defects caused by Htt-103Q overexpression	92
Figure 3.9	The presence of $[RNQ^+]$ prions in the nucleus exacerbates Htt-103Q toxicity	94
Figure 3.10	Rnq1-GFP-NLS exacerbates Htt-103Q toxicity in $[RNQ^+]$ cells but has no affect on Htt-103Q toxicity in $[rnq^-]$ cells	95
Figure 3.11	Expression of Rnq1-mRFP-NLS was unable to sequester the non-Q-rich Het-S prion to the nucleus	97
Figure 3.12	$[RNQ^+]$ prions form an immunoprecipitable complex with high molecular weight Htt-103Q	98
Figure 3.13	Nuclear $[RNQ^+]$ prions hinder the assembly of Htt-103Q into high molecular weight, SDS-resistant aggregates	100
Figure 3.14	Htt-103Q-GFP-NLS forms SDS-resistant aggregates with reduced efficiency and is dramatically more toxic than Htt-103Q-GFP	101

LIST OF ABBREVIATIONS

aa	amino acid
AAA ATPase	AAA family of ATPases
A β ₄₂	proteolytically cleaved peptide from the amyloid precursor protein
APP	amyloid precursor protein
ATP	adenine triphosphate
BAG	Bcl2-associated athanogene
BSA	bovine serum albumin
CHIP	carboxy-terminus of Hsp70 interacting protein
CMA	chaperone-mediated autophagy
coIP	co-immunoprecipitation
CUP1	copper-inducible promoter
CuSO ₄	copper sulfate
DAPI	4'-6-Diamidino-2-phenylindole
DTT	dithiothreitol
EDTA	ethylenedinitrolo-tetraacetic acid disodium salt
ECL	enhanced chemiluminescent substrate
ER	endoplasmic reticulum
GAL1	galactose inducible promoter
GFP	green fluorescent protein
GPI	glycosylphosphatidylinositol

His	poly-histidine
HIV	human immunodeficiency virus
Hrs	hours
Hsc	heat shock cognate
HSF	heat shock factor
Hsp	heat shock protein
Htt	huntingtin protein
IGF	insulin growth factor
IP	immunoprecipitation
kDa	kilodalton
L94A	amino acid substitution of leucine to alanine at the 94 th residue of the Rnq1 protein
mg	milligram
ml	milliliter
mm	millimeter
mM	milli Molar
mRFP	monomeric red fluorescent protein
N	asparagine
NaCl	sodium chloride
NEF	nucleotide exchange factor
NES	nuclear export signal

NLS	nuclear import signal
PBS	phosphate buffer saline
pH	potential of hydrogen
PI	protease inhibitor cocktail
PKI	protein kinase inhibitor
PMSF	phenylmethsulfonyl fluoride
polyQ	multiple glutamine residues
PrP	mammalian prion protein
Q	glutamine
Rnq1	yeast prion protein rich in asparagine and glutamine
S	sulfur
SDD-AGE	semi-denaturing detergent agarose gel electrophoresis
SDS	sodium dodecylsulfate
SDS-PAGE	SDS-polyacrylamide gel electrophoresis
SCA3	spinocerebellar ataxia type 3
SOD	superoxide dismutase
Sup35	yeast translational termination factor
SV-40	simian virus 40
WT	wild type
YFP	yellow fluorescent protein

Chapter One

Molecular Chaperones antagonize proteotoxicity by differentially modulating protein aggregation pathways

1.1 Abstract

The self-association of misfolded or damaged proteins into ordered amyloid-like aggregates characterizes numerous neurodegenerative disorders. Insoluble amyloid plaques are diagnostic of many disease states. Yet soluble, oligomeric intermediates in the aggregation pathway appear to represent the toxic culprit. Molecular chaperones regulate the fate of misfolded proteins and thereby influence their aggregation state. Chaperones conventionally antagonize aggregation of misfolded, disease proteins and assist in refolding or degradation pathways. Recent work suggests that chaperones may also suppress neurotoxicity by converting toxic, soluble oligomers into benign aggregates. Chaperones can therefore suppress or promote aggregation of disease proteins to ameliorate the proteotoxic accumulation of soluble, assembly intermediates.

1.2 Introduction

Many neurodegenerative disorders are characterized by the misfolding and subsequent aggregation of toxic proteins. Alzheimer's, Parkinson's, and the glutamine-encoding expansion diseases are examples of conformational disorders which show late onset symptoms of progressive neuronal dysfunction and eventual neuronal loss within certain brain regions (Carrell and Lomas, 1997). The disease-causing protein can adopt aberrant conformations due to age or stress which enables its aggregation and ultimate accumulation in amyloid fibrils (Figure 1.1) (Balch et al., 2008; Morimoto, 2008). Amyloids share a β -sheet-rich, fibrillar protein conformation in which the β -sheets stack parallel or anti-parallel to one another and run perpendicular to the fiber axis (Caughey and Lansbury, 2003; Nelson et al., 2005). Numerous pathogenic substrates as well as yeast prion proteins can exist in alternate, amyloid-like states that are characterized by a defined set of biochemical parameters including the ability to bind indicator dyes such as Thioflavin or Congo Red as well as resistance to both protease digestion and detergent solubilization (Chiti and Dobson, 2006). Though the appearance of amyloid is diagnostic of the disease state, the extent of amyloid accumulation often does not correlate with the disease symptoms (Caughey and Lansbury, 2003; Haass and Selkoe, 2007). In fact, a wide variety of organisms utilize functional forms of amyloid-like structures to perform important cellular processes such as phenotypic adaptation in yeast (Shorter and Lindquist, 2005; True et al., 2004; Uptain and Lindquist, 2002) and melanin synthesis in humans (Fowler et al., 2006). These and other lines of evidence suggest that amyloid formation per se is not toxic but may represent a benign by-product or even a protective mechanism (Arrasate et al., 2004; Cheng et al., 2007; Douglas et al., 2008).

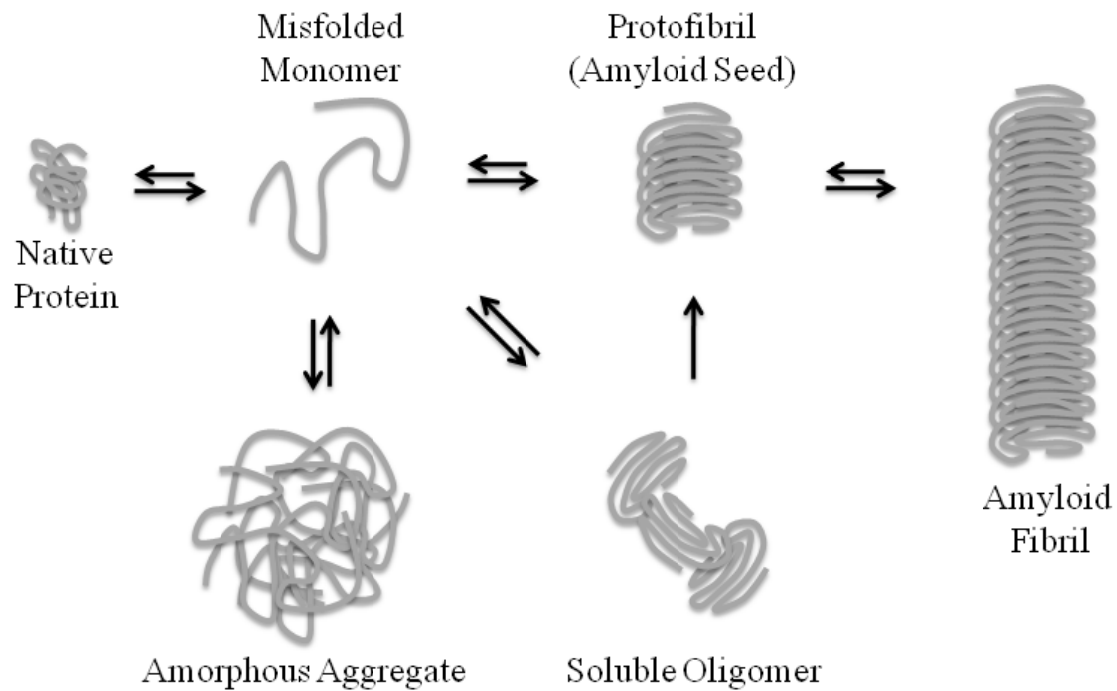


Figure 1.1 Schematic representation of the amyloid assembly pathway. A disease causing protein can adopt a non-native conformation due to intrinsic and/or environmental stress. The misfolded, disease protein can then self-associate into different intermediate structures such as detergent-soluble oligomers and/or protofibrils whose intracellular accumulation correlate with cell death. In this model, we speculate about the structural properties of the ill-defined intermediates. Alternatively, the misfolded protein can accumulate as non-specific, amorphous aggregates. The formation of amyloid seeds drives the autocatalytic conversion of native and misfolded protein monomers into β -sheet-rich, amyloid aggregates.

Soluble intermediates in the amyloid assembly pathway appear to represent the toxic species (Haass and Selkoe, 2007; Kaye et al., 2003). Relatively little is known about the exact nature of the assembly intermediates due to their dynamic structure (Figure 1.1). Antibodies generated against the A β ₄₂-peptide (proteolytically cleaved peptide from the Amyloid Precursor Protein, APP, and a causative agent for Alzheimer's disease) could recognize assembly intermediates formed by numerous amyloidogenic substrates and buffer their cytotoxicity (Kaye et al., 2003). Subsequent work demonstrated that the same conformational-specific antibodies could selectively inhibit spontaneous amyloid formation of yeast prions *in vitro* (Shorter and Lindquist, 2004; Vitrenko et al., 2007). Thus, amyloid assembly intermediates, which include soluble oligomers, do exhibit common conformation-dependent structures that are unique to the intermediates regardless of the amino acid sequence.

The accumulation of oligomeric amyloid assembly intermediates closely correlates with cell death (Haass and Selkoe, 2007), and distinct clearance pathways maintain the proteotoxic oligomers at low levels (Cohen et al., 2006). This can be accomplished by either solubilizing the aggregation-prone substrate or driving its assembly into higher-ordered amyloid-like aggregates. The ability to promote aggregation does not necessarily represent the cell's primary means of clearance but may provide backup pathways when solubilization machinery has become compromised by age or environmental insult (Cohen et al., 2006). The nature and identity of the unfavorable interactions between the soluble oligomers and other cellular components is just being defined and may result in transcriptional deregulation (Burke et al., 1996; Dunah et al., 2002; Steffan et al., 2000), proteasomal inactivation (Bence et al., 2001), aberrant signaling (Small et al., 2001), or

membrane damage (Arispe et al., 1993; Kremer et al., 2001; Volles et al., 2001). It should be noted that disease proteins associated with conformational disorders perform a wide variety of cellular functions and scenarios may exist where protein species other than amyloid assembly intermediates represent the predominant toxic species.

All cells contain quality control machinery termed molecular chaperones to maintain the appropriate folding state of proteins. Many of these molecular chaperones have been termed Heat-Shock Proteins (HSP) due to their increased expression upon heat treatment of cell and have been divided into six major families including HSP100, HSP90, HSP70, HSP60, HSP40, and the small HSPs (Muchowski and Wacker, 2005). Chaperones recognize misfolded protein conformers and ultimately coordinate the appropriate folding or degradation pathways. As the first line of defense against conformational disorders, chaperones maintain the solubility of misfolded, disease-related substrates by directly binding to non-native conformers or disassembling aggregates formed by the disease protein (Muchowski and Wacker, 2005). Alternatively, recent evidence suggests that chaperones can also promote aggregation and thereby prevent the toxic accumulation of amyloid assembly intermediates (Behrends et al., 2006; Douglas et al., 2008). Herein we discuss how molecular chaperones manage proteotoxic misfolding events of numerous amyloidogenic substrates.

1.3 Molecular chaperones antagonize aggregation of disease proteins

Chaperones act by multiple means to maintain the solubility of disease-causing proteins. Chaperone-mediated solubilization can occur in the initial stages of the amyloid assembly pathway by preventing the self-association of misfolded, disease proteins into toxic, oligomeric intermediates. Alternatively, chaperones also act later in the assembly

pathway to dismantle amyloid-like aggregates and resolubilize the disease protein. Thus chaperone intervention can either maintain or generate disease protein monomers which can be properly refolded or marked for degradation by the ubiquitin-proteasome system or autophagy pathways. This reduces the flux of misfolded, disease proteins through different stages of the amyloid assembly pathway and decreases the cellular concentration of proteotoxic assembly intermediates.

1.3.1 Chaperones prevent disease proteins from assembling into amyloid-like aggregations

Chaperone machinery can act early in the amyloid assembly pathway by recognizing misfolded, disease proteins and subsequently preventing their aggregation. The Hsp70 chaperone system has been well-defined in its role of preventing the assembly of different, disease-causing proteins into amyloid-like aggregates (Bonini, 2002; Muchowski and Wacker, 2005). The Hsp70 family of chaperone proteins is abundantly expressed throughout the cell and contains 11 known isoforms in humans (Tavaria et al., 1996). Though not as abundant as its Hsp70 partner, the Hsp40 co-chaperone (also referred to as J-proteins due to their highly conserved J-domain) represent a more diverse family of proteins which contain 41 isoforms in humans and are present in most every intracellular compartment (Qiu et al., 2006). The structural and functional diversity of Hsp40 co-chaperones provide specific substrate recognition properties for the Hsp70 work horse (Fan et al., 2003).

The misfolding of disease proteins can arise from numerous intrinsic or environmental stresses (Balch et al., 2008), and Hsp70 cooperates with different Hsp40 co-chaperones to ultimately recognize and refold the non-native protein conformers

(Figure 1.2). Hsp40 can bind hydrophobic peptides which are normally buried in the core of natively folded proteins but become solvent-exposed in misfolded states (Rudiger et al., 2001). The polypeptide binding domain of Hsp40 binds non-native proteins and delivers them to Hsp70 (Cheetham and Caplan, 1998; Cyr and Douglas, 1994). The ability of Hsp70 to bind the misfolded substrate is tightly regulated through an ATP hydrolytic cycle. Once in a complex with Hsp70, the J-domain of Hsp40 stimulates ATP hydrolysis on Hsp70 which promotes a conformational change in the Hsp70 substrate-binding domain and increases its binding affinity for the misfolded substrate (Cyr et al., 1992; Langer et al., 1992; Liberek et al., 1991). Hsp40 is liberated from the Hsp70:substrate complex following ATP hydrolysis yet it is unclear how co-chaperone release occurs. The substrate in complex with Hsp70 can be properly refolded, marked for degradation via Hsp70 coordination with degradation machinery, or released to re-enter this binding cycle. The substrate remains tightly bound to Hsp70 until ADP is exchanged for ATP via a diverse class of nucleotide exchange factors (NEF) (Bukau et al., 2006). It is in this manner that cooperation between Hsp40 and Hsp70 prevents the proteotoxic accumulation of misfolded, aggregation-prone proteins.

The involvement of nucleotide exchange factors (NEF) adds yet another level of regulation to the Hsp70 system. This diverse family of exchange factors is critical for the functional cycle of Hsp70 because they replace ADP for ATP on Hsp70 and trigger substrate release (Bukau et al., 2006). Well characterized NEFs include the bacterial GrpE, which facilitates nucleotide dissociation from the Hsp70 (DnaK) (Liberek et al., 1991; Zylicz et al., 1987), and the BAG family of eukaryotic proteins which are NEFs for different cytosolic Hsp70s (Bimston et al., 1998). A third family of proteins which

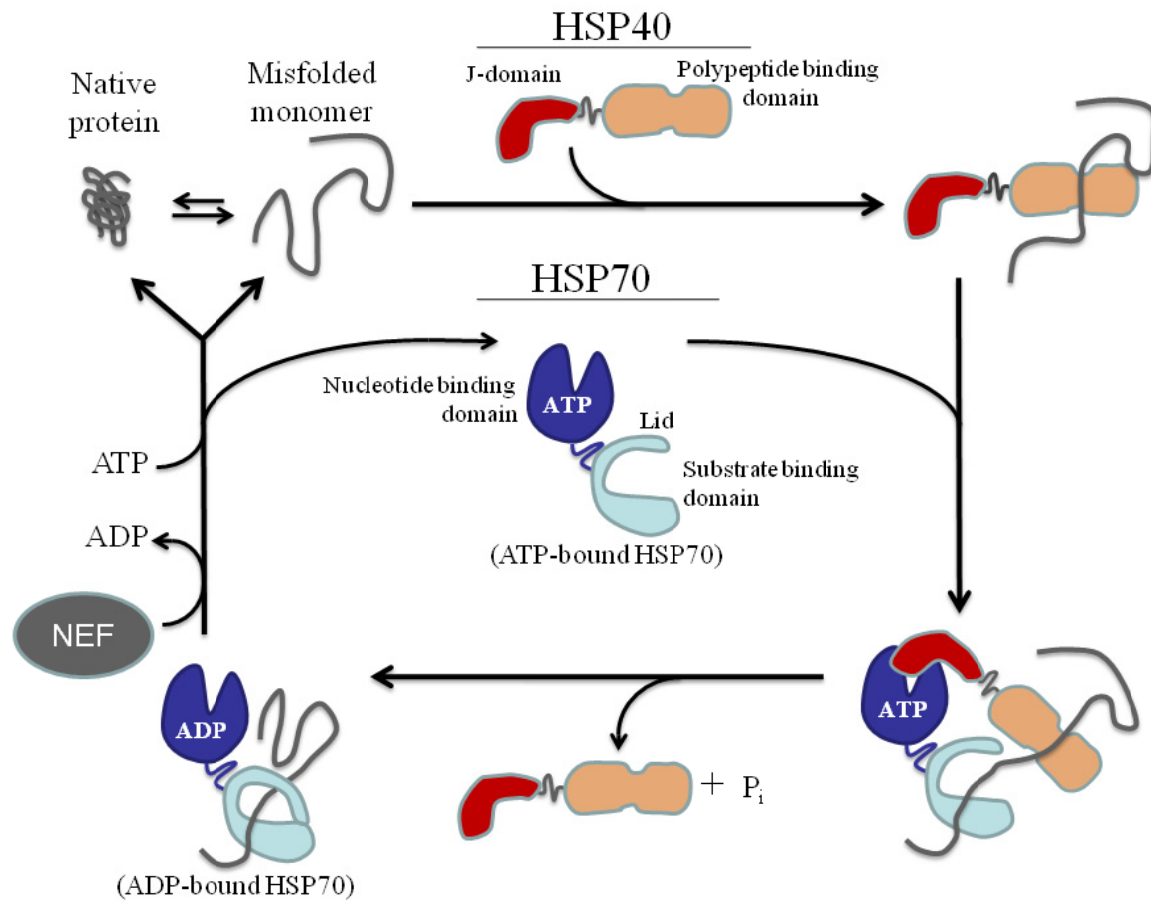


Figure 1.2 Hsp70-Hsp40 hydrolytic cycle for the binding and refolding of non-native proteins. A native protein can adopt a non-native conformation. Hsp40 co-chaperones can recognize the misfolded protein and bind it via its polypeptide binding domain. Hsp40 delivers the non-native substrate to Hsp70 and its J-domain stimulates ATP hydrolysis on Hsp70. This promotes a conformational change in Hsp70 via closure of the lid domain and increases the binding affinity of Hsp70 for the substrate. Hsp70 along with other cellular components not shown in this model can assist in the proper refolding of the substrate. Nucleotide exchange factors (NEF) release ADP and load ATP back onto the nucleotide binding domain of Hsp70 which promotes substrate release.

possess nucleotide exchange activity including the cytosolic Fes1 and ER luminal Sls1 in *Saccharomyces cerevisiae* (Kabani et al., 2002; Kabani et al., 2000), and the human ortholog HspBP1 (Hsp70 binding protein 1) (Raynes and Guerriero, 1998). Interestingly, other molecular chaperones are capable of nucleotide exchange on Hsp70. The yeast Hsp110, Sse1, regulates nucleotide exchange on different cytosolic Hsp70s (Raviol et al., 2006), while the Hsp170, Lhs1, stimulates nucleotide exchange of the ER Hsp70, Kar2 (Steel et al., 2004). Sse1 is a particularly interesting exchange factor because its activity in yeast is required for the propagation of the [URE3] prion (Kryndushkin and Wickner, 2007), as well as the formation and propagation of the [PSI⁺] prion (Sadlish et al., 2008). The recent findings which implicate Sse1 in the formation and propagation of amyloid-like prions may establish a better understanding of how nucleotide exchange on Hsp70 affects amyloid dynamics. Thus, the cell can utilize this diverse family of NEFs to regulate the different activities of Hsp70 in distinct subcellular compartments.

The ability of Hsp70 and Hsp40 to suppress the assembly of disease proteins into amyloid-like aggregates has been well documented in numerous model systems (Muchowski and Wacker, 2005), yet only a few examples will be discussed. Glutamine-encoding repeats within a set of unrelated proteins are the cause of at least nine different late onset neurodegenerative disorders (Ross, 2002; Zoghbi and Orr, 2000). Elevating intracellular pools of Hsp70 as well as Hsp40 reduce expanded-polyQ aggregate formation and suppressed toxicity in cultured cells (Chai et al., 1999; Jana et al., 2000; Kobayashi and Sobue, 2001). Due to the high conservation of chaperone machinery between eukaryotic cells, *Saccharomyces cerevisiae* has emerged as a model system to study protein aggregation and toxicity. Overexpression of the yeast Hsp70, Ssa1, or the

Hsp40, Ydj1, inhibit the formation of large, detergent-insoluble aggregates by an expanded-polyQ protein containing the N-terminal sequence of the huntingtin protein, the causative gene for Huntington's disease (Muchowski et al., 2000). Ydj1 also reduced the aggregation of the Q/N-rich prion domain of the yeast prion, Rnq1, which correlated with its ability to suppress prion toxicity (Summers et al., 2008). Elevated expression of another yeast Hsp40, Sis1, reduced the aggregation of expanded-polyQ Htt protein and suppressed toxicity in [psi⁻] yeast, which are void of the amyloid-like [PSI⁺] prion (Gokhale et al., 2005). Hsp70 and Hsp40 have also been shown to suppress the aggregation and toxicity of numerous other disease-causing proteins including mutant superoxide dismutase 1 (SOD) (Takeuchi et al., 2002), a causative gene for familial amyotrophic lateral sclerosis, and α -synuclein (Klucken et al., 2004), a causative gene for Parkinson disease. Thus, the ability of Hsp70 and Hsp40 to prevent assembly of amyloid-like aggregates and suppress cytotoxicity extends to numerous disease-causing proteins in a variety of model organisms.

1.3.2 Molecular chaperones solubilize protein aggregates

Chaperones can act later in the aggregation pathway to disassemble amyloid-like particles. Although it is unclear whether mammalian cells possess this disaggregation activity, fungi, plants and bacteria express the AAA ATPase protein remodeling factor, Hsp104 (ClpB in *E. coli*) (Shorter, 2008). The hexameric Hsp104 works synergistically with the Hsp70 chaperone system to not only resolubilize misfolded substrates, but to also restore their proper function (Glover and Lindquist, 1998). Interestingly, normal Hsp104 function is required in a yeast model to maintain different prion proteins in their

amyloid-like prion conformation (Chernoff et al., 1995; Derkatch et al., 1997; Moriyama et al., 2000; Sondheimer and Lindquist, 2000) by generating small prion seeds via fragmentation of larger prion aggregates which enables new rounds of prion propagation (Wegrzyn et al., 2001). Further *in vitro* studies demonstrated that Hsp104 couples ATP hydrolysis with the rapid disassembly of amyloid-like fibers and oligomeric intermediates formed by the yeast prions [*PSI*⁺] and [*URE3*] (Shorter and Lindquist, 2004; Shorter and Lindquist, 2006). Thus, it is not surprising that Hsp104 overexpression was able to efficiently solubilize amyloid-like aggregates formed by the expanded-polyQ huntingtin (Htt) fragment and reduce cell death in a yeast model (Cashikar et al., 2005). Yet removal of Hsp104 via gene deletion also subdued the toxicity caused by overexpression of the expanded-polyQ Htt fragment (Meriin et al., 2002). Thus, Hsp104 may indirectly affect polyQ aggregation and toxicity in yeast by acting through the yeast prions, [*PSI*⁺] and/or [*RNQ*⁺] [also termed [*PIN*⁺]](Derkatch et al., 1997)], which can serve as Q/N-rich templates to alter the conformation of the expanded-polyQ protein into an aggregation-prone, toxic form (Derkatch et al., 2004; Gokhale et al., 2005; Meriin et al., 2002).

To clarify the role of Hsp104 in polyQ aggregation and toxicity, the yeast Hsp104 chaperone was introduced into a number of higher eukaryotes and retained its ability to remodel amyloid-like assemblies. In a *C. elegans* model, expression of Hsp104 reduced the aggregation of expanded-polyQ proteins and abrogated developmental delays (Satyal et al., 2000). Similarly in a rat model, the presence of Hsp104 suppressed expanded-polyQ toxicity in a manner which correlated with altered distribution and number of the polyQ assemblies (Perrin et al., 2007). The small heat shock proteins, Hsp26 in yeast and Hsp27 in rats, were identified as potentiators for Hsp104-mediated suppression of polyQ

aggregation and toxicity (Cashikar et al., 2005; Perrin et al., 2007). Utilizing a Parkinson disease model in rats, Hsp104 was also shown to antagonize the formation oligomeric intermediates and amyloid fibers by α -synuclein which reduced dopaminergic degeneration (Lo Bianco et al., 2008). Thus, molecular chaperones can act at multiple stages in the aggregation pathway to both coordinate the disassembly of amyloid-like aggregates and prevent the self-association of non-native protein monomers.

1.3.3 Molecular chaperones participate in the degradation of proteotoxic substrates by the ubiquitin-proteasome system or chaperone-mediated autophagy

Under certain conditions, chaperone machinery cannot repair the misfolded protein and must coordinate its degradation by either the ubiquitin-proteasome pathway or lysosomal-mediated autophagy. CHIP (carboxy terminus of Hsc70-interacting protein) is a versatile protein that acts as a co-chaperone to Hsc70 (Heat shock cognate 70) or Hsp70, possesses intrinsic chaperone activity in its own right and functions as an E3 ligase to mediate the transfer of polyubiquitin chains to misfolded substrates (Cyr et al., 2002; Jiang et al., 2001; Rosser et al., 2007). The Hsp70 interacting protein, Bag2 (Bcl2-associated athanogene 2), can inhibit the ubiquitin ligase activity of CHIP and promote substrate refolding by Hsp70 (Arndt et al., 2005; Dai et al., 2005). Overexpression of CHIP increased the ubiquitination and degradation of expanded-polyQ huntingtin and ataxin-3, the causative gene for Spinocerebellar ataxia type 3 (SCA3) (Jana et al., 2005). This subsequently reduced polyQ aggregation levels and suppressed cell death. The suppressive activity by CHIP overexpression became more prominent when Hsc70 levels were also elevated. Similar results were obtained which demonstrated CHIP's ability to

reduce aggregation of expanded-polyQ substrates and suppress cell death in transfected cell lines, primary neurons and zebrafish models (Miller et al., 2005). Therefore, CHIP along with other cofactors can partition Hsp70 substrates between refolding and degradation pathways.

The autophagy pathway represents a mechanism independent of the ubiquitin-proteasome system which participates in the intracellular bulk degradation of organelles as well as misfolded and aggregated proteins. Autophagy entails the packaging/engulfment of cytoplasmic contents into autophagosome vesicles which fuse with lysosomes, wherein the contents are degraded (Levine and Klionsky, 2004). Loss of autophagy in mice via disruption of ATG5 manifested features characteristic of neurodegeneration even in the absence of any disease-associated mutant proteins (Hara et al., 2006). Molecular chaperones have been shown to participate in the recognition and subsequent packaging of misfolded proteins into autophagosomes which has become termed chaperone-mediated autophagy (CMA) (Terlecky et al., 1991). CMA involves the selective targeting of proteins containing a KFERQ peptide motif to lysosomes (Olson et al., 1991). The rate-limiting step in CMA involves chaperone/cargo binding to the lysosomal receptor, Lamp2a (Cuervo and Dice, 1996). In this manner, chaperones can recognize misfolded or aggregated proteins and target them via the KFERQ motif to lysosomes for degradation. The causative agent in Parkinson's disease, α -synuclein, possesses a pentapeptide sequence which is consistent with the CMA recognition motif and targets the disease protein to lysosomes (Cuervo et al., 2004). The pathogenic A53T and A30P mutations in α -synuclein were capable of binding the lysosomal receptors but inhibited both their own degradation as well as other substrates. Additionally, CMA has

also been linked to polyQ-expanded huntingtin toxicity through the small heat shock protein, HspB8, and Bag3. In cultured cells, elevated expression of HspB8 prevented the intracellular accumulation of polyQ-expanded huntingtin protein (Carra et al., 2005). Subsequent work demonstrated that HspB8 works in complex with Bag3 to stimulate the degradation of polyQ-expanded huntingtin protein by macroautophagy (Carra et al., 2008). Thus, chaperones can couple their activity with multiple degradation pathways to remove toxic, disease proteins.

1.4 Chaperones promote aggregation of toxic proteins

Chaperones are also capable of packaging disease proteins into tight, amyloid-like aggregates and thereby reducing the accumulation of soluble, oligomeric intermediates. Elevated expression of the human Hsp40, Hdj2, increased the aggregation of expanded-polyQ huntingtin protein in COS-7 cells (Wytttenbach et al., 2000). Subsequent *in vitro* studies demonstrated that purified forms of Hsp70 and Hsp40, Hdj1, were able to attenuate polyQ oligomer assembly and drive the formation of amyloid-like fibrillar structures (Wacker et al., 2004). These data suggest that chaperones can partition disease proteins between oligomeric and fibrillar aggregation states. Chaperones other than Hsp70 and Hsp40 can take an active role in promoting protein aggregation. The proteasomal chaperones, Rpt4 and Rpt6 (AAA ATPase subunits of the 19S proteasomal particle), facilitated the aggregation of different expanded-polyQ disease proteins, huntingtin and ataxin-3, without affecting proteasomal degradation (Rousseau et al., 2009). Furthermore, *in vitro* reconstitution experiments showed that purified 19S proteasomal particles enhanced aggregation of expanded-polyQ huntingtin protein

(Rousseau et al., 2009). Thus, a number of molecular chaperones can promote the assembly of disease proteins into amyloid-like aggregates.

1.4.1 Chaperone-mediated aggregation reduces proteotoxicity

Recent work has begun to link chaperone-mediated aggregation of toxic proteins with suppression of toxicity. The chaperonin TriC complex was identified as potent suppressor of polyQ-mediated toxicity in *C. Elegans* (Nollen et al., 2004). This family of chaperonins form multi-subunit, cage-like structures that sequester non-native proteins (Fenton and Horwich, 2003) and work alongside Hsp70 chaperone systems to promote substrate refolding in the cytosol upon rounds of ATP hydrolysis (Farr et al., 1997; Frydman and Hartl, 1996). Substrate refolding occurs within the central cavity of the chaperonin complex and substrate release occurs after folding is complete (Meyer et al., 2003). Interestingly, reducing the cellular concentration of TriC resulted in the accumulation of low-molecular weight, soluble oligomers by polyQ-expansions which correlated with toxicity in cell culture lines and yeast (Behrends et al., 2006; Kitamura et al., 2006; Tam et al., 2006). One group demonstrated by size exclusion chromatography that toxic oligomers were approximately 200 kDa in size (Schaffar et al., 2004), yet the chaperonin complex remodeled the polyQ-expansions into higher molecular weight aggregates around the 500 kDa size range (Behrends et al., 2006). The ability of the chaperonin complex to remodel polyQ-expanded disease proteins worked synergistically with Hsp70, Ssa1, and Hsp40, Ydj1. In contrast, studies in [*psi*⁻] yeast demonstrate that excess Ydj1 increased aggregation of expanded-polyQ Htt, yet enhanced toxicity (Gokhale et al., 2005). Though these data seems contrary to the work done with TriC, the nature and size of the polyQ aggregates may differ between experimental conditions and

account for whether the polyQ protein elicits a toxic or benign outcome. Additionally, cellular factors such as endogenous prions add to complexity of how chaperone networks buffer the accumulation of expanded-polyQ aggregates in a yeast model. Nevertheless, this provides correlative evidence that chaperonin complexes can not only solubilize their substrates but also promote the efficient packaging of proteotoxic species into benign aggregates.

Related studies in yeast have recently demonstrated the protective effects of Hsp40-mediated aggregate formation. The Hsp40, Sis1, is an essential chaperone (Luke et al., 1991) that participates in protein refolding (Lu and Cyr, 1998), protein translocation (Caplan et al., 1992), and translation initiation (Zhong and Arndt, 1993). Sis1 activity is also required to maintain the Rnq1 yeast prion in its $[RNQ^+]$ amyloid-like, prion conformation (Sondheimer et al., 2001). Endogenous Rnq1 is not toxic to yeast yet modest elevation of Rnq1 levels induced cell death (Douglas et al., 2008). Rnq1 toxicity is dependent on the presence of pre-existing $[RNQ^+]$ prions as elevated Rnq1 levels are not toxic to $[rnq^-]$ cells in which the $[RNQ^+]$ prion conformer is absent. Thus, $[RNQ^+]$ prion seeds provide a template which can alter the conformation of native Rnq1 into a toxic form (Douglas et al., 2008). Elevating Sis1 levels was able to suppress Rnq1 toxicity in a manner that correlated with increased formation of $[RNQ^+]$ prion assemblies and decreased amounts of soluble Rnq1. Point mutations (Rnq1 L94A) within the Sis1 binding site of Rnq1 enabled it to assume an aberrant conformation which formed SDS-soluble aggregates and became toxic in $[rnq^-]$ cells. Interestingly, Sis1 overexpression was able to detoxify excess Rnq1 L94A in $[RNQ^+]$ cells yet was unable to suppress Rnq1 L94A toxicity in $[rnq^-]$ cells. Therefore, Sis1 detoxification requires $[RNQ^+]$ prion seeds

so that nascent Rnq1 can be efficiently packaged into benign, amyloid-like aggregates. Inefficiencies in the $[RNQ^+]$ prion assembly pathway due to compromised Sis1 activity exacerbated cell death.

The molecular mechanism by which chaperones facilitate Rnq1 assembly into amyloid-like prions is not clear. Sis1 was previously shown to work in concert with Hsp104 to mediate the fragmentation of larger $[RNQ^+]$ prion aggregates (Aron et al., 2007). This generates more $[RNQ^+]$ prion seeds and more nucleation points to further drive the autocatalytic conversion of nascent Rnq1 into the prion conformer. The Ssa subclass of Hsp70 chaperones positively affects the formation and propagation of amyloid-like $[PSI^+]$ prions in yeast (Allen et al., 2005; Jung et al., 2000; Newnam et al., 1999). Yet the role of Hsp70 in $[RNQ^+]$ prion assembly remains elusive. It does appear that $[RNQ^+]$ prion shearing alone is not sufficient to suppress Rnq1 toxicity as overexpression of Hsp104 or different Hsp70 members was unable to suppress Rnq1 toxicity like excess Sis1 (Douglas et al., 2008). Therefore, we suggest that Sis1 may perform an additional function as an elongation factor in the $[RNQ^+]$ prion assembly process (Figure 1.3). Sis1 was shown to bind a region of Rnq1 outside the Q/N-rich prion domain (Douglas et al., 2008) in equimolar ratios (Lopez et al., 2003). Thus Sis1 may coat $[RNQ^+]$ prions and facilitate the stable association of nascent Rnq1 with $[RNQ^+]$ prions which would subsequently promote its efficient conversion into the growing amyloid-like $[RNQ^+]$ aggregate. Yet it is difficult to judge the relative importance of Sis1 action in fragmentation versus elongation of $[RNQ^+]$ prions.

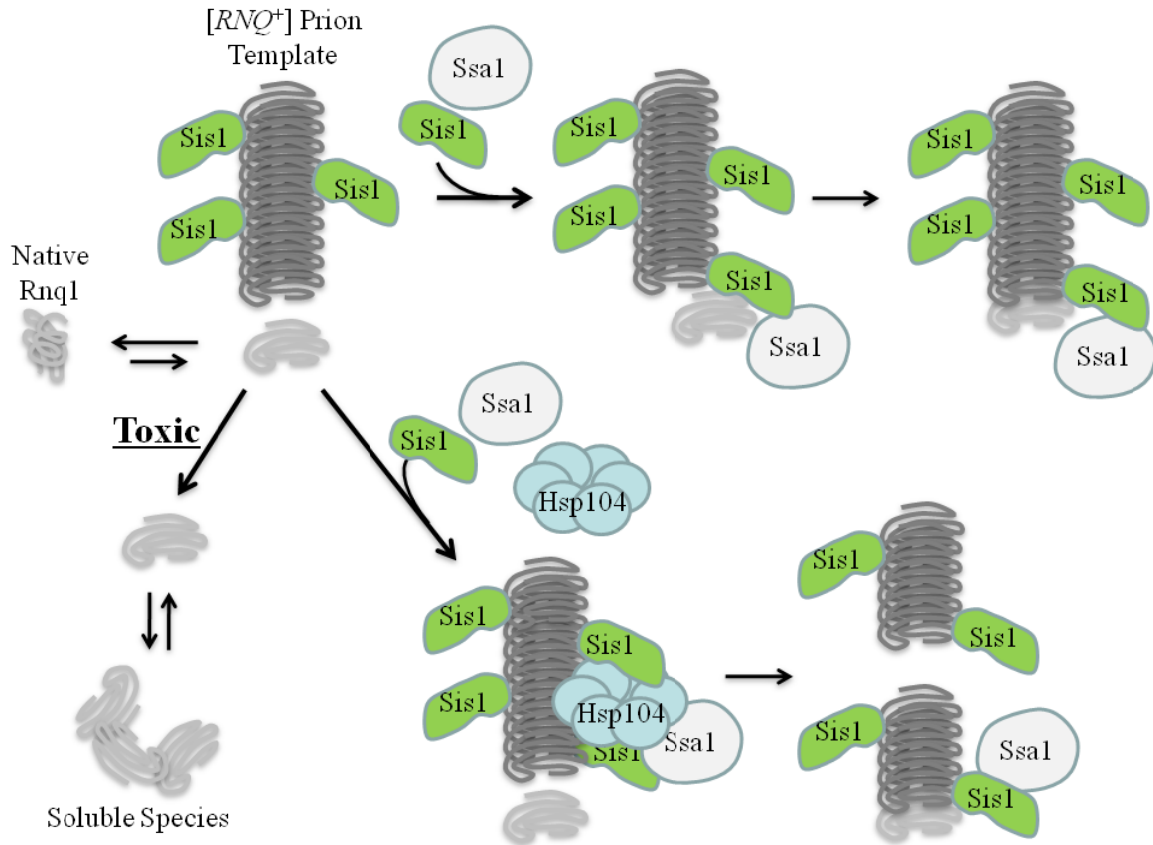


Figure 1.3 Roles for Sis1 in $[RNQ^+]$ prion assembly. The $[RNQ^+]$ prion acts as a template to alter the conformation of native Rnq1 into an assembly competent monomer. Sis1 promotes the appropriate packaging of templated Rnq1 monomers into higher-ordered $[RNQ^+]$ prions via a fragmentation and elongation model. Inefficiencies in this assembly process by Rnq1 overexpression or Sis1 depletion enable templated monomers to accumulate as soluble, proteotoxic species.

1.4.2 Distinct signaling pathways facilitate protein detoxification via opposing mechanisms

Cells can manage the proteotoxic accumulation of soluble, oligomeric species by both disaggregation and aggregation methods. *C. Elegans* have become a valuable tool to dissect the dynamics of amyloid assembly pathways in aging organisms. Distinct signaling pathways exist which both prevent the formation of amyloid aggregates as well as promote efficient amyloid assembly. The heat shock factor-1 (HSF-1) signaling pathway promoted the solubilization of toxic, A β ₁₋₄₂ assemblies (Cohen et al., 2006). HSF-1 activity is induced by a variety of stress signals including heat-shock which subsequently promotes the expression of numerous chaperones (Morimoto, 1998; Sorger, 1990; Wu et al., 1987). In contrast, the DAF-16 signaling pathway appears to promote efficient assembly of A β ₁₋₄₂ peptides into amyloid particles. The FOXO transcription factor, DAF-16 (Lin et al., 1997; Ogg et al., 1997), is a downstream target of insulin/insulin growth factor (IGF)-1-like signaling pathway which regulated life span and youthfulness in worms, flies and mammals (Kenyon, 2005). Although HSF-1 and DAF-16 signaling pathways promote longevity and cell survival, they appear to act by opposing mechanisms to accomplish this feat.

1.5 Conclusions

Molecular chaperones can intervene at multiple points in the amyloid assembly pathway to buffer the proteotoxic accumulation of misfolded protein intermediates. As a first line of defense, chaperone networks can coordinate the solubilization and subsequent refolding or degradation of different toxic proteins. Alternatively, the cell possesses a second line of defense which can package misfolded proteins into benign aggregates and thereby minimize the cell's exposure to the toxic assembly intermediates. Although the formation of amyloid-like aggregates appears to protect cells against protein misfolding events, the gradual stockpiling of amyloid fibrils into intra- and extra-cellular plaques can clearly have a negative impact on normal cellular processes over extended periods of time (Ehrnhoefer et al., 2008; Fiala, 2007; Lorenzo et al., 1994). Additionally, the general decline in protein homeostasis or proteostasis (Balch et al., 2008) by age or chronic stress may compromise chaperone networks (Morimoto, 2008) resulting in the destruction of benign aggregates and the generation of soluble, toxic oligomers. Two distinct signaling cascades appear to regulate the flux of misfolded, amyloidogenic proteins between solubilization and aggregation pathways (Cohen et al., 2006). HSF-1 regulates the expression of numerous molecular chaperones (Morimoto, 1998) and can antagonize aggregation through control of the integrated chaperone network. However, it is unclear in the DAF-16 signaling pathway which downstream components are involved in the remodeling of misfolded, disease proteins into ordered aggregates. Sis1 and the chaperonin complex were shown to drive protective aggregate formation, yet both proteins historically act to suppress non-specific aggregation (Frydman et al., 1992; Lu and Cyr, 1998). Therefore, different signaling pathways such as DAF-16 and HSF-1 may enable an individual chaperone such as Sis1 or the TriC chaperonin complex to perform

opposing functions on misfolded proteins. Alternatively, the disease substrate may possess intrinsic, structural properties which determine the action of the interacting chaperone. Further studies will elucidate the means by which opposing chaperone activities are regulated at a molecular and cellular level.

1.6 References

- Allen, K.D., R.D. Wegrzyn, T.A. Chernova, S. Muller, G.P. Newnam, P.A. Winslett, K.B. Wittich, K.D. Wilkinson, and Y.O. Chernoff. 2005. Hsp70 chaperones as modulators of prion life cycle: novel effects of Ssa and Ssb on the *Saccharomyces cerevisiae* prion [PSI⁺]. *Genetics*. 169:1227-42.
- Arispe, N., E. Rojas, and H.B. Pollard. 1993. Alzheimer disease amyloid beta protein forms calcium channels in bilayer membranes: blockade by tromethamine and aluminum. *Proc Natl Acad Sci U S A*. 90:567-71.
- Arndt, V., C. Daniel, W. Nastainczyk, S. Alberti, and J. Hohfeld. 2005. BAG-2 acts as an inhibitor of the chaperone-associated ubiquitin ligase CHIP. *Mol Biol Cell*. 16:5891-900.
- Aron, R., T. Higurashi, C. Sahi, and E.A. Craig. 2007. J-protein co-chaperone Sis1 required for generation of [RNQ⁺] seeds necessary for prion propagation. *EMBO J*. 26:3794-803.
- Arrasate, M., S. Mitra, E.S. Schweitzer, M.R. Segal, and S. Finkbeiner. 2004. Inclusion body formation reduces levels of mutant huntingtin and the risk of neuronal death. *Nature*. 431:805-10.
- Balch, W.E., R.I. Morimoto, A. Dillin, and J.W. Kelly. 2008. Adapting proteostasis for disease intervention. *Science*. 319:916-9.
- Behrends, C., C.A. Langer, R. Boteva, U.M. Bottcher, M.J. Stemp, G. Schaffar, B.V. Rao, A. Giese, H. Kretschmar, K. Siegers, and F.U. Hartl. 2006. Chaperonin TRiC promotes the assembly of polyQ expansion proteins into nontoxic oligomers. *Mol Cell*. 23:887-97.
- Bence, N.F., R.M. Sampat, and R.R. Kopito. 2001. Impairment of the ubiquitin-proteasome system by protein aggregation. *Science*. 292:1552-5.
- Bimston, D., J. Song, D. Winchester, S. Takayama, J.C. Reed, and R.I. Morimoto. 1998. BAG-1, a negative regulator of Hsp70 chaperone activity, uncouples nucleotide hydrolysis from substrate release. *EMBO J*. 17:6871-8.
- Bonini, N.M. 2002. Chaperoning brain degeneration. *Proc Natl Acad Sci U S A*. 99 Suppl 4:16407-11.

- Bukau, B., J. Weissman, and A. Horwich. 2006. Molecular chaperones and protein quality control. *Cell*. 125:443-51.
- Burke, J.R., J.J. Enghild, M.E. Martin, Y.S. Jou, R.M. Myers, A.D. Roses, J.M. Vance, and W.J. Strittmatter. 1996. Huntingtin and DRPLA proteins selectively interact with the enzyme GAPDH. *Nat Med*. 2:347-50.
- Caplan, A.J., D.M. Cyr, and M.G. Douglas. 1992. YDJ1p facilitates polypeptide translocation across different intracellular membranes by a conserved mechanism. *Cell*. 71:1143-55.
- Carra, S., S.J. Seguin, H. Lambert, and J. Landry. 2008. HspB8 chaperone activity toward poly(Q)-containing proteins depends on its association with Bag3, a stimulator of macroautophagy. *J Biol Chem*. 283:1437-44.
- Carra, S., M. Sivilotti, A.T. Chavez Zobel, H. Lambert, and J. Landry. 2005. HspB8, a small heat shock protein mutated in human neuromuscular disorders, has in vivo chaperone activity in cultured cells. *Hum Mol Genet*. 14:1659-69.
- Carrell, R.W., and D.A. Lomas. 1997. Conformational disease. *Lancet*. 350:134-8.
- Cashikar, A.G., M. Duennwald, and S.L. Lindquist. 2005. A chaperone pathway in protein disaggregation. Hsp26 alters the nature of protein aggregates to facilitate reactivation by Hsp104. *J Biol Chem*. 280:23869-75.
- Caughey, B., and P.T. Lansbury. 2003. Protofibrils, pores, fibrils, and neurodegeneration: separating the responsible protein aggregates from the innocent bystanders. *Annu Rev Neurosci*. 26:267-98.
- Chai, Y., S.L. Koppenhafer, N.M. Bonini, and H.L. Paulson. 1999. Analysis of the role of heat shock protein (Hsp) molecular chaperones in polyglutamine disease. *J Neurosci*. 19:10338-47.
- Cheetham, M.E., and A.J. Caplan. 1998. Structure, function and evolution of DnaJ: conservation and adaptation of chaperone function. *Cell Stress Chaperones*. 3:28-36.
- Cheng, I.H., K. Scearce-Levie, J. Legleiter, J.J. Palop, H. Gerstein, N. Bien-Ly, J. Puolivali, S. Lesne, K.H. Ashe, P.J. Muchowski, and L. Mucke. 2007.

- Accelerating amyloid-beta fibrillization reduces oligomer levels and functional deficits in Alzheimer disease mouse models. *J Biol Chem.* 282:23818-28.
- Chernoff, Y.O., S.L. Lindquist, B. Ono, S.G. Inge-Vechtsov, and S.W. Liebman. 1995. Role of the chaperone protein Hsp104 in propagation of the yeast prion-like factor [psi⁺]. *Science.* 268:880-4.
- Chiti, F., and C.M. Dobson. 2006. Protein misfolding, functional amyloid, and human disease. *Annu Rev Biochem.* 75:333-66.
- Cohen, E., J. Bieschke, R.M. Perciavalle, J.W. Kelly, and A. Dillin. 2006. Opposing activities protect against age-onset proteotoxicity. *Science.* 313:1604-10.
- Cuervo, A.M., and J.F. Dice. 1996. A receptor for the selective uptake and degradation of proteins by lysosomes. *Science.* 273:501-3.
- Cuervo, A.M., L. Stefanis, R. Fredenburg, P.T. Lansbury, and D. Sulzer. 2004. Impaired degradation of mutant alpha-synuclein by chaperone-mediated autophagy. *Science.* 305:1292-5.
- Cyr, D.M., and M.G. Douglas. 1994. Differential regulation of Hsp70 subfamilies by the eukaryotic DnaJ homologue YDJ1. *J Biol Chem.* 269:9798-804.
- Cyr, D.M., J. Hohfeld, and C. Patterson. 2002. Protein quality control: U-box-containing E3 ubiquitin ligases join the fold. *Trends Biochem Sci.* 27:368-75.
- Cyr, D.M., X. Lu, and M.G. Douglas. 1992. Regulation of Hsp70 function by a eukaryotic DnaJ homolog. *J Biol Chem.* 267:20927-31.
- Dai, Q., S.B. Qian, H.H. Li, H. McDonough, C. Borchers, D. Huang, S. Takayama, J.M. Younger, H.Y. Ren, D.M. Cyr, and C. Patterson. 2005. Regulation of the cytoplasmic quality control protein degradation pathway by BAG2. *J Biol Chem.* 280:38673-81.
- Derkatch, I.L., M.E. Bradley, P. Zhou, Y.O. Chernoff, and S.W. Liebman. 1997. Genetic and environmental factors affecting the de novo appearance of the [PSI⁺] prion in *Saccharomyces cerevisiae*. *Genetics.* 147:507-19.

- Derkatch, I.L., S.M. Uptain, T.F. Outeiro, R. Krishnan, S.L. Lindquist, and S.W. Liebman. 2004. Effects of Q/N-rich, polyQ, and non-polyQ amyloids on the de novo formation of the [PSI⁺] prion in yeast and aggregation of Sup35 in vitro. *Proc Natl Acad Sci U S A*. 101:12934-9.
- Douglas, P.M., S. Treusch, H.Y. Ren, R. Halfmann, M.L. Duennwald, S. Lindquist, and D.M. Cyr. 2008. Chaperone-dependent amyloid assembly protects cells from prion toxicity. *Proc Natl Acad Sci U S A*. 105:7206-11.
- Dunah, A.W., H. Jeong, A. Griffin, Y.M. Kim, D.G. Standaert, S.M. Hersch, M.M. Mouradian, A.B. Young, N. Tanese, and D. Krainc. 2002. Sp1 and TAFII130 transcriptional activity disrupted in early Huntington's disease. *Science*. 296:2238-43.
- Ehrnhoefer, D.E., J. Bieschke, A. Boeddrich, M. Herbst, L. Masino, R. Lurz, S. Engemann, A. Pastore, and E.E. Wanker. 2008. EGCG redirects amyloidogenic polypeptides into unstructured, off-pathway oligomers. *Nat Struct Mol Biol*. 15:558-66.
- Fan, C.Y., S. Lee, and D.M. Cyr. 2003. Mechanisms for regulation of Hsp70 function by Hsp40. *Cell Stress Chaperones*. 8:309-16.
- Farr, G.W., E.C. Scharl, R.J. Schumacher, S. Sondak, and A.L. Horwich. 1997. Chaperonin-mediated folding in the eukaryotic cytosol proceeds through rounds of release of native and nonnative forms. *Cell*. 89:927-37.
- Fenton, W.A., and A.L. Horwich. 2003. Chaperonin-mediated protein folding: fate of substrate polypeptide. *Q Rev Biophys*. 36:229-56.
- Fiala, J.C. 2007. Mechanisms of amyloid plaque pathogenesis. *Acta Neuropathol*. 114:551-71.
- Fowler, D.M., A.V. Koulov, C. Alory-Jost, M.S. Marks, W.E. Balch, and J.W. Kelly. 2006. Functional amyloid formation within mammalian tissue. *PLoS Biol*. 4:e6.
- Frydman, J., and F.U. Hartl. 1996. Principles of chaperone-assisted protein folding: differences between in vitro and in vivo mechanisms. *Science*. 272:1497-502.

- Frydman, J., E. Nimmesgern, H. Erdjument-Bromage, J.S. Wall, P. Tempst, and F.U. Hartl. 1992. Function in protein folding of TRiC, a cytosolic ring complex containing TCP-1 and structurally related subunits. *EMBO J.* 11:4767-78.
- Glover, J.R., and S. Lindquist. 1998. Hsp104, Hsp70, and Hsp40: a novel chaperone system that rescues previously aggregated proteins. *Cell.* 94:73-82.
- Gokhale, K.C., G.P. Newnam, M.Y. Sherman, and Y.O. Chernoff. 2005. Modulation of prion-dependent polyglutamine aggregation and toxicity by chaperone proteins in the yeast model. *J Biol Chem.* 280:22809-18.
- Haass, C., and D.J. Selkoe. 2007. Soluble protein oligomers in neurodegeneration: lessons from the Alzheimer's amyloid beta-peptide. *Nat Rev Mol Cell Biol.* 8:101-12.
- Hara, T., K. Nakamura, M. Matsui, A. Yamamoto, Y. Nakahara, R. Suzuki-Migishima, M. Yokoyama, K. Mishima, I. Saito, H. Okano, and N. Mizushima. 2006. Suppression of basal autophagy in neural cells causes neurodegenerative disease in mice. *Nature.* 441:885-9.
- Jana, N.R., P. Dikshit, A. Goswami, S. Kotliarova, S. Murata, K. Tanaka, and N. Nukina. 2005. Co-chaperone CHIP associates with expanded polyglutamine protein and promotes their degradation by proteasomes. *J Biol Chem.* 280:11635-40.
- Jana, N.R., M. Tanaka, G. Wang, and N. Nukina. 2000. Polyglutamine length-dependent interaction of Hsp40 and Hsp70 family chaperones with truncated N-terminal huntingtin: their role in suppression of aggregation and cellular toxicity. *Hum Mol Genet.* 9:2009-18.
- Jiang, J., C.A. Ballinger, Y. Wu, Q. Dai, D.M. Cyr, J. Hohfeld, and C. Patterson. 2001. CHIP is a U-box-dependent E3 ubiquitin ligase: identification of Hsc70 as a target for ubiquitylation. *J Biol Chem.* 276:42938-44.
- Jung, G., G. Jones, R.D. Wegrzyn, and D.C. Masison. 2000. A role for cytosolic hsp70 in yeast [PSI(+)] prion propagation and [PSI(+)] as a cellular stress. *Genetics.* 156:559-70.
- Kabani, M., J.M. Beckerich, and J.L. Brodsky. 2002. Nucleotide exchange factor for the yeast Hsp70 molecular chaperone Ssa1p. *Mol Cell Biol.* 22:4677-89.

- Kabani, M., J.M. Beckerich, and C. Gaillardin. 2000. Sls1p stimulates Sec63p-mediated activation of Kar2p in a conformation-dependent manner in the yeast endoplasmic reticulum. *Mol Cell Biol.* 20:6923-34.
- Kayed, R., E. Head, J.L. Thompson, T.M. McIntire, S.C. Milton, C.W. Cotman, and C.G. Glabe. 2003. Common structure of soluble amyloid oligomers implies common mechanism of pathogenesis. *Science.* 300:486-9.
- Kenyon, C. 2005. The plasticity of aging: insights from long-lived mutants. *Cell.* 120:449-60.
- Kitamura, A., H. Kubota, C.G. Pack, G. Matsumoto, S. Hirayama, Y. Takahashi, H. Kimura, M. Kinjo, R.I. Morimoto, and K. Nagata. 2006. Cytosolic chaperonin prevents polyglutamine toxicity with altering the aggregation state. *Nat Cell Biol.* 8:1163-70.
- Klucken, J., Y. Shin, E. Masliah, B.T. Hyman, and P.J. McLean. 2004. Hsp70 Reduces alpha-Synuclein Aggregation and Toxicity. *J Biol Chem.* 279:25497-502.
- Kobayashi, Y., and G. Sobue. 2001. Protective effect of chaperones on polyglutamine diseases. *Brain Res Bull.* 56:165-8.
- Kremer, J.J., D.J. Sklansky, and R.M. Murphy. 2001. Profile of changes in lipid bilayer structure caused by beta-amyloid peptide. *Biochemistry.* 40:8563-71.
- Kryndushkin, D., and R.B. Wickner. 2007. Nucleotide exchange factors for Hsp70s are required for [URE3] prion propagation in *Saccharomyces cerevisiae*. *Mol Biol Cell.* 18:2149-54.
- Langer, T., C. Lu, H. Echols, J. Flanagan, M.K. Hayer, and F.U. Hartl. 1992. Successive action of DnaK, DnaJ and GroEL along the pathway of chaperone-mediated protein folding. *Nature.* 356:683-9.
- Levine, B., and D.J. Klionsky. 2004. Development by self-digestion: molecular mechanisms and biological functions of autophagy. *Dev Cell.* 6:463-77.
- Liberek, K., J. Marszalek, D. Ang, C. Georgopoulos, and M. Zylicz. 1991. *Escherichia coli* DnaJ and GrpE heat shock proteins jointly stimulate ATPase activity of DnaK. *Proc Natl Acad Sci U S A.* 88:2874-8.

- Lin, K., J.B. Dorman, A. Rodan, and C. Kenyon. 1997. daf-16: An HNF-3/forkhead family member that can function to double the life-span of *Caenorhabditis elegans*. *Science*. 278:1319-22.
- Lo Bianco, C., J. Shorter, E. Regulier, H. Lashuel, T. Iwatsubo, S. Lindquist, and P. Aebischer. 2008. Hsp104 antagonizes alpha-synuclein aggregation and reduces dopaminergic degeneration in a rat model of Parkinson disease. *J Clin Invest*. 118:3087-97.
- Lopez, N., R. Aron, and E.A. Craig. 2003. Specificity of class II Hsp40 Sis1 in maintenance of yeast prion [RNQ+]. *Mol Biol Cell*. 14:1172-81.
- Lorenzo, A., B. Razzaboni, G.C. Weir, and B.A. Yankner. 1994. Pancreatic islet cell toxicity of amylin associated with type-2 diabetes mellitus. *Nature*. 368:756-60.
- Lu, Z., and D.M. Cyr. 1998. Protein folding activity of Hsp70 is modified differentially by the hsp40 co-chaperones Sis1 and Ydj1. *J Biol Chem*. 273:27824-30.
- Luke, M.M., A. Sutton, and K.T. Arndt. 1991. Characterization of SIS1, a *Saccharomyces cerevisiae* homologue of bacterial dnaJ proteins. *J Cell Biol*. 114:623-38.
- Meriin, A.B., X. Zhang, X. He, G.P. Newnam, Y.O. Chernoff, and M.Y. Sherman. 2002. Huntington toxicity in yeast model depends on polyglutamine aggregation mediated by a prion-like protein Rnq1. *J Cell Biol*. 157:997-1004.
- Meyer, A.S., J.R. Gillespie, D. Walther, I.S. Millet, S. Doniach, and J. Frydman. 2003. Closing the folding chamber of the eukaryotic chaperonin requires the transition state of ATP hydrolysis. *Cell*. 113:369-81.
- Miller, V.M., R.F. Nelson, C.M. Gouvion, A. Williams, E. Rodriguez-Lebron, S.Q. Harper, B.L. Davidson, M.R. Rebagliati, and H.L. Paulson. 2005. CHIP suppresses polyglutamine aggregation and toxicity in vitro and in vivo. *J Neurosci*. 25:9152-61.
- Morimoto, R.I. 1998. Regulation of the heat shock transcriptional response: cross talk between a family of heat shock factors, molecular chaperones, and negative regulators. *Genes Dev*. 12:3788-96.

- Morimoto, R.I. 2008. Proteotoxic stress and inducible chaperone networks in neurodegenerative disease and aging. *Genes Dev.* 22:1427-38.
- Moriyama, H., H.K. Edskes, and R.B. Wickner. 2000. [URE3] prion propagation in *Saccharomyces cerevisiae*: requirement for chaperone Hsp104 and curing by overexpressed chaperone Ydj1p. *Mol Cell Biol.* 20:8916-22.
- Muchowski, P.J., G. Schaffar, A. Sittler, E.E. Wanker, M.K. Hayer-Hartl, and F.U. Hartl. 2000. Hsp70 and hsp40 chaperones can inhibit self-assembly of polyglutamine proteins into amyloid-like fibrils. *Proc Natl Acad Sci U S A.* 97:7841-6.
- Muchowski, P.J., and J.L. Wacker. 2005. Modulation of neurodegeneration by molecular chaperones. *Nat Rev Neurosci.* 6:11-22.
- Nelson, R., M.R. Sawaya, M. Balbirnie, A.O. Madsen, C. Riek, R. Grothe, and D. Eisenberg. 2005. Structure of the cross-beta spine of amyloid-like fibrils. *Nature.* 435:773-8.
- Newnam, G.P., R.D. Wegrzyn, S.L. Lindquist, and Y.O. Chernoff. 1999. Antagonistic interactions between yeast chaperones Hsp104 and Hsp70 in prion curing. *Mol Cell Biol.* 19:1325-33.
- Nollen, E.A., S.M. Garcia, G. van Haften, S. Kim, A. Chavez, R.I. Morimoto, and R.H. Plasterk. 2004. Genome-wide RNA interference screen identifies previously undescribed regulators of polyglutamine aggregation. *Proc Natl Acad Sci U S A.* 101:6403-8.
- Ogg, S., S. Paradis, S. Gottlieb, G.I. Patterson, L. Lee, H.A. Tissenbaum, and G. Ruvkun. 1997. The Fork head transcription factor DAF-16 transduces insulin-like metabolic and longevity signals in *C. elegans*. *Nature.* 389:994-9.
- Olson, T.S., S.R. Terlecky, and J.F. Dice. 1991. Targeting specific proteins for lysosomal proteolysis. *Biomed Biochim Acta.* 50:393-7.
- Perrin, V., E. Regulier, T. Abbas-Terki, R. Hassig, E. Brouillet, P. Aebischer, R. Luthi-Carter, and N. Deglon. 2007. Neuroprotection by Hsp104 and Hsp27 in lentiviral-based rat models of Huntington's disease. *Mol Ther.* 15:903-11.

- Qiu, X.B., Y.M. Shao, S. Miao, and L. Wang. 2006. The diversity of the DnaJ/Hsp40 family, the crucial partners for Hsp70 chaperones. *Cell Mol Life Sci.* 63:2560-70.
- Raviol, H., H. Sadlish, F. Rodriguez, M.P. Mayer, and B. Bukau. 2006. Chaperone network in the yeast cytosol: Hsp110 is revealed as an Hsp70 nucleotide exchange factor. *EMBO J.* 25:2510-8.
- Raynes, D.A., and V. Guerriero, Jr. 1998. Inhibition of Hsp70 ATPase activity and protein renaturation by a novel Hsp70-binding protein. *J Biol Chem.* 273:32883-8.
- Ross, C.A. 2002. Polyglutamine pathogenesis: emergence of unifying mechanisms for Huntington's disease and related disorders. *Neuron.* 35:819-22.
- Rosser, M.F., E. Washburn, P.J. Muchowski, C. Patterson, and D.M. Cyr. 2007. Chaperone functions of the E3 ubiquitin ligase CHIP. *J Biol Chem.* 282:22267-77.
- Rousseau, E., R. Kojima, G. Hoffner, P. Djian, and A. Bertolotti. 2009. Misfolding of proteins with a polyglutamine expansion is facilitated by proteasomal chaperones. *J Biol Chem.* 284:1917-29.
- Rudiger, S., J. Schneider-Mergener, and B. Bukau. 2001. Its substrate specificity characterizes the DnaJ co-chaperone as a scanning factor for the DnaK chaperone. *EMBO J.* 20:1042-50.
- Sadlish, H., H. Rampelt, J. Shorter, R.D. Wegrzyn, C. Andreasson, S. Lindquist, and B. Bukau. 2008. Hsp110 chaperones regulate prion formation and propagation in *S. cerevisiae* by two discrete activities. *PLoS ONE.* 3:e1763.
- Satyral, S.H., E. Schmidt, K. Kitagawa, N. Sondheimer, S. Lindquist, J.M. Kramer, and R.I. Morimoto. 2000. Polyglutamine aggregates alter protein folding homeostasis in *Caenorhabditis elegans*. *Proc Natl Acad Sci U S A.* 97:5750-5.
- Schaffar, G., P. Breuer, R. Boteva, C. Behrends, N. Tzvetkov, N. Strippel, H. Sakahira, K. Siegers, M. Hayer-Hartl, and F.U. Hartl. 2004. Cellular toxicity of polyglutamine expansion proteins: mechanism of transcription factor deactivation. *Mol Cell.* 15:95-105.
- Shorter, J. 2008. Hsp104: a weapon to combat diverse neurodegenerative disorders. *Neurosignals.* 16:63-74.

- Shorter, J., and S. Lindquist. 2004. Hsp104 catalyzes formation and elimination of self-replicating Sup35 prion conformers. *Science*. 304:1793-7.
- Shorter, J., and S. Lindquist. 2005. Prions as adaptive conduits of memory and inheritance. *Nat Rev Genet*. 6:435-50.
- Shorter, J., and S. Lindquist. 2006. Destruction or potentiation of different prions catalyzed by similar Hsp104 remodeling activities. *Mol Cell*. 23:425-38.
- Small, D.H., S.S. Mok, and J.C. Bornstein. 2001. Alzheimer's disease and Abeta toxicity: from top to bottom. *Nat Rev Neurosci*. 2:595-8.
- Sondheimer, N., and S. Lindquist. 2000. Rnq1: an epigenetic modifier of protein function in yeast. *Mol Cell*. 5:163-72.
- Sondheimer, N., N. Lopez, E.A. Craig, and S. Lindquist. 2001. The role of Sis1 in the maintenance of the [RNQ+] prion. *EMBO J*. 20:2435-42.
- Sorger, P.K. 1990. Yeast heat shock factor contains separable transient and sustained response transcriptional activators. *Cell*. 62:793-805.
- Steel, G.J., D.M. Fullerton, J.R. Tyson, and C.J. Stirling. 2004. Coordinated activation of Hsp70 chaperones. *Science*. 303:98-101.
- Steffan, J.S., A. Kazantsev, O. Spasic-Boskovic, M. Greenwald, Y.Z. Zhu, H. Gohler, E.E. Wanker, G.P. Bates, D.E. Housman, and L.M. Thompson. 2000. The Huntington's disease protein interacts with p53 and CREB-binding protein and represses transcription. *Proc Natl Acad Sci U S A*. 97:6763-8.
- Summers, D.W., P.M. Douglas, H.Y. Ren, and D.M. Cyr. 2008. The type I HSP40 YDJ1 utilizes a farnesyl moiety and zinc finger like-region to suppress prion toxicity. *J Biol Chem*.
- Takeuchi, H., Y. Kobayashi, T. Yoshihara, J. Niwa, M. Doyu, K. Ohtsuka, and G. Sobue. 2002. Hsp70 and Hsp40 improve neurite outgrowth and suppress intracytoplasmic aggregate formation in cultured neuronal cells expressing mutant SOD1. *Brain Res*. 949:11-22.

- Tam, S., R. Geller, C. Spiess, and J. Frydman. 2006. The chaperonin TRiC controls polyglutamine aggregation and toxicity through subunit-specific interactions. *Nat Cell Biol.* 8:1155-62.
- Tavaria, M., T. Gabriele, I. Kola, and R.L. Anderson. 1996. A hitchhiker's guide to the human Hsp70 family. *Cell Stress Chaperones.* 1:23-8.
- Terlecky, S.R., T.S. Olson, and J.F. Dice. 1991. A pathway of lysosomal proteolysis mediated by the 73-kilodalton heat shock cognate protein. *Acta Biol Hung.* 42:39-47.
- True, H.L., I. Berlin, and S.L. Lindquist. 2004. Epigenetic regulation of translation reveals hidden genetic variation to produce complex traits. *Nature.* 431:184-7.
- Uptain, S.M., and S. Lindquist. 2002. Prions as protein-based genetic elements. *Annu Rev Microbiol.* 56:703-41.
- Vitrenko, Y.A., E.O. Gracheva, J.E. Richmond, and S.W. Liebman. 2007. Visualization of aggregation of the Rnq1 prion domain and cross-seeding interactions with Sup35NM. *J Biol Chem.* 282:1779-87.
- Volles, M.J., S.J. Lee, J.C. Rochet, M.D. Shtilerman, T.T. Ding, J.C. Kessler, and P.T. Lansbury, Jr. 2001. Vesicle permeabilization by protofibrillar alpha-synuclein: implications for the pathogenesis and treatment of Parkinson's disease. *Biochemistry.* 40:7812-9.
- Wacker, J.L., M.H. Zareie, H. Fong, M. Sarikaya, and P.J. Muchowski. 2004. Hsp70 and Hsp40 attenuate formation of spherical and annular polyglutamine oligomers by partitioning monomer. *Nat Struct Mol Biol.* 11:1215-22.
- Wegrzyn, R.D., K. Bapat, G.P. Newnam, A.D. Zink, and Y.O. Chernoff. 2001. Mechanism of prion loss after Hsp104 inactivation in yeast. *Mol Cell Biol.* 21:4656-69.
- Wu, C., S. Wilson, B. Walker, I. Dawid, T. Paisley, V. Zimarino, and H. Ueda. 1987. Purification and properties of Drosophila heat shock activator protein. *Science.* 238:1247-53.

- Wytenbach, A., J. Carmichael, J. Swartz, R.A. Furlong, Y. Narain, J. Rankin, and D.C. Rubinsztein. 2000. Effects of heat shock, heat shock protein 40 (HDJ-2), and proteasome inhibition on protein aggregation in cellular models of Huntington's disease. *Proc Natl Acad Sci U S A.* 97:2898-903.
- Zhong, T., and K.T. Arndt. 1993. The yeast SIS1 protein, a DnaJ homolog, is required for the initiation of translation. *Cell.* 73:1175-86.
- Zoghbi, H.Y., and H.T. Orr. 2000. Glutamine repeats and neurodegeneration. *Annu Rev Neurosci.* 23:217-47.
- Zylicz, M., D. Ang, and C. Georgopoulos. 1987. The grpE protein of Escherichia coli. Purification and properties. *J Biol Chem.* 262:17437-42.

Chapter Two

Chaperone-dependent amyloid assembly protects against prion toxicity

2.1 Abstract

Protein conformational diseases are associated with the aberrant accumulation of amyloid protein aggregates, but whether amyloid formation is cytotoxic or protective is unclear. To address this issue, we investigated a normally benign amyloid formed by the yeast prion $[RNQ^+]$. Surprisingly, modest overexpression of Rnq1 protein was deadly, but only when preexisting Rnq1 was in the $[RNQ^+]$ prion conformation. Molecular chaperones protect against protein aggregation diseases and are generally believed to do so by solubilizing their substrates. The Hsp40 chaperone, Sis1, suppressed Rnq1 proteotoxicity, but instead of blocking Rnq1 protein aggregation, it stimulated conversion of soluble Rnq1 to $[RNQ^+]$ amyloid. Furthermore, interference with Sis1-mediated $[RNQ^+]$ amyloid formation exacerbated Rnq1 toxicity. These and other data establish that even subtle changes in the folding homeostasis of an amyloidogenic protein can create a severe proteotoxic gain-of-function phenotype and that chaperone-mediated amyloid assembly can be cytoprotective. The possible relevance of these findings to other phenomena, including prion-driven neurodegenerative diseases and heterokaryon incompatibility in fungi, is discussed.

2.2 Introduction

Alzheimer's disease, transmissible spongiform encephalopathies, and polyglutamine diseases are representatives of a large group of neurodegenerative disorders that are associated with the misfolding and conversion of particular proteins into amyloids (Carrell and Lomas, 1997). Amyloids form in response to many perturbations in protein homeostasis, namely mutations in the amino acid sequence of a disease-related protein, expansion of simple sequence elements in disease genes, elevated protein levels, and age-associated cell stress (Chiti and Dobson, 2006). Amyloid fibrils share a cross- β structural motif, in which β -strands run perpendicular to the long fiber axis and accumulate in intra- and extracellular inclusions (Caughey and Lansbury, 2003; Nelson et al., 2005). Fibril formation requires that a misfolded protein expose a pleated β -surface that is capable of serving as a template and hydrogen-bonding partner with an extra β -strand (Carrell and Lomas, 1997). Biochemical parameters for the classification of protein aggregates as amyloids include resistance to solubilization by the detergent SDS and the ability to bind indicator dyes such as thioflavin-T (Chiti and Dobson, 2006).

Amyloid deposits in the brain are a hallmark of protein conformational disease, but often there is only a poor correlation between the detection of amyloid fibrils and other markers of neurodegeneration (Haass and Selkoe, 2007). Thus, there is still intense debate about whether amyloids are the causative toxic protein species in neurodegenerative diseases. In fact, recent, still controversial work suggests that amyloids might be benign or cytoprotective and that difficult-to-characterize soluble oligomeric conformers are the toxic species of disease-causing proteins (Cheng et al., 2007; Kaye et al., 2003; Shorter and Lindquist, 2005).

Cells buffer proteotoxic events related to intracellular protein misfolding via chaperone-mediated partitioning of nonnative conformers between pathways for proper folding, inclusion body formation, and degradation (Muchowski and Wacker, 2005). Molecular chaperones also play a critical role in the propagation of yeast prions (Chernoff et al., 1995), which are examples of intracellular amyloids that, in general, are not inherently toxic (Lindquist, 1997; Wickner, 1994). However, the conversion of active soluble Sup35 and Ure2 into their prion states [*PSI*⁺] and [*URE3*], respectively, inactivates these proteins (Lindquist, 1997; Wickner, 1994). Yeast prion formation occurs spontaneously at a low frequency, and the prion state is then perpetuated through the templating of newly synthesized prion proteins by preexisting amyloid-like prions (Chien et al., 2004). Templated prion proteins then undergo stable changes in structure and function to enter an amyloid-like state that is propagated and passed from mother cells to their daughters in a molecular chaperone-dependent manner (Chernoff et al., 1995). Yeast prions thereby constitute cytoplasmically transmitted, protein-based elements of inheritance that are dominant in genetic crosses (prions are denoted by brackets, italics, and capital letters to reflect these properties).

The yeast prion [*RNQ*⁺] is determined by the conformational state of the Rnq1 protein, which contains a C-terminal asparagine- and glutamine-rich prion domain and an N-terminal non-prion-forming domain (Derkatch et al., 2000; Sondheimer and Lindquist, 2000). The native form of Rnq1 has no known normal biological function and is nonessential. Yet the [*RNQ*⁺] prion can have important effects on yeast cells because it influences certain other proteins to convert to amyloid-like states (Meriin et al., 2002; Osherovich and Weissman, 2001; Taneja et al., 2007). For example, [*RNQ*⁺] prions are

required for the initial conversion of native Sup35 to the $[PSI^+]$ state. Indeed, $[RNQ^+]$ constitutes the cytoplasmically inherited factor known as $[PIN^+]$ and is the only known yeast prion that is commonly found in wild strains (Derkatch et al., 2001; Nakayashiki et al., 2005). $[RNQ^+]$ prions also cause the exon 1 fragment of huntingtin protein, containing glutamine repeats, to become toxic in yeast (Meriin et al., 2002). Thus, $[RNQ^+]$ prions can interact with other amyloid-forming proteins and thereby help drive their conversion into benign or toxic amyloid-like species.

2.2 Results

Overexpression of Rnq1 Is Toxic in $[RNQ^+]$ Cells

We recently discovered that moderate (i.e., ≈ 5 - to 10-fold) overexpression of Rnq1 from the GAL1 promoter was severely toxic in cells that harbored the $[RNQ^+]$ prion (Figure 2.1a, *Upper panel* shows growth of serially diluted liquid cultures on agar and *Lower panel* shows protein levels detected by western blot). This finding was surprising because Rnq1 overexpression was not toxic when endogenous Rnq1 was in the $[rnq^-]$ non-prion conformation, nor was it toxic in cells carrying a deletion of the *RNQ1* gene, $\Delta rnq1$ (Figure 2.1a). Cell growth defects observed were more extreme than any we have observed with other misfolded proteins in yeast (Cooper et al., 2006; Duennwald et al., 2006a; Duennwald et al., 2006b). At this modest level of Rnq1 overexpression, $\approx 25\%$ of $[RNQ^+]$ cells were dead within 4 h, as determined by the percentage of colony-forming units and dye exclusion (data not shown). Toxicity was accompanied by the accumulation of Rnq1 aggregates that stained with the common amyloid diagnostic dye thioflavin-T (Figure 2.1b). Rnq1 overexpression was found to be toxic in $[RNQ^+]$ laboratory strains (W303, 74D-694, BY23, and BY4741), clinical strains (YJM269, YJM421, YJM436, and YJM653), a fermentation strain (Y12), and wine strains (I14, T73, and WE372) (M. Taipale and S.L., unpublished observations). Thus, Rnq1 toxicity is pervasive and not strain-specific.

Although not quite as deadly, a carboxy-terminal Rnq1-YFP fusion protein behaved similarly to untagged Rnq1 and exhibited the same pattern of toxicity: toxic in $[RNQ^+]$ cells but not in $[rnq^-]$ or $\Delta rnq1$ cells. This result allowed us to correlate changes in toxicity with changes in protein distribution (Figure 2.1 and 2.2). While aggregated in

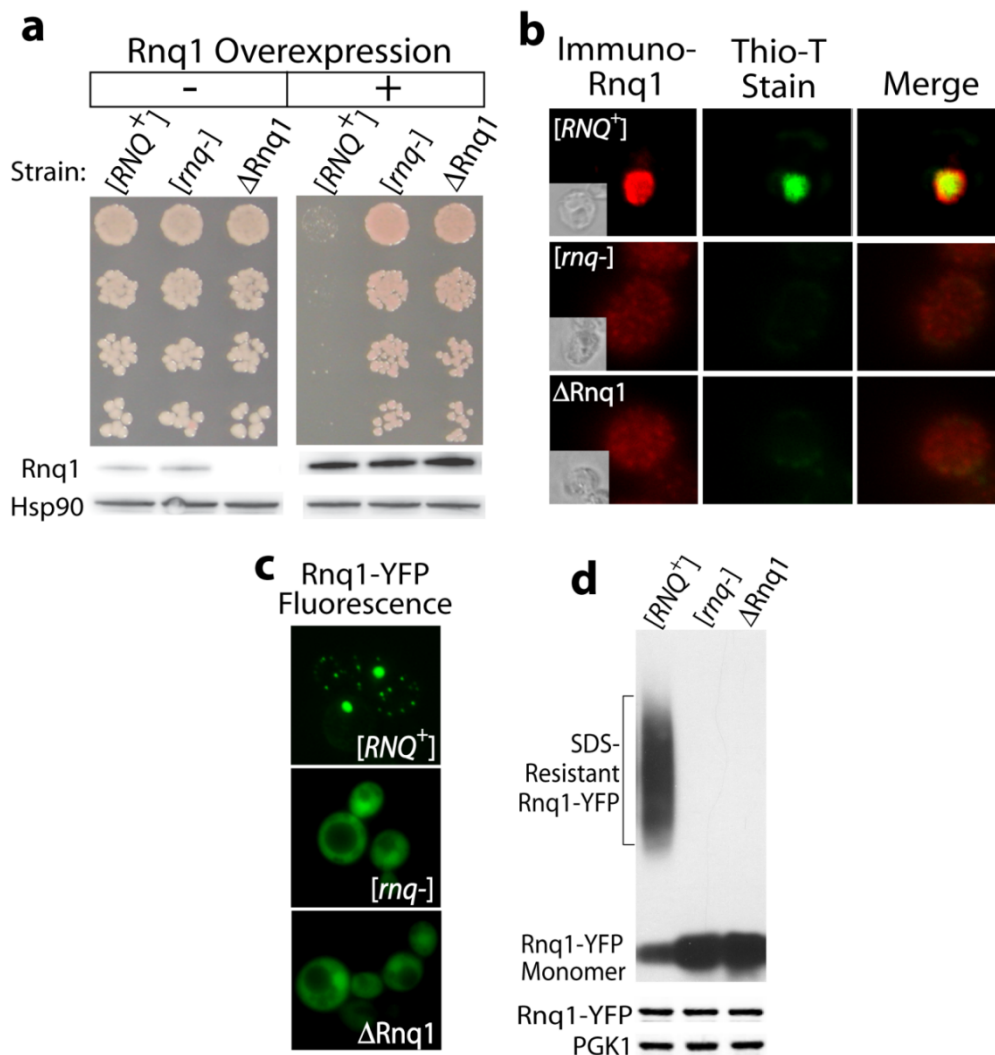


Figure 2.1 Overexpression of Rnq1 is toxic to [RNQ⁺] cells. (a) The effect of Rnq1 overexpression on yeast cell viability in the presence and absence of the [RNQ⁺] prion. (b) Thioflavin-T staining of Rnq1 in [RNQ⁺], [rnq⁻] and ΔRnq1 cells. Fixed yeast were decorated with α-Rnq1 sera that was detected with a fluorescent secondary antibody. The same cells were simultaneously stained with the amyloid indicator dye, thioflavin-T. (c) Visualization of the aggregation state of Rnq1-YFP by fluorescence microscopy. (d) The assembly status of Rnq1-YFP as determined by SDD-AGE. The lower panels represent western blots of cell extracts probed with the indicated antibodies.

[*RNQ*⁺] cells, Rnq1-YFP was distributed throughout the cytosol in [*rnq*⁻] or Δ *rnq1* cells. Using low- and high-copy plasmids that express Rnq1-YFP at different levels, we found that toxicity positively correlated with the degree of overexpression (Figure 2.2a). Western blots of cell lysates separated by semidenaturing-detergent-agarose gel electrophoresis (SDD-AGE) demonstrated that, in [*RNQ*⁺] but not [*rnq*⁻] cells, Rnq1-YFP assembled into a SDS-resistant high-molecular-weight species typical of amyloid assemblies of yeast prions (Figure 2.1d and Figure 2.2b) (Kryndushkin et al., 2003). Yet a pool of soluble Rnq1-YFP, which ran at the position of a monomer on SDD-AGE gels, also was present in [*RNQ*⁺] cells.

Growth of [*RNQ*⁺] cells overexpressing just the non-prion-forming domain or just the prion-forming domain of Rnq1, amino acids 1–153 and 154–405, respectively, was not hindered (Figure 2.2c). When the prion-forming domain is expressed on its own, it assembles into an SDS-resistant species that runs as an amyloid on SDD-AGE gels (Figure 2.2d). Therefore, the mechanism for Rnq1 toxicity does not appear related to the accumulation of large quantities of amyloid-like [*RNQ*⁺] prions *per se*.

The toxicity of Rnq1 overexpression in the presence of the [*RNQ*⁺] prion might seem similar to the toxicity of overexpressed Sup35 in the presence of its prion [*PSI*⁺]. Overexpression of Sup35 is toxic in [*PSI*⁺] cells because it drives too much of the essential Sup35 protein into an inactive amyloid conformation (Derkatch et al., 1997). In contrast, Rnq1 toxicity cannot be due to an inhibition of Rnq1 function because deletion of the gene-encoding Rnq1 has no detectable effect on yeast growth under hundreds of conditions tested (T.F. Outeiro and S.L., unpublished data). Furthermore, in contrast to

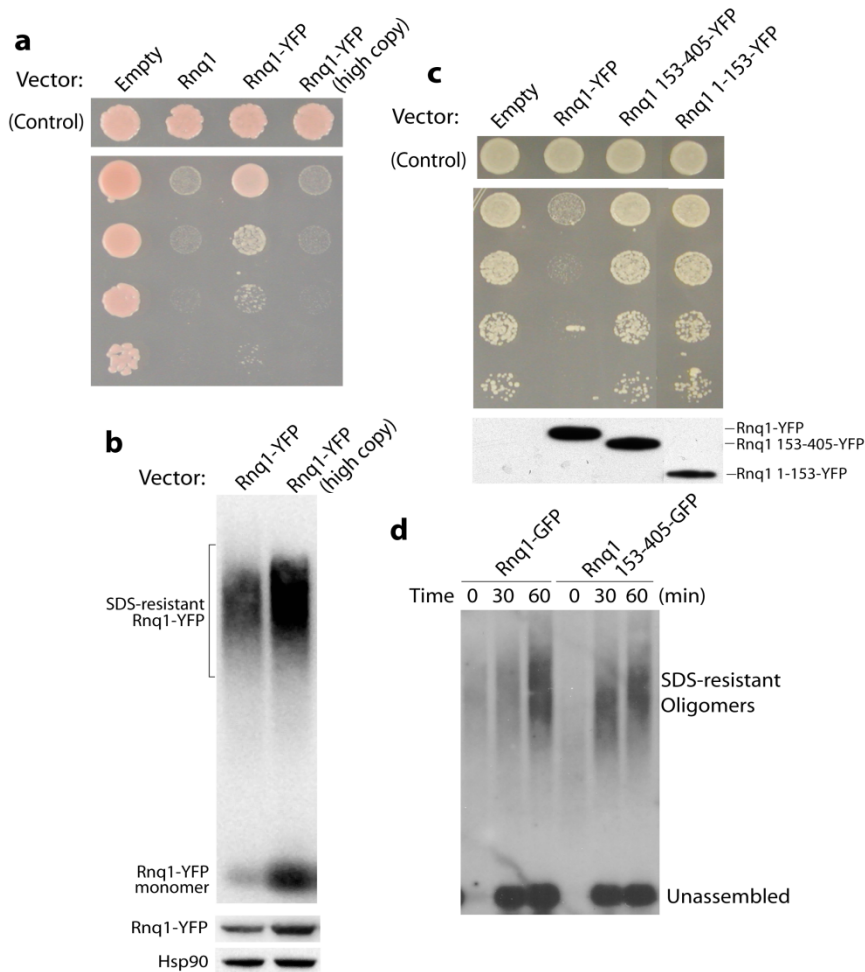


Figure 2.2 Factors influencing Rnq1 toxicity include the expression level and presence of a carboxy-terminal tag. (a) Comparison of the toxicity of untagged Rnq1 to Rnq1-YFP that is expressed at different levels. **(b)** SDD-AGE analysis of the assembly status of Rnq1-YFP expressed from low and high copy expression vectors. The bottom panel represents Western blots depicting Rnq1-YFP levels in the indicated extracts. **(c)** The effect on growth of $[RNQ^+]$ yeast caused by overexpression of full length and truncated Rnq1-YFP fusion. Rnq1 1-153 corresponds to the Rnq1 N-terminal non-prion forming domain. Rnq1 154-405 corresponds to the Rnq1 C-terminal prion forming domain. Spots that contain 10-fold serial dilutions of indicated yeast strains were positioned horizontally across the plate. The lower panel is a western blot of cell extracts that express the indicated YFP fusion with GFP anti-sera. **(d)** SDS-resistance of Rnq1-GFP or PrD-GFP fusions expressed under control of the CUP1 promoter as analyzed by SDD-AGE.

Sup35, expression of Rnq1's non-prion-forming domain does not rescue the toxicity caused by Rnq1 overexpression (data not shown).

The Hsp40 Sis1 Can Suppress Rnq1 Toxicity

Sis1, an essential Hsp40 chaperone, is required for the propagation of the $[RNQ^+]$ prion state (Sondheimer et al., 2001). Sis1 specifies Hsp70 function and is required for protein synthesis, protein folding, and cell stress protection (Fan et al., 2004; Zhong et al., 1996). Overexpressing Sis1 by as little as 3-fold strongly suppressed Rnq1 toxicity (Figure 2.3a). To examine whether other chaperones were capable of suppressing Rnq1 toxicity, an expression library of 4,954 yeast genes was screened (Cooper et al., 2006). Sis1 was the only chaperone in this library able to protect from Rnq1 toxicity (data not shown). This library includes, among many other chaperones, Ydj1, which is a member of the large Hsp40 family that is closely related to Sis1. It also includes Hsp70 Ssa1 (Hsp70) and Hsp104, which assist in shearing $[RNQ^+]$ prions to form seeds required for the propagation of the $[RNQ^+]$ state (Aron et al., 2007). Therefore, the effect of Sis1 on the toxicity of Rnq1 overexpression is unique.

Sis1 not only promotes $[RNQ^+]$ prion formation, but it remains stably bound to the prion in a 1:1 complex (Lopez et al., 2003). This finding could provide an explanation for the toxicity of overexpressed Rnq1: Elevation of $[RNQ^+]$ prion levels could kill cells by sequestering Sis1 away from its essential substrates. But this explanation is unlikely because cells in which Sis1 is depleted by nearly 100-fold grow for extended time periods and exhibit delayed lethality (Luke et al., 1991). In contrast, cells start to die within 4 h of the induction of Rnq1 overexpression.

To directly eliminate the possibility that cell death is due to the sequestration of Sis1, we deleted the domain of Sis1 that is required for interaction with the prion, the glycine- and phenylalanine-rich (G/F) region (Lopez et al., 2003). A Sis1 Δ G/F variant fails to promote the propagation of $[RNQ^+]$, but can carry out Sis1's essential functions. We overexpressed Sis1 Δ G/F and found that, unlike Sis1, it could not suppress Rnq1 toxicity (Figure 2.3a).

Sis1-Mediated Amyloid Formation Protects from Rnq1 Toxicity

The toxicity produced by the overexpression of Rnq1 represents a dominant gain of function that requires endogenous Rnq1 protein to be in a $[RNQ^+]$ prion conformation. It may be Sis1's ability to facilitate $[RNQ^+]$ prion propagation that ameliorates Rnq1 toxicity. Indeed, the suppression of Rnq1 toxicity by Sis1 overexpression was accompanied by a substantial increase in the formation of SDS-resistant $[RNQ^+]$ amyloids (Figure 2.3b). This seemed to be accompanied by a decrease in the pool of unassembled SDS-sensitive Rnq1. We have found, however, that although SDD-AGE is a reliable method for quantitatively detecting SDS-resistant species, it is not reliable for SDS-soluble species. To examine SDS-soluble species, we used gel-filtration chromatography. As shown in Figure 2.3c, a large pool of unassembled Rnq1-YFP accumulated on Rnq1-YFP overexpression (Figure 2.3c, compare *Top* and *Middle*). Suppression of Rnq1 toxicity by Sis1 correlated with a dramatic decrease in unassembled Rnq1-YFP pools and a corresponding increase in the pools of assembled forms (Figure 2.3c, compare *Middle* and *Bottom*). These results suggest that cytotoxic Rnq1 conformers accumulate when levels of Rnq1 protein exceed the cell's capacity to efficiently promote

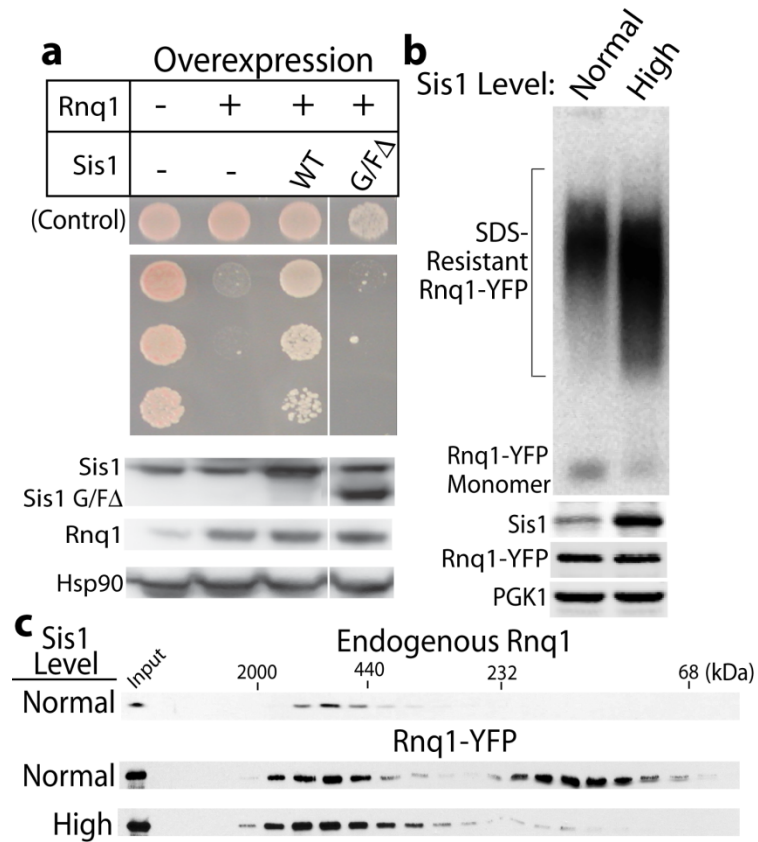


Figure 2.3 Sis1 overexpression protects against Rnq1 toxicity. (a) The effect of Sis1 or Sis1 Δ G/F overexpression on Rnq1 toxicity. **(b)** The effect of Sis1 overexpression on the formation of SDS-resistant [RNQ^+] conformers as determined by SDD-AGE. **(c)** Gel filtration analysis of intracellular pools of overexpressed Rnq1-YFP. The lower panels in **a** and **b** represent Western blots of the indicated proteins.

the template-driven formation of the SDS-resistant $[RNQ^+]$ prion species. To test this hypothesis, we asked whether Rnq1 toxicity would be exacerbated when the efficiency of $[RNQ^+]$ amyloid assembly was reduced.

Identification of the Sis1-Binding Site in Rnq1

First, we identified and mutated the chaperone-binding motif that Sis1 uses to interact with Rnq1. A peptide array was created that contained 25 residue *N*-acetylated peptides spanning the entire Rnq1 amino acid sequence. This array was incubated with purified Sis1 and washed, and Sis1-interacting peptides were identified by western blot after transfer of bound chaperone to nitrocellulose (Figure 2.4*b* and 2.5*a*). Tight binding of Sis1 was observed only with a few neighboring Rnq1 peptides, and these peptides were located in the non-prion-forming domain.

The amino acid sequence of this region is conserved in all known Rnq1 homologues and contains a classic, hydrophobic, chaperone-binding motif, LGKLALL (Figure 2.5*b* and Figure 2.4*a*) (Rudiger et al., 2001). Hsp40 proteins stimulate the binding of their Hsp70 cochaperones to specific substrates. Indeed, Sis1 stimulated binding of its Hsp70 cochaperone, Ssa1, to the peptides containing this motif in an ATP-dependent manner (Figure 2.4*b*). Thus, Sis1 forms a functional chaperone:substrate complex with peptides containing this chaperone-binding motif.

Next, to reduce the efficiency of Sis1's interaction with $[RNQ^+]$ prions, we replaced hydrophobic leucine residues in the Rnq1 chaperone-binding motif with alanines (L91A, L94A, and L97A). As demonstrated by coimmunoprecipitation, the capacity of

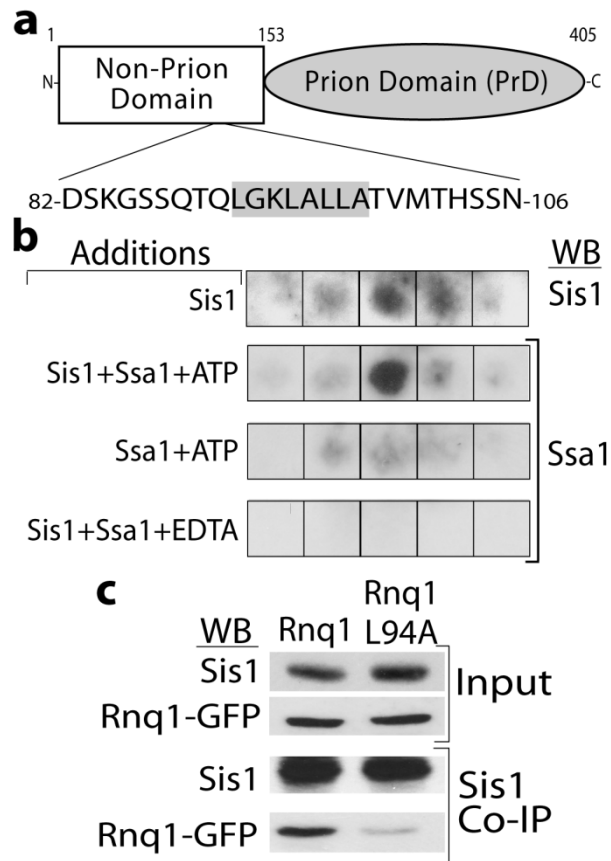


Figure 2.4 Sis1 binding to a conserved chaperone-binding motif in the non-prion domain of Rnq1. **(a)** A schematic showing the domain structure of Rnq1. The underlined region in non-prion domain of Rnq1 represents a chaperone binding motif identified via screening a cellulose peptide array (see Fig. S2). **(b)** Sis1 dependent binding of Hsp70 Ssa1 to the peptide in the Rnq1 peptide array that is bound most strongly by Sis1. **(c)** Mutation of L94A in the chaperone-binding motif reduces the ability of Sis1 to form co-immunoprecipitable complexes with Rnq1-GFP in $[RNQ^+]$ cells. Levels of the indicated proteins in c were visualized by western blot analysis (WB).

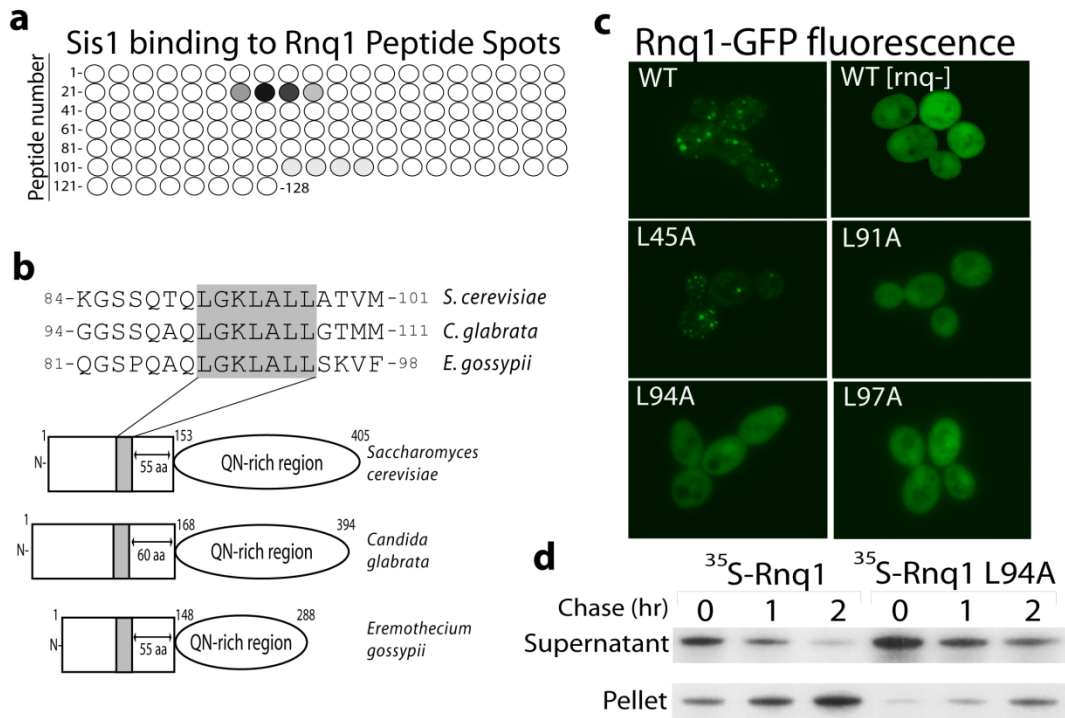


Figure 2.5 Mutation of the chaperone-binding motif slows the rate of Rnq1 assembly into $[RNQ^+]$ prions. (a) Peptide spots in a 25-residue Rnq1 peptide array that were bound by purified Sis1. Shown is a schematic of the Rnq1 peptide array in which circles represent the peptide spots starting at amino acid 1 of Rnq1 and sequentially shift in register by 3 amino acids until the terminal peptide. Filled circles represent peptide spots where Sis1 binding could be detected as significant levels above background. The darkness of the spots correlates with the intensity of Sis1 binding signal. **(b)** Comparison of the Sis1 binding site in Rnq1 with similar regions in the two known Rnq1 homologs from *C. glabrata* and *E. gossypii*. The hydrophobic core within the peptide identified in **b** is conserved between species both in sequence as well as in proximity to the carboxy-terminal, Q/N rich prion-forming domain. The term aa is an abbreviation for amino acid. **(c)** Fluorescence microscopy of live $[RNQ^+]$ cells after the indicated form of Rnq1-GFP was expressed for 1 hr. **(d)** Pulse-Chase analysis of the assembly of nascent Rnq1 into pelletable $[RNQ^+]$ prions. $[RNQ^+]$ cells were labeled with ^{35}S -translabel. At the indicated times cells were lysed and fractionated by centrifugation with an airfuge. Rnq1-GFP present in supernatant and pellet fractions of cell extracts was then isolated by immunoprecipitation with α -GFP sera.

Rnq1-GFP to interact with Sis1 was strongly, but not completely, reduced by these mutations (Figure 2.4c and data not shown).

Mutations in the Sis1-Binding Site of Rnq1 Interfere with $[RNQ^+]$ Amyloid Assembly

To determine whether the Rnq1 chaperone-binding motif mutants were defective in the assembly of $[RNQ^+]$ amyloid, we expressed them as Rnq1-GFP fusions from an extrachromosomal plasmid in cells expressing WT Rnq1 in its prion state. The L91A, L94A, and L97A mutations were expressed at levels similar to those of WT Rnq1 by using the CUP1 promoter, but they had a reduced capacity to form fluorescent foci (Figure 2.5c). An L45A mutation, which also is located in the non-prion-forming domain, but lies outside of the chaperone-binding motif, had no detectable effect on the assembly of $[RNQ^+]$ prions. Further, a time-course analysis by SDD-AGE (Figure 2.6a) and pulse-chase (Figure 2.5d) revealed that the rate at which newly synthesized Rnq1-GFP protein was converted into SDS-resistant conformers *in vivo* was reduced several fold by the L94A mutation in comparison with the WT protein. In addition, *in vitro*-purified Rnq1 L94A could be templated by prion “seeds” present in $[RNQ^+]$ cell extracts to form SDS-resistant species (Figure 2.6b). However, it was templated and converted to an SDS-resistant form with lower efficiency than the WT Rnq1 protein.

Finally, we asked whether the impairment of Rnq1 amyloid assembly increased the toxicity of Rnq1 overexpression. As we hypothesized, Rnq1 L94A was more toxic than WT Rnq1 when overexpressed in $[RNQ^+]$ cells (Figure 2.6c). A triple mutant, Rnq1

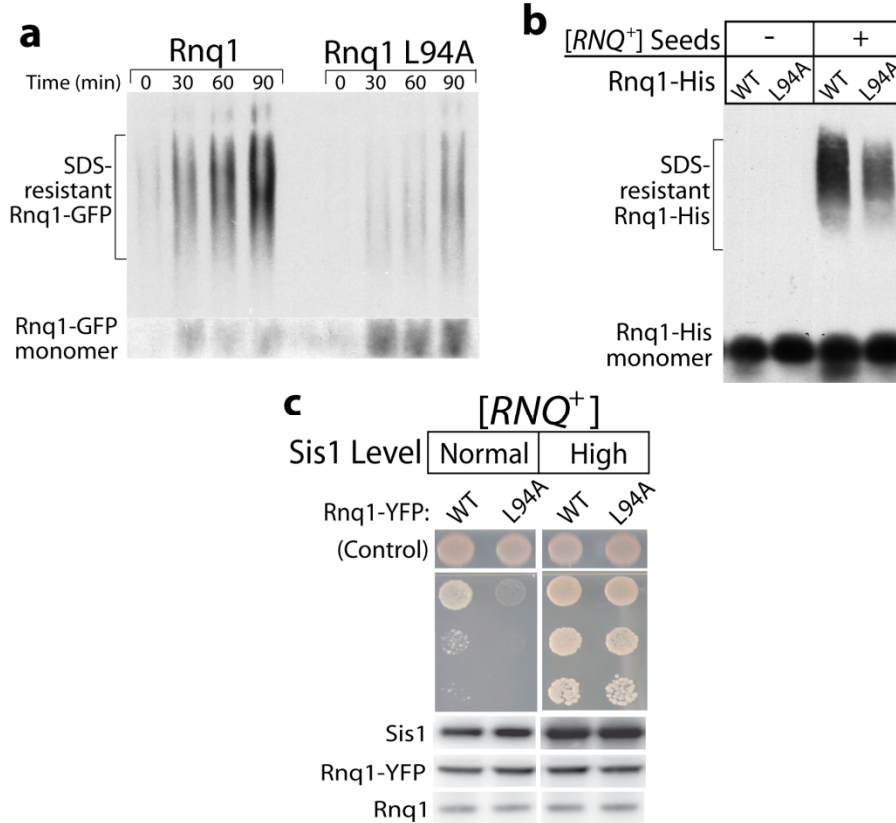


Figure 2.6 Mutations in the chaperone-binding motif of Rnq1 reduce the efficiency of [RNQ⁺] amyloid assembly. (a) Kinetics of Rnq1-GFP L94A assembly into SDS-resistant aggregates in [RNQ⁺] yeast determined by SDD-AGE. **(b)** [RNQ⁺] seed dependent assembly of purified Rnq1-His and Rnq1-His L94A into SDS-resistant amyloid. **(c)** Growth of 10 fold serial dilutions of [RNQ⁺] strains in which WT or L94A Rnq1 was overexpressed from the GAL1 promoter. Where indicated, Sis1 was overexpressed from the GPD promoter. Lower panels show the relative expression level of the specified proteins as determined by Western blot.

L94A–L96A–L97A, was even more toxic than Rnq1 L94A (data not shown). As expected from the fact that the Rnq1 L94A mutation impaired, but did not eliminate, interaction with Sis1, the overexpression of Sis1 3-fold was still able to suppress the toxicity of the mutant protein (Figure 2.6c).

Thus far, we have shown that interfering with the assembly of Rnq1 into the $[RNQ^+]$ amyloid state is extremely toxic. Toxicity occurs when Rnq1 expression is higher than normal (Figures 2.1, 2.2 and 2.3) or when mutations in Rnq1 interfere with the efficiency of Sis1 interaction (Figures 2.4, 2.5 and 2.6). In addition, depletion of Sis1 from the cytosol reduces the efficiency of $[RNQ^+]$ prion assembly and exacerbates Rnq1 toxicity (Figure 2.7). These collective data indicate that the efficient conversion of native Rnq1 into its SDS-resistant amyloid form prevents the accumulation of a toxic Rnq1 conformer.

Suppression of Rnq1 Toxicity by Sis1 Requires $[RNQ^+]$ Prion Assembly

Rnq1 L94A exhibits a higher propensity than WT Rnq1 to form SDS-soluble aggregates when $[RNQ^+]$ assembly is impeded via depletion of Sis1 (Figure 2.7). The inability of cells to maintain Rnq1 L94A in a soluble state correlates with the enhanced toxicity of the L94A mutant. In this sense, Rnq1 L94A is similar to alleles of amyloidogenic proteins whose subtle defects in folding kinetics cause devastating protein conformational diseases (Carrell and Lomas, 1997). Thus, we wondered whether Rnq1 L94A would assume a toxic conformation in the absence of templating by $[RNQ^+]$ prion seeds. Indeed, the overexpression of Rnq1 L94A, but not WT Rnq1, was toxic in $[rnq^-]$

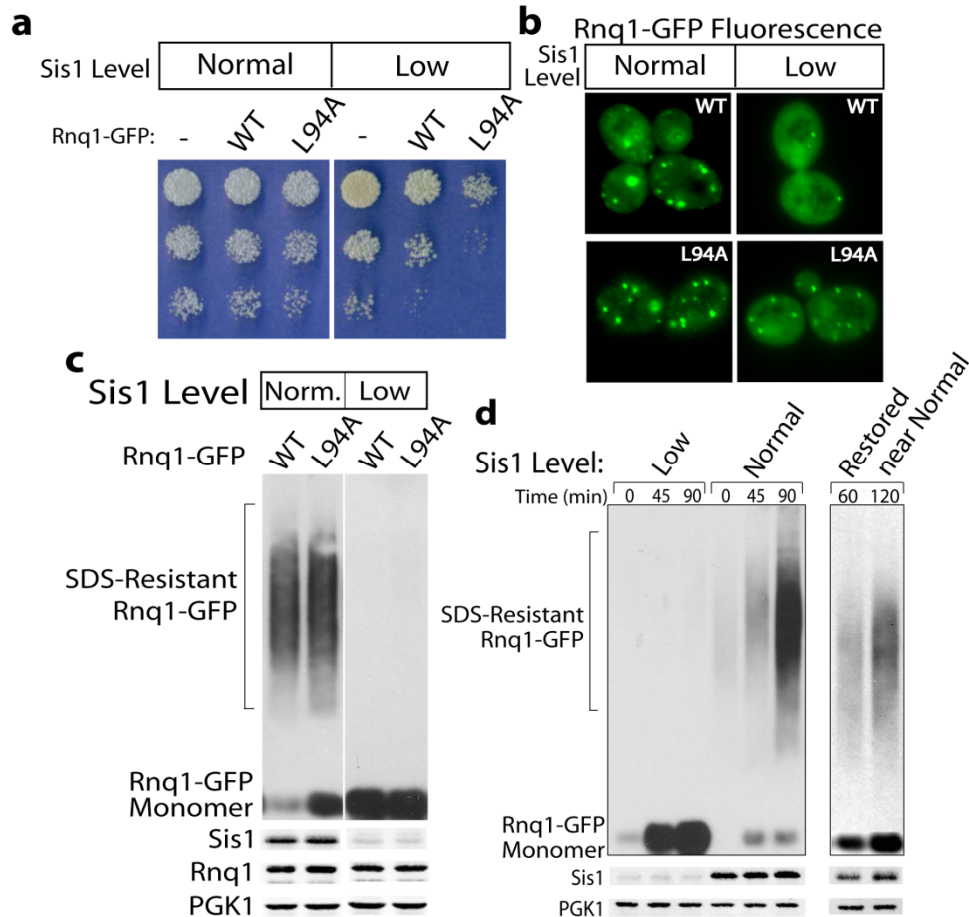


Figure 2.7 Depletion of Sis1 hinders assembly of nascent Rnq1-GFP into SDS-resistant $[RNQ^+]$ aggregates. (a) The influence of Rnq1-GFP and Rnq1-GFP L94A overexpression on cell viability when Sis1 levels are normal or low. A $[RNQ^+]$ $\Delta sis1$ strain that harbored pGAL1-*SIS1* was grown on plates that contained galactose or glucose as the carbon source to maintain Sis1 at normal or low levels. Rnq1-GFP and Rnq1-GFP L94A were expressed from the CUP1 promoter in the presence of 500 μ M CuSO₄. Sis1 was depleted from $\Delta sis1$ that was maintained pGAL1-*SIS1* from galactose to glucose medium. Consistent with a previous report (Luke et al., 1991), the near complete depletion of Sis1 did not cause yeast to exhibit growth defects on its own, but it did exacerbate Rnq1-GFP cytotoxicity. Further, this effect was far more severe for the L94A mutant than for wild-type Rnq1. (b) Coalescence of Rnq1-GFP and Rnq1-GFP L94A into foci in Sis1 depleted cells. (c) SDD-AGE analysis of Rnq1-GFP and Rnq1-GFP L94A assembly into SDS-resistant conformers at normal and low Sis1 levels. The lower panels depict levels of the indicated proteins as determined by Western blot. These data demonstrate that the foci formed by Rnq1 L94A under toxic conditions are sensitive to SDS-treatment, and thus, do not appear to represent $[RNQ^+]$ prions. (d) Restoration of $[RNQ^+]$ prion formation in Sis1 depleted cells upon reintroduction of normal Sis1 expression. Bottom panels depict Sis1 and PGK1 levels in the indicated extracts as determined by western blot. Data in panel (d) indicate that defects in the assembly of Rnq1 and Rnq1 L94A into SDS-resistant species observed upon depletion of Sis1, are not resultant from curing $[RNQ^+]$ prion seeds from cells.

strains (Figure 2.8a). Hence, a small amino acid substitution can cause Rnq1 to be toxic even in the absence of $[RNQ^+]$ amyloid formation.

Sis1-dependent $[RNQ^+]$ amyloid formation appears to protect cells from toxicity caused by the overexpression of Rnq1. If amyloid formation is a critical aspect of Sis1's ability to suppress Rnq1 toxicity, then Sis1 overexpression should not protect $[rnq^-]$ cells from Rnq1 L94A-mediated death because these cells lack the $[RNQ^+]$ prion seeds required for amyloid assembly. Indeed, overexpression of Sis1, which binds Rnq1 L94A with reduced efficiency, protected $[RNQ^+]$, but not $[rnq^-]$, strains from Rnq1 L94A toxicity. This finding further confirms that Rnq1 toxicity is not caused by the sequestration of Sis1 into $[RNQ^+]$ prion complexes. Furthermore, the presence of the $[RNQ^+]$ prion assembly pathway and Sis1 overexpression are both required for the suppression of Rnq1 toxicity.

Rnq1 L94A Does Not Form Prion Amyloids in $[rnq^-]$ Cells

To rule out the possibility that Rnq1 L94A assembled into $[RNQ^+]$ prions spontaneously in $[rnq^-]$ cells, we compared its assembly status to that of WT Rnq1 in $[rnq^-]$ strains (Figure 2.8b–e). In $[rnq^-]$ cells, Rnq1 L94A exhibited a higher propensity than WT Rnq1 to coalesce into foci (Figure 2.8b). Gel-filtration chromatography showed that Rnq1 L94A formed high-molecular-weight aggregates in these cells (Figure 2.9). Notably, these aggregates were not SDS-resistant and (Figure 2.8c) were unable to bind the amyloid indicator thioflavin-T (Figure 2.8d). Thus, Rnq1 toxicity is not related to the accumulation of excess pools of $[RNQ^+]$ amyloid and may be caused by a SDS-soluble Rnq1 species.

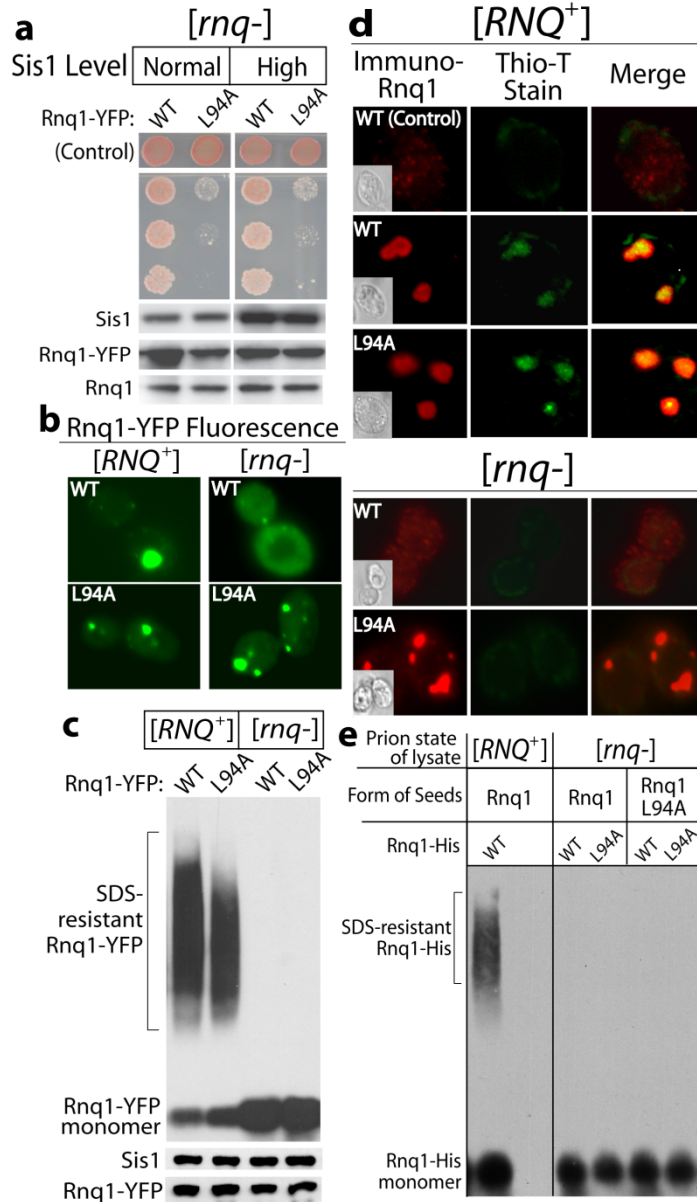


Figure 2.8 Rnq1 L94A toxicity and assembly status in [rnq-] yeast. (a) Growth of 10 fold serial dilutions of [rnq-] strains in which WT or L94A Rnq1 was overexpressed from the GAL1 promoter. Sis1 was overexpressed from the GPD promoter. **(b)** Fluorescent foci formed by Rnq1-YFP and Rnq1-YFP L94A in [RNQ⁺] and [rnq-] cells. **(c)** SDD-AGE analysis of aggregates formed by Rnq1-YFP and Rnq1-YFP L94A in [RNQ⁺] and [rnq-] cells. **(d)** Thioflavin-T staining of untagged Rnq1 and Rnq1 L94A in [RNQ⁺] and [rnq-] cells. Fixed yeast were decorated with α -Rnq1 sera that was detected with a fluorescent secondary antibody. The same cells were simultaneously stained with the amyloid indicator dye, thioflavin-T. **(e)** Cell extracts from [rnq-] cells overexpressing either Rnq1 or Rnq1 L94A were incubated with purified Rnq1-His or Rnq1-His L94A. The assembly status of purified Rnq1-His was determined by SDD-AGE. As a control, the assembly status of purified Rnq1-His incubated with [RNQ⁺] cell extract was also determined. Lower panels in **(a)** and **(b)** are western blots of cell extracts.

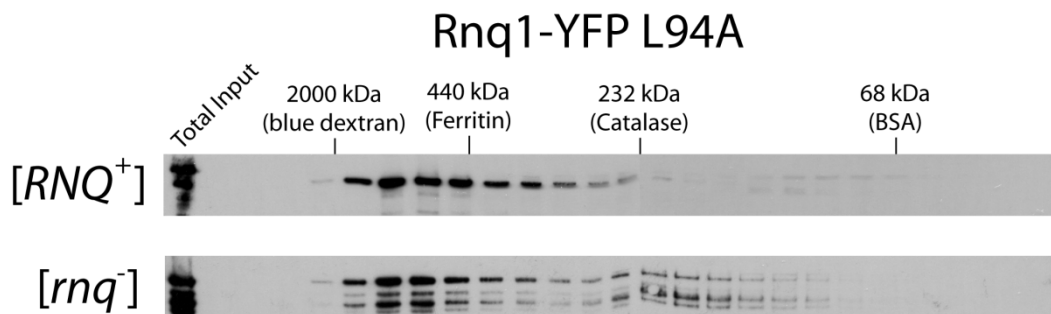


Figure 2.9 Analysis of the mobility of Rnq1 L94A in extracts from $[RNQ^+]$ and $[rnq^-]$ strains by gel filtration chromatography. Rnq1-YFP L94A was expressed from the GAL1 promoter for 4 hrs in the indicated strain. Extracts were prepared under native buffer conditions and loaded onto a Superose 12S column. The mobility of Rnq1-YFP L94A was determined with Western blot of column fractions with anti-GFP sera.

Because small prion seeds in the form of detergent-soluble prefibrillar species could have escaped detection by SDD-AGE and thioflavin-T staining, we applied another test for the existence of such forms of Rnq1 L94A in [*rnq*⁻] cell extracts (Figure 2.8e). Prion seeds in cell extracts can be sensitively detected through their ability to catalyze the conversion of exogenously added native prion protein into SDS-resistant amyloids. Prion seeds were readily detected in lysates of [*RNQ*⁺] cells overexpressing Rnq1 L94A (Figure 2.6b). However, extracts of [*rnq*⁻] cells that contained toxic levels of Rnq1 L94A failed to seed assembly of purified His-Rnq1 or His-Rnq1-L94A into SDS-resistant amyloids (Figure 2.8e).

The Rnq1 L94A assemblies in [*rnq*⁻] cells fail to meet three classification standards of [*RNQ*⁺] amyloid. They are SDS-soluble, they do not stain with thioflavin-T, and they do not seed polymerization of soluble Rnq1 protein. Rnq1 L94A is more lethal than Rnq1 and can assume a toxic conformation in the absence of [*RNQ*⁺] templates. Rescue from Rnq1 L94A toxicity requires Sis1 overexpression and active propagation of the [*RNQ*⁺] prion. Therefore, it appears that the conversion of Rnq1 L94A to [*RNQ*⁺] amyloid prevents the accumulation of toxic Rnq1 conformer whose true nature remains obscure.

2.4 Discussion

Our data suggest a model in which efficient chaperone-dependent conversion of soluble Rnq1 into SDS-resistant $[RNQ^+]$ amyloid is critical to prevent the formation of other toxic Rnq1 conformers. We demonstrate that toxic Rnq1 conformers accumulate in a nonamyloid form when $[RNQ^+]$ assembly is made inefficient by multiple means. We propose that nonproductive templating of Rnq1 monomers by $[RNQ^+]$ seeds predisposes Rnq1 to leave the amyloid pathway and accumulate as a toxic species, whose exact nature is not yet clear. Templating of native proteins to form amyloid is a basic feature of amyloidogenesis, and we suggest that inefficiencies in this process contribute to the proteotoxicity associated with certain protein conformational diseases. This templating model explains how amyloid formation can serve a protective function, whereas the $[RNQ^+]$ prion state is a prerequisite for toxicity of the WT Rnq1 protein.

One of Sis1's functions in $[RNQ^+]$ prion propagation appears to be promoting the shearing of $[RNQ^+]$ amyloid fibers into smaller pieces, thereby creating new surfaces to more efficiently seed the assembly of the prion (Aron et al., 2007). This reaction also requires Hsp104 and Hsp70. Hence, binding of Sis1 to the non-prion-forming domain of full-length Rnq1 may help facilitate this shearing process. However, because overexpression of Hsp70 and Hsp104 does not suppress Rnq1 toxicity, Sis1 may have additional functions in $[RNQ^+]$ prion propagation that do not overlap with those of other chaperones. Sis1 stably associates with assembled $[RNQ^+]$ conformers in a 1:1 molar ratio (Lopez et al., 2003). Therefore, Sis1's binding to the non-prion-forming domain has the potential to stabilize $[RNQ^+]$ prions in a conformation that is optimal for efficient amyloid fibril growth.

Many neurodegenerative diseases involve the accumulation of intracellular and/or extracellular amyloid protein aggregates. In the past, these amyloid aggregates were thought to be the cytotoxic, disease-causing protein conformer. However, recent studies have begun to question this view. As one striking example in mice, deletion of the GPI anchor of the prion protein PrP leads to massive extracellular amyloid plaque formation in mice injected with infective scrapie, but causes no overt clinical manifestations of scrapie (Chesebro et al., 2005). Furthermore, it has been suggested that neurodegenerative diseases are caused by the ability of very different proteins to adopt common toxic nonamyloid conformers such as protofibrils or soluble oligomers (Caughey and Lansbury, 2003; Haass and Selkoe, 2007). Hence, amyloid formation may serve to convert oligomeric amyloid precursors into a highly stable, nontoxic form (Piccardo et al., 2007).

Although amyloid is not toxic, its interaction with soluble protein forms could give rise to pathogenic species via nonproductive templating. Case in point, when GPI-anchorless PrP was expressed together with WT PrP, it accelerated scrapie disease and resulted in increased deposits of both amyloid and nonamyloid proteinase K-resistant PrP (Chesebro et al., 2005). Similarly, in yeast, the toxicity of Huntington exon 1 depends on the $[RNQ^+]$ prion state (Duennwald et al., 2006a; Meriin et al., 2002). This concept may even extend to the heterokaryon incompatibility mediated by the [Het-s] prion in *Podospora anserina* (Coustou-Linares et al., 2001). HET-s in its prion form only leads to cell death when coexpressed with the HET-S allele that cannot form amyloid. Templating of the nonamyloidogenic HET-S protein by [Het-s] prion seeds could lead to the

formation of a toxic species, whereas templating of HET-s protein would result in the nontoxic prion amyloid species.

The aggregation state and the toxicity of aggregation-prone proteins are strongly modulated by host factors such as Hsp70 and its associated cochaperones, but the mechanisms for chaperone function in this process are just being defined (Muchowski and Wacker, 2005). Molecular chaperones generally act to antagonize protein aggregation. Yet our observations that the chaperone-dependent assembly of amyloid conformers can be cytoprotective provide a different view of the effects of chaperones in conformational disease. Thus, molecular chaperones can antagonize protein toxicity in conformational disorders by two different mechanisms: They can solubilize misfolded proteins or aid in sequestering them into benign, amyloid-like species. The most central aspect of antagonizing toxicity of misfolded proteins appears to be preventing accumulation of the detergent-soluble misfolded species, rather than preventing the formation of amyloid conformers.

2.5 Materials and methods

Strains and Plasmids. W303, *MATa can1-100 ade2-1, his3-11,15 leu2-3,112 ura3-1 trp1-1*; W303 Δ *rnq1*, *MATa can1-100 ade2-1 his3-11,15 leu2-3,112 ura3-1 trp1-1 \Delta**rnq1:KanMX4*; 74D-694, *MATa ade1-14 trp1-289 his3\Delta-300 ura3-52 leu2-3,112*; W303 Δ *sis1*, *MATa ade2-1 his3-11,15 leu2-3,112 ura3-1 trp1-1 ssd1-d2 sis1::HIS* pRS316-SIS1. All the above strains harbored Rnq1 in its [RNQ⁺] form and the generation of isogenic [*rnq-*] strains was accomplished via sequential passage of cells on plates containing 3 mM guanidinium-HCl (Eaglestone et al., 2000). W303 and 74D-694 strains were utilized to take advantage of the different markers or gene deletions. Identical results were obtained in studies carried out with both of these strains, so Rnq1 toxicity is not strain specific.

Strains were transformed with plasmids and cultured in synthetic media as previously described (Caplan and Douglas, 1991). Plasmids that express the indicated protein under control of the GAL1 promoter include pRS416-*RNQ1*, pRS416-*RNQ1-YFP*, and pYES3-*SIS1*, termed pGAL1-*SIS1*. Plasmids that express *RNQ1* under control of the CUP1 promoter include pRS316-*RNQ1-GFP*, pRS315-*RNQ1-GFP*. The glyceraldehyde-3-phosphate dehydrogenase (GPD) promoter controlled expression of *SIS1* in pRS414-*SIS1* and pRS414-*sis1\Delta**g/f*. The QuikChange site-directed mutagenesis kit (Stratagene) was used to create the indicated point mutations in *RNQ1*.

Analysis of Rnq1 cytotoxicity. W303 strains harboring pRS416-*RNQ1* or pRS416-*RNQ1-YFP* were grown overnight in synthetic drop-out media containing 2% raffinose before 5-fold serial dilutions were spotted on plates containing either 2% galactose or

glucose. Alternatively, strains that harbored pRS316-*RNQ1-GFP* or pRS315-*RNQ1-GFP* were cultured overnight in synthetic media containing glucose before serial dilutions were spotted on agarose plates that contained 500 μ M CuSO₄. Plates were incubated for 3-5 days at 30 °C and then photographed.

Screening of a Rnq1 peptide array. A 25mer Rnq1 cellulose bound peptide array was prepared by automated spot synthesis (Jerini Peptide Technologies). The array was screened according the manufactures instructions with 100 nM Sis1 or Hsp70 Ssa1 in the presence or absence of 1 mM EDTA or Mg-ATP. Bound chaperones were transferred to a nitrocellulose membrane and the peptide spots were identified by western blot. Hsp70 Ssa1 bound a number of different peptides that contained clusters of hydrophobic amino acids (data not shown), yet peptides 27-30 were the only peptides that Sis1 bound reproducibly with high affinity. In addition, peptide 28, which contains residues 82-106 of Rnq1, was the only peptide that was bound by Hsp70 Ssa1 in a Sis1 and ATP dependent manner (Figure 2.5).

Pulse-chase analysis of [*RNQ*⁺] prion formation. 74D-694 cultures were grown overnight in synthetic media and then diluted and starved in methionine free media. Log phase cultures were first supplemented with 50 μ M CuSO₄ to induce Rnq1-GFP or Rnq1-GFP L94A expression for 1 hr before the addition of Trans³⁵S-label (100 μ Ci/ml). Cultures were labeled for 10 min, then 1 mg/ml of cold methionine was added and cells were washed. Cultures were incubated for the indicated time period at 30°C before samples were collected. Cell lysis was achieved by glass bead disruption in a buffer

composed of 50 mM Hepes pH 7.4, 150 mM NaCl, 1 mM EDTA, 0.1% Tween-20, 2 mM phenylmethanesulfonyl fluoride and a protease inhibitor cocktail mixture. Cell debris was removed and the resulting lysate was spun at 4 °C at $165,000 \times g$ for 45 min in a TLA-100 rotor (Beckman Coulter). Rnq1-GFP present in the supernatant and pellet fractions was then immunoprecipitated with α -GFP (Roche) in the presence of 0.1% SDS. ^{35}S -labeled proteins in immunoprecipitates were resolved by SDS-PAGE and detected by autoradiography.

Analysis of $[\text{RNQ}^+]$ prion formation by fluorescence microscopy. To examine the assembly of newly synthesized Rnq1 into of $[\text{RNQ}^+]$ prions Rnq1-GFP expression was induced from the CUP1 promoter by the addition of 50 μM CuSO_4 to log-phase cultures and live cells were photographed 1 hr later. To examine the aggregation pattern of Rnq1, Rnq1-GFP or Rnq1-YFP under condition where growth defects are observed, protein expression under control of the CUP1 or GAL1 promoter was induced by the addition of either 500 μM CuSO_4 or 2% galactose, respectively, and 4 hrs later live cells were photographed.

Indirect immunofluorescence of Rnq1 and thioflavin-T staining of Rnq1 aggregates were performed as follows. Log phase cells harboring pRS416-*RNQ1* that were cultured in synthetic raffinose media were supplemented with 2% galactose for 4 hrs to induce expression of either Rnq1 or Rnq1 L94A. Cells were fixed with 4% formaldehyde for 1 hr and washed twice in buffer containing 1.2 M sorbitol before being converted to spheroplasts via 45 min incubations at 30°C in the presence of 5 mg/ml zymolyase-20T. Cells were then permeabilized in phosphate buffer saline (PBS)

containing 0.1% Triton X-100 for 5 min. Cells were washed and incubated with PBS that contained 0.001% Thioflavin-T for 10 min. Next, thioflavin-T stained cells were washed 4 times and incubated in PBS containing 1.0% BSA and 0.025% Triton X-100. Blocked cells were then incubated with polyclonal rabbit α -Rnq1 (1:50 dilution) for 1 hr and then washed 4 times. Cells were then decorated with goat α -rabbit conjugated Texas Red (1:1000) second antibody (Molecular Probes). Decorated cells were spotted on glass slides and photographed with a Nikon fluorescence microscope and images were processed with Metamorph and Adobe Photoshop Software.

Semi-denaturing detergent agarose gel electrophoresis (SDD-AGE). Rnq1 assembly into SDS-resistant [RNQ^+] prions was monitored by SDD-AGE as previously described (Kryndushkin et al., 2003) with the following exceptions. Cells were lysed in buffer containing 2% SDS, 5% glycerol, 75 mM Tris-HCl pH 6.8, 2 mM EDTA, 8% 2-mercaptoethanol, 0.05% coomassie blue, 2 mM phenylmethanesulfonyl fluoride and a protease inhibitor cocktail (Roche). Proteins resolved by the 1.5% agarose gel were electrophoretically transferred to PVDF in a submerged transfer apparatus for 2 hrs at 24 V. PVDF membranes were then decorated with α -GFP and bands were visualized with ECL reagent.

Rnq1 co-immunoprecipitation. Expression of Rnq1-GFP in log phase cells harboring the indicated form of pRS316-Rnq1-GFP was induced by supplementation with 50 μ M $CuSO_4$. Cell extracts were prepared 1 hr later under the non-denaturing conditions described above for the pulse-chase analysis. Cell debris was removed by centrifugation

and the resulting supernatant was supplemented with either α -Sis1 or α -GFP. Samples were incubated at 4°C for 1 hr before being supplemented with pre-blocked protein G agarose beads. After 1 hr, the beads were isolated by centrifugation and washed 3 times with lysis buffer. Immunoprecipitated proteins were resolved by SDS-PAGE and detected by western blot.

Rnq1 toxicity and $[RNQ^+]$ assembly in Sis1 depleted cells. A strain in which Rnq1-GFP expression was controlled by the CUP1 promoter and Sis1 expression was controlled the GAL1 promoter was constructed by transforming W303 Δ *sis1* with pRS315-*Rnq1-GFP* and pGAL1-*SIS1*. To examine $[RNQ^+]$ toxicity at different Sis1 levels, strains were generated by the plasmid shuffle technique (Boeke et al., 1987) and then grown on synthetic drop-out plates containing 2% glucose. A single colony was picked, diluted into sterile H₂O and 5-fold serial dilutions were spotted onto plates containing either galactose or glucose in the presence of 500 μ M CuSO₄. To examine the effect that depletion of Sis1 had on $[RNQ^+]$ assembly, transformants grown on galactose plates were transferred to liquid media containing either glucose or galactose and cultured overnight at 30°C. Cells were then diluted and grown an additional 12 hrs. Rnq1-GFP expression was then induced by the addition of 500 μ M CuSO₄ and the formation of SDS-resistant $[RNQ^+]$ particles was measured by SDD-AGE. To demonstrate that Sis1 depleted cells were still capable of $[RNQ^+]$ prion assembly, Sis1 levels were restored by spotting cells cultured in glucose media back onto synthetic galactose plates. After the restoration of Sis levels, $[RNQ^+]$ assembly was monitored as described by SDD-AGE.

Seeded polymerization of purified Rnq1. His-Rnq1 WT and L94A were expressed from pDEST17 vector in BL21 cells for 4 hrs at 30 °C followed by lysis in a buffer that contained 6 M guanidium-HCl and 100 mM potassium phosphate buffer pH 7.0. His-Rnq1 was purified by standard techniques on Ni-NTA agarose that was washed with 8 M urea and 100 mM potassium phosphate buffer pH 7.0. His-Rnq1 was eluted with the same buffer at pH 3.0, concentrated by methanol precipitation and stored at -80 °C. Prior to use His-Rnq1 was resuspended in 6 M guanidium-HCl and filtered through a Microcon YM-100 spin-column. Yeast extracts containing [RNQ⁺] seeds were prepared as follows. The indicated form of Rnq1 was expressed from the GAL1 promoter for 4 hrs. Cells were isolated by centrifugation and extracts were created by bead disruption in buffer composed of 40 mM Hepes, pH 7.5, 150 mM KCL, 2 mM DTT, 5% glycerol, 8 mM PMSF, 10 mg/ml aprotinin, and 10 mg/ml leupeptin. An aliquot of purified Rnq1 was adjusted to a final concentration of 5 μM in cell lysate and incubated at 25 °C for 30 min, without agitation. Samples were then analyzed by SDD-AGE described above.

2.6 References

- Aron, R., T. Higurashi, C. Sahi, and E.A. Craig. 2007. J-protein co-chaperone Sis1 required for generation of [RNQ+] seeds necessary for prion propagation. *EMBO J.* 26:3794-803.
- Boeke, J.D., J. Trueheart, G. Natsoulis, and G.R. Fink. 1987. 5-Fluoroorotic acid as a selective agent in yeast molecular genetics. *Methods in Enzymology.* 154:164-75.
- Caplan, A.J., and M.G. Douglas. 1991. Characterization of YDJ1: a yeast homologue of the bacterial dnaJ protein. *J Cell Biol.* 114:609-21.
- Carrell, R.W., and D.A. Lomas. 1997. Conformational disease. *Lancet.* 350:134-8.
- Caughey, B., and P.T. Lansbury. 2003. Protofibrils, pores, fibrils, and neurodegeneration: separating the responsible protein aggregates from the innocent bystanders. *Annu Rev Neurosci.* 26:267-98.
- Cheng, I.H., K. Scarce-Levie, J. Legleiter, J.J. Palop, H. Gerstein, N. Bien-Ly, J. Puolivali, S. Lesne, K.H. Ashe, P.J. Muchowski, and L. Mucke. 2007. Accelerating amyloid-beta fibrillization reduces oligomer levels and functional deficits in Alzheimer disease mouse models. *J Biol Chem.* 282:23818-28.
- Chernoff, Y.O., S.L. Lindquist, B. Ono, S.G. Inge-Vechtomov, and S.W. Liebman. 1995. Role of the chaperone protein Hsp104 in propagation of the yeast prion-like factor [psi+]. *Science.* 268:880-4.
- Chesebro, B., M. Trifilo, R. Race, K. Meade-White, C. Teng, R. LaCasse, L. Raymond, C. Favara, G. Baron, S. Priola, B. Caughey, E. Masliah, and M. Oldstone. 2005. Anchorless prion protein results in infectious amyloid disease without clinical scrapie. *Science.* 308:1435-9.
- Chien, P., J.S. Weissman, and A.H. DePace. 2004. Emerging principles of conformation-based prion inheritance. *Annu Rev Biochem.* 73:617-56.
- Chiti, F., and C.M. Dobson. 2006. Protein misfolding, functional amyloid, and human disease. *Annu Rev Biochem.* 75:333-66.

- Cooper, A.A., A.D. Gitler, A. Cashikar, C.M. Haynes, K.J. Hill, B. Bhullar, K. Liu, K. Xu, K.E. Strathearn, F. Liu, S. Cao, K.A. Caldwell, G.A. Caldwell, G. Marsischky, R.D. Kolodner, J. Lobaer, J.C. Rochet, N.M. Bonini, and S. Lindquist. 2006. Alpha-synuclein blocks ER-Golgi traffic and Rab1 rescues neuron loss in Parkinson's models. *Science*. 313:324-8.
- Coustou-Linares, V., M.L. Maddelein, J. Begueret, and S.J. Saupe. 2001. In vivo aggregation of the HET-s prion protein of the fungus *Podospora anserina*. *Mol Microbiol*. 42:1325-35.
- Derkatch, I.L., M.E. Bradley, J.Y. Hong, and S.W. Liebman. 2001. Prions affect the appearance of other prions: the story of [PIN(+)]. *Cell*. 106:171-82.
- Derkatch, I.L., M.E. Bradley, S.V. Masse, S.P. Zadorsky, G.V. Polozkov, S.G. Inge-Vechtomov, and S.W. Liebman. 2000. Dependence and independence of [PSI(+)] and [PIN(+)] : a two-prion system in yeast? *EMBO J*. 19:1942-52.
- Derkatch, I.L., M.E. Bradley, P. Zhou, Y.O. Chernoff, and S.W. Liebman. 1997. Genetic and environmental factors affecting the de novo appearance of the [PSI+] prion in *Saccharomyces cerevisiae*. *Genetics*. 147:507-19.
- Duennwald, M.L., S. Jagadish, F. Giorgini, P.J. Muchowski, and S. Lindquist. 2006a. A network of protein interactions determines polyglutamine toxicity. *Proc Natl Acad Sci U S A*. 103:11051-6.
- Duennwald, M.L., S. Jagadish, P.J. Muchowski, and S. Lindquist. 2006b. Flanking sequences profoundly alter polyglutamine toxicity in yeast. *Proc Natl Acad Sci U S A*. 103:11045-50.
- Eaglestone, S.S., L.W. Ruddock, B.S. Cox, and M.F. Tuite. 2000. Guanidine hydrochloride blocks a critical step in the propagation of the prion-like determinant [PSI(+)] of *Saccharomyces cerevisiae*. *Proc Natl Acad Sci U S A*. 97:240-4.
- Fan, C.Y., S. Lee, H.Y. Ren, and D.M. Cyr. 2004. Exchangeable chaperone modules contribute to specification of type I and type II Hsp40 cellular function. *Mol Biol Cell*. 15:761-73.

- Haass, C., and D.J. Selkoe. 2007. Soluble protein oligomers in neurodegeneration: lessons from the Alzheimer's amyloid beta-peptide. *Nat Rev Mol Cell Biol.* 8:101-12.
- Kayed, R., E. Head, J.L. Thompson, T.M. McIntire, S.C. Milton, C.W. Cotman, and C.G. Glabe. 2003. Common structure of soluble amyloid oligomers implies common mechanism of pathogenesis. *Science.* 300:486-9.
- Kryndushkin, D.S., I.M. Alexandrov, M.D. Ter-Avanesyan, and V.V. Kushnirov. 2003. Yeast [PSI+] prion aggregates are formed by small Sup35 polymers fragmented by Hsp104. *J Biol Chem.* 278:49636-43.
- Lindquist, S. 1997. Mad cows meet psi-chotic yeast: the expansion of the prion hypothesis. *Cell.* 89:495-8.
- Lopez, N., R. Aron, and E.A. Craig. 2003. Specificity of class II Hsp40 Sis1 in maintenance of yeast prion [RNQ+]. *Mol Biol Cell.* 14:1172-81.
- Luke, M.M., A. Sutton, and K.T. Arndt. 1991. Characterization of SIS1, a *Saccharomyces cerevisiae* homologue of bacterial dnaJ proteins. *J Cell Biol.* 114:623-38.
- Meriin, A.B., X. Zhang, X. He, G.P. Newnam, Y.O. Chernoff, and M.Y. Sherman. 2002. Huntington toxicity in yeast model depends on polyglutamine aggregation mediated by a prion-like protein Rnq1. *J Cell Biol.* 157:997-1004.
- Muchowski, P.J., and J.L. Wacker. 2005. Modulation of neurodegeneration by molecular chaperones. *Nat Rev Neurosci.* 6:11-22.
- Nakayashiki, T., C.P. Kurtzman, H.K. Edskes, and R.B. Wickner. 2005. Yeast prions [URE3] and [PSI+] are diseases. *Proc Natl Acad Sci U S A.* 102:10575-80.
- Nelson, R., M.R. Sawaya, M. Balbirnie, A.O. Madsen, C. Riek, R. Grothe, and D. Eisenberg. 2005. Structure of the cross-beta spine of amyloid-like fibrils. *Nature.* 435:773-8.
- Osherovich, L.Z., and J.S. Weissman. 2001. Multiple Gln/Asn-rich prion domains confer susceptibility to induction of the yeast [PSI(+)] prion. *Cell.* 106:183-94.

- Piccardo, P., J.C. Manson, D. King, B. Ghetti, and R.M. Barron. 2007. Accumulation of prion protein in the brain that is not associated with transmissible disease. *Proc Natl Acad Sci U S A*. 104:4712-7.
- Rudiger, S., J. Schneider-Mergener, and B. Bukau. 2001. Its substrate specificity characterizes the DnaJ co-chaperone as a scanning factor for the DnaK chaperone. *EMBO J*. 20:1042-50.
- Shorter, J., and S. Lindquist. 2005. Prions as adaptive conduits of memory and inheritance. *Nat Rev Genet*. 6:435-50.
- Sondheimer, N., and S. Lindquist. 2000. Rnq1: an epigenetic modifier of protein function in yeast. *Mol Cell*. 5:163-72.
- Sondheimer, N., N. Lopez, E.A. Craig, and S. Lindquist. 2001. The role of Sis1 in the maintenance of the [RNQ+] prion. *EMBO J*. 20:2435-42.
- Taneja, V., M.L. Maddelein, N. Talarek, S.J. Saupe, and S.W. Liebman. 2007. A non-Q/N-rich prion domain of a foreign prion, [Het-s], can propagate as a prion in yeast. *Mol Cell*. 27:67-77.
- Wickner, R.B. 1994. [URE3] as an altered URE2 protein: evidence for a prion analog in *Saccharomyces cerevisiae*. *Science*. 264:566-9.
- Zhong, T., M.M. Luke, and K.T. Arndt. 1996. Transcriptional regulation of the yeast DnaJ homologue SIS1. *J Biol Chem*. 271:1349-56.

Chapter Three

**Hsp40 dependent localization of $[RNQ^+]$ prions to the nucleus
reciprocally effects Rnq1 and Huntingtin toxicity**

3.1 Abstract

Cellular environment influences whether misfolded disease proteins are benign or toxic. Yet, how the cellular milieu impacts detoxification of disease proteins is unclear. Herein we demonstrate that interplay between chaperone systems, nucleocytoplasmic traffic, and protein interaction networks impacts the efficiency of benign aggregate formation and proteotoxicity. Increasing Hsp40 chaperone activity shifted the site of $[RNQ^+]$ prion assembly from the cytosol to the nucleus. Nuclear Rnq1 was less toxic as its assembly into benign $[RNQ^+]$ prions was more efficient. $[RNQ^+]$ prions are environmental factors that act via an ill-defined mechanism to promote toxicity of a huntingtin's protein exon-1 fragment with an expanded polyglutamine tract (Htt-103Q). $[RNQ^+]$ prions were found to form stable complexes with Htt-103Q, which enabled nuclear $[RNQ^+]$ prions to attract Htt-103Q from the cytosol to the nucleus. The efficiency of nuclear Htt-103Q assembly into SDS-resistant aggregates was dramatically reduced and this exacerbated Htt-103Q toxicity. Molecular chaperones directly and indirectly impact the cellular location of amyloid-like aggregate formation. This has a profound impact on proteotoxicity because the cytosol and nucleus have different capacities to package disease proteins into benign assemblies.

3.2 Introduction

Protein misfolding and accumulation of amyloid-like aggregates are the hallmarks of a broad class of protein conformational diseases, which include Alzheimer's Disease, frontotemporal dementia, spongiform encephalopathies and polyglutamine expansion diseases (Carrell and Lomas, 1997). Factors that initiate protein aggregation and disease onset include inheritance of a mutant protein, aberrant protein processing, expansion of glutamine or alanine-rich tracts of amino acids, and environmental stress (Chiti and Dobson, 2006). The amino acid sequence of individual, disease-causing proteins defines the neurodegenerative disorder as well as the affected brain regions. Though it is unclear why some neuronal populations are more vulnerable to toxicity while others are more apt to efficiently manage protein misfolding events (Taylor et al., 2002). The differential susceptibility of various neuronal subtypes to proteotoxicity indicates that the cellular environment plays a major role in dictating whether a misfolded disease protein is toxic (Balch et al., 2008).

The exact nature of the neurotoxic conformer formed by individual, disease proteins remains controversial (Caughey and Lansbury, 2003). Aggregates formed by disease proteins can sequester essential cellular proteins (Burke et al., 1996; Steffan et al., 2000) and/or inhibit the activity of the proteasome (Bence et al., 2001) and thereby cause cell death. Yet, the extent of disease protein aggregation does not always correlate with the observed pathology (Caughey and Lansbury, 2003; Haass and Selkoe, 2007) and small oligomers formed by disease proteins have been implicated as the toxic species (Haass and Selkoe, 2007; Kaye et al., 2003).

A primary mechanism to prevent the accumulation of toxic protein species is chaperone-dependent suppression of disease protein aggregation and subsequent degradation (Cohen et al., 2006; Muchowski and Wacker, 2005). Emerging evidence demonstrates that the conversion of disease proteins into ordered, benign aggregates also serves to prevent the accumulation of toxic protein oligomers (Behrends et al., 2006; Cheng et al., 2007). Paradoxically, the ability of disease proteins to assemble into ordered benign aggregates is critically dependent upon molecular chaperone action (Behrends et al., 2006; Douglas et al., 2008). Thus, molecular chaperones can protect against proteotoxicity by either suppressing or promoting protein aggregation.

Cell stress or subtle age-dependent changes in the activity of chaperone networks appear to enable pools of disease proteins to escape surveillance and accumulate as toxic conformers (Morimoto, 2008). Epigenetic factors control molecular chaperone expression and the capacity of chaperone networks in different cell types and subcellular compartments is variable (Balch et al., 2008; Morimoto, 2008). Therefore, selective vulnerability to conformational disease could result from differences in the neuron's ability to promote efficient flux of disease proteins through degradation and aggregation pathways.

The cytosol and nucleus have different capacities to buffer the presence of mutant disease proteins, but the mechanism behind this occurrence is unknown (Ross, 1997). For example, normal Huntingtin protein (Htt) contains a 25-residue polyglutamine (polyQ) sequence within exon I and predominately resides within the cytosol (De Rooij et al., 1996). Huntington's disease is caused by the expansion of the polyQ region in Htt beyond 39 residues and is associated with the nuclear accumulation of mutant Htt in

striatal neurons (DiFiglia et al., 1997; Saudou et al., 1998). Conversion of mutant Htt to a toxic species in the nucleus may occur through its interactions with new nuclear neighbors (Duennwald et al., 2006). In addition, the cytoplasmic chaperonin TriC, which functions to assemble mutant Htt into benign aggregates (Behrends *et al.*, 2006), is not present in the nucleus (Kim et al., 1994). Therefore, when mutant Htt enters the nucleus, it appears to face a combination of negative environmental influences that enable it to assume a toxic conformation. However, attaining a mechanistic understanding of the environmental conditions that permit accumulation of toxic Htt species requires further study.

To define how the cellular environment buffers the accumulation of proteotoxic species, we study features of Rnq1 prion and Htt toxicity in yeast. The yeast prion Rnq1 belongs to a class of glutamine/asparagine-rich (Q/N) proteins that exist in native and alternate, self-propagating amyloid-like forms (Sondheimer and Lindquist, 2000). Though benign at low levels, elevated expression of Rnq1 protein induces cell death (Douglas et al., 2008). Formation of toxic Rnq1 species requires the presence of pre-existing $[RNQ^+]/[PIN^+]$ prions (Derkatch *et al.*, 1997; Douglas *et al.*, 2008). Rnq1 toxicity is suppressed by increasing the levels of the Hsp40 chaperone, Sis1, which enhances $[RNQ^+]$ prion formation and reduces accumulation of a detergent-soluble Rnq1 species (Douglas et al., 2008). These data demonstrate that chaperone-dependent conversion of a toxic protein into its amyloid-like prion can serve as a protective mechanism. In addition, the efficiency of disease protein flux through amyloid assembly pathways appears to strongly influence whether or not cells tolerate disease protein expression.

[RNQ^+] prions also represent a model system to study the mechanism by which environmental factors promote the conversion of disease proteins to a toxic state (Meriin *et al.*, 2002). It is proposed that [RNQ^+] prions expose surfaces that serve as templates that foster conversion of endogenous yeast prions and foreign prions from other organisms, which are expressed in yeast, into amyloid-like states (Derkatch *et al.*, 1997; Taneja *et al.*, 2007). Furthermore, [RNQ^+] prions act via an unknown mechanism to facilitate the conformational switching of the polyQ expanded exon-1 fragment from Huntingtin's protein (Htt-103Q) from a benign to toxic state (Meriin *et al.*, 2002). Thus, the study of interactions between [RNQ^+] prions and Htt-103Q provides an excellent model to understand how members of a disease protein's neighborhood influence whether it becomes benign or toxic. Such information will help explain enigmatic observations of selective neuronal vulnerability to specific disease proteins.

To investigate how a disease protein's environment influences its toxicity, we examined the impact of relocating [RNQ^+] prions from the cytosol to the nucleus on cell death caused by Rnq1 and Htt-103Q. Hsp40 dependent accumulation of Rnq1 in the nucleus dramatically enhanced the accumulation of [RNQ^+] prions and suppressed Rnq1 toxicity. Relocation of the [RNQ^+] prion assembly pathway from the cytosol to the nucleus also had dramatic effects on Htt-103Q localization and toxicity. Nuclear [RNQ^+] prions sequestered Htt-103Q and interfered with the formation of SDS-resistant, Htt-103Q aggregates. The resultant accumulation of detergent-soluble forms of Htt-103Q correlated with a dramatic increase in Htt toxicity. The presence of [RNQ^+] prions in the nuclear environment reciprocally impacts the toxicity of Rnq1 and Htt-103Q. The differences in toxicity tightly correlate with the ability of the cytosol and the nucleus to

package Rnq1 and Htt-103Q in SDS-resistant aggregates. These data demonstrate that the capacity of the cytosol and nucleus to package proteins into benign aggregates varies in a manner that is dependent upon the nature of individual disease proteins.

3.3 Results

Sis1-mediated suppression of Rnq1 toxicity is accompanied by movement of [RNQ⁺] prions the nucleus

To explore how changes in chaperone activity within the cellular environment impact toxicity of disease proteins, we examined the ability of the Hsp40 Sis1 to subdue the rapid onset of Rnq1 toxicity in relation to the subcellular distribution of the [RNQ⁺] prions. The yeast plasma membrane becomes permeable to sytox dye (Zakrzewska et al., 2007) within 5 hrs of inducing Rnq1 overexpression (Figure 3.1a). Elevating Sis1 expression within the physiologic levels observed during heat-stress (Bardwell et al., 1986), prevents Rnq1 from permeablizing the yeast plasma membrane to sytox, which correlates with suppression of Rnq1 induced cell death (Douglas et al., 2008). Interestingly, Sis1-dependent suppression of Rnq1 toxicity was also associated with a dramatic change in the localization of fluorescent [RNQ⁺] prion foci containing Rnq1-mRFP from the cytosol to the nucleus (Figure 3.1b).

The link between suppression of Rnq1 toxicity by Sis1 and the relocation of [RNQ⁺] prions to the nucleus is intriguing because, until now, changes in the nucleocytoplasmic distribution of disease-causing proteins has been associated with the onset of cell death (DiFiglia et al., 1997; Neumann et al., 2006; Saudou et al., 1998). Type II Hsp40s such as Sis1 have been implicated in mediating the accumulation of a range of proteins in the nucleus (Cheng et al., 2008; Zhang et al., 2008). Thus, we sought to establish the concept that molecular chaperones can impact proteotoxicity by influencing the cellular location of a disease protein.

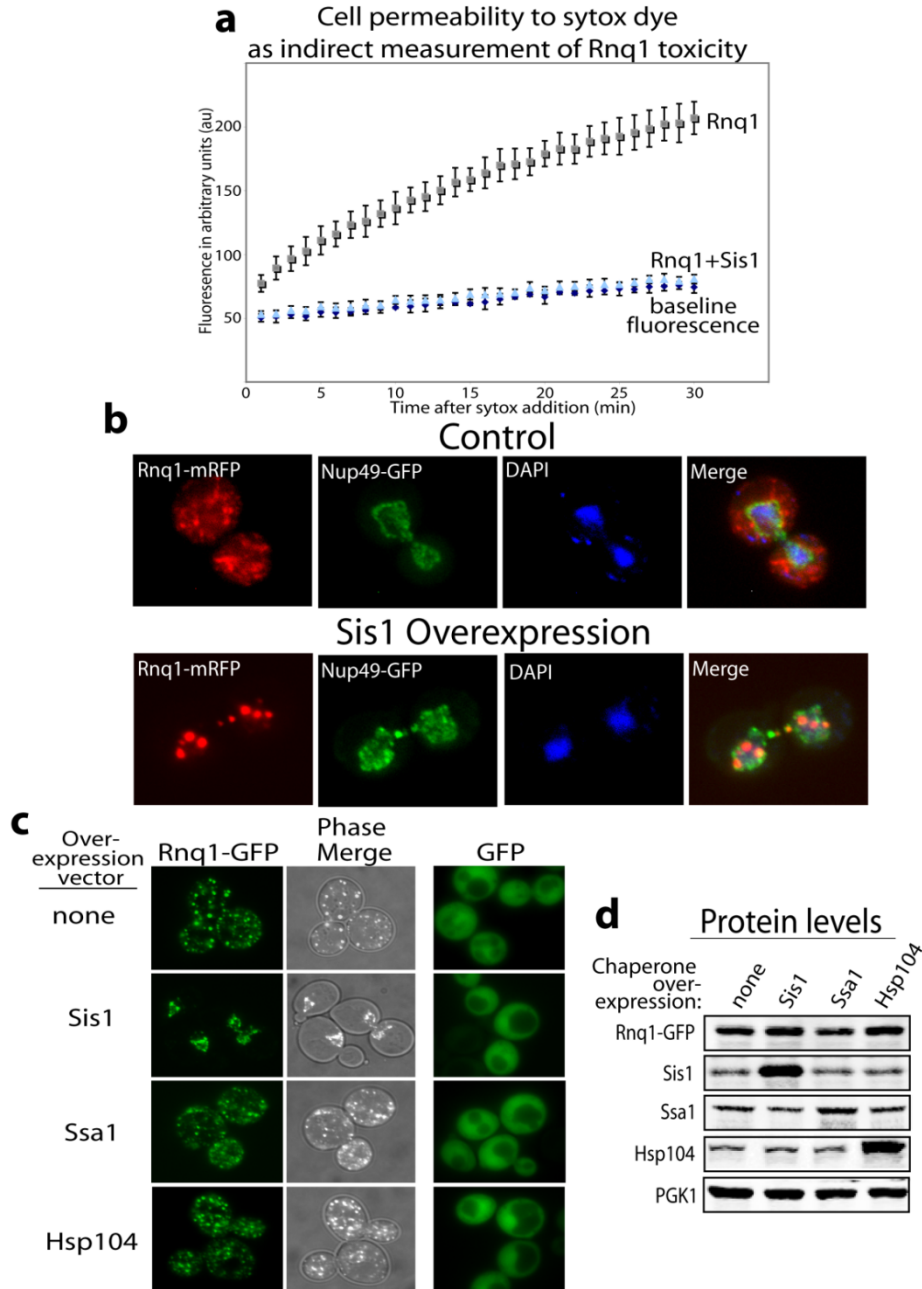


Figure 3.1 Suppression of Rnq1 toxicity by Sis1 correlates with nuclear accumulation of $[RNQ^+]$ prions. (a) Sytox dye uptake into cells expressing Rnq1 with and without excess Sis1. Rnq1 overexpression was induced for 5 hrs prior to the addition of sytox dye, at which point fluorescent readings were taken every min for 30 min. **(b)** Localization of Rnq1-mRFP in the nucleus resultant from Sis1 overexpression. Nup49-GFP is a marker of the nuclear envelope boundary. DAPI denotes the localization of nuclear DNA. **(c)** The effect of chaperone overexpression on the cellular distribution of Rnq1-GFP. **(d)** Western blot analysis of the indicated proteins from cell extracts in panel c.

Control studies demonstrate that the effect of Sis1 on $[RNQ^+]$ prion localization was a specific result of Sis1 action in Rnq1 detoxification. The Hsp70, Ssa1, as well as Hsp104 play important roles in $[RNQ^+]$ prion propagation (Schwimmer and Masison, 2002; Sondheimer and Lindquist, 2000), but do not suppress Rnq1 toxicity (Douglas et al., 2008). Accordingly, overexpression of either of these chaperones did not detectably alter the subcellular distribution or expression level of Rnq1-GFP (Figure 3.1c and d). In addition, elevating Sis1 levels did not have a pleiotropic effect on nucleocytoplasmic traffic. Sis1 overexpression did not alter the cellular location of GFP (Figure 3.1c, *right column*), $[PSI^+]$ prions formed by Sup35-GFP (Figure 3.2a), or a GFP reporter of nucleocytoplasmic transport that contains both NLS (nuclear localization signal) and NES (nuclear export signal) moieties (Figure 3.2b) (Stade et al., 1997).

Eukaryotic cells clear some misfolded protein conformers from the cytosol by partitioning protein aggregates into aggresome-like assemblies (Johnston et al., 1998) and non-aggregated ubiquitinated proteins to a perinuclear compartment for degradation (Kaganovich et al., 2008). Our data suggest that an additional route for detoxification exists, so it was important to further demonstrate that detoxification of Rnq1 was actually dependent upon nuclear transport machinery. This was accomplished by identification of three nuclear pore proteins (Nup84, Nup120, Nup188) and one nuclear transport receptor (Kap123) whose deletion hindered the ability of Sis1 to promote nuclear $[RNQ^+]$ prion accumulation (Figure 3.3a). These same nuclear import pathway genes were also shown to be required for Rnq1 detoxification in the absence of Sis1 overexpression because their deletion enhanced Rnq1 toxicity (Figure 3.3b). Thus, Rnq1 toxicity is exacerbated by removal of nuclear protein import machinery that is required for Sis1-

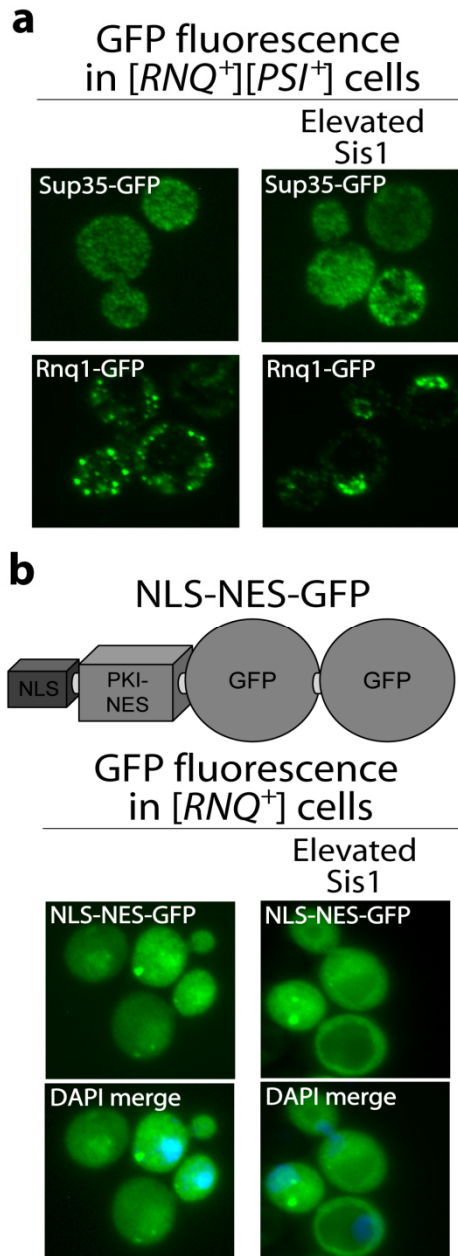


Figure 3.2 Sis1 overexpression does not promote the nuclear accumulation of $[PSI^+]$ prions or a nucleocytoplasmic transport reporter protein. **(a)** The localization of Rnq1-GFP or Sup35-GFP was monitored in $[RNQ^+][PSI^+]$ cells by fluorescence microscopy. Right panels show prion localization in the presence of Sis1 overexpression. **(b)** Model of the tandem GFP reporter protein with an N-terminal NLS and NES. The cellular distribution of NLS-NES-GFP was monitored in the presence or absence of Sis1 overexpression by fluorescence microscopy. DAPI stained images were overlaid with the GFP channel in the merge.

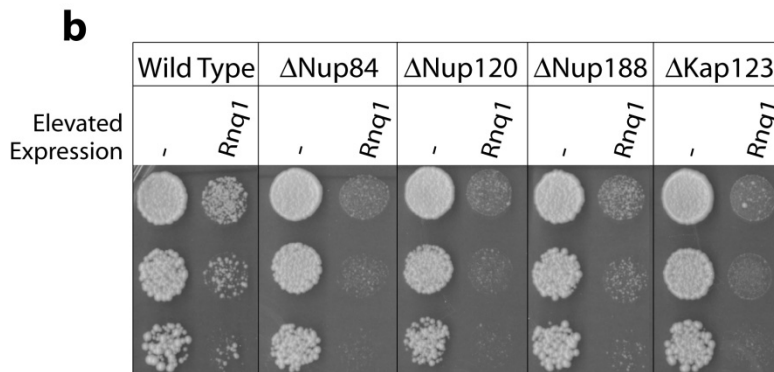
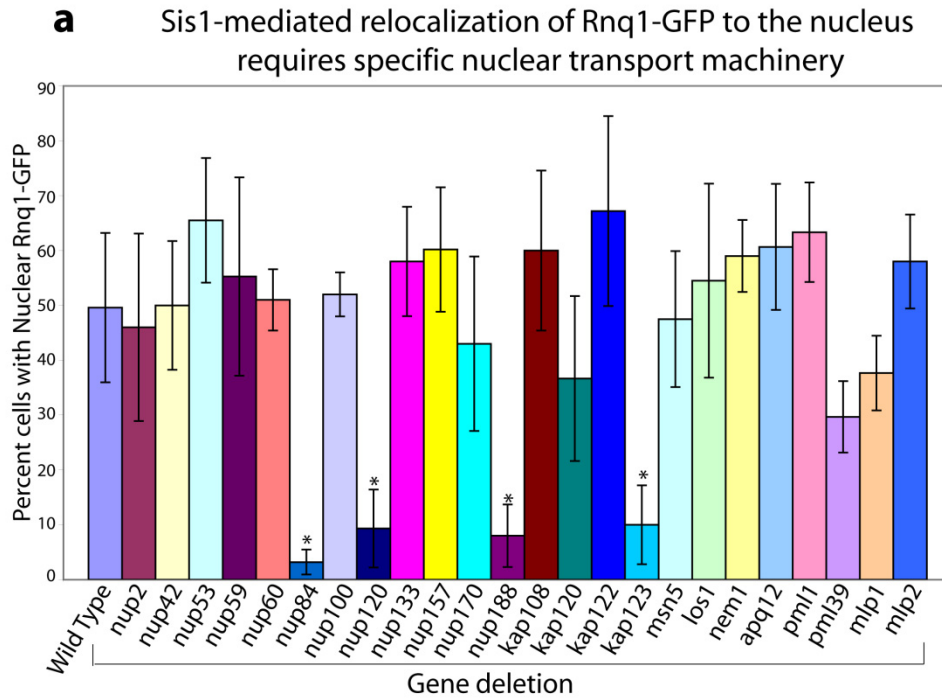


Figure 3.3 Identification of nuclear import factors that are required for Sis1-mediated concentration of Rnq1-GFP to the nucleus. (a) Deletion strains of 24 non-essential nuclear transport factors were sequentially transformed with plasmids expressing Sis1 and then Rnq1-GFP. The localization of Rnq1-GFP in 200 cells from 3-5 different transformations was scored via fluorescence microscopy as in Figure 3.1c. Deletion strains in which there was a significant decrease in Sis1 dependent nuclear accumulation of Rnq1-GFP are indicated (*), which denotes a p-value of <0.005. (b) Exacerbation of Rnq1 toxicity via deletion of genes required for Sis1 dependent nuclear Rnq1 accumulation. Analysis of toxicity in 5 fold serial dilutions of cells grown on plates supplemented with galactose to induce Rnq1 expression from the GAL1 promoter.

dependent $[RNQ^+]$ prion accumulation in the nucleus. These data, combined with Rnq1 localization data, indicate that Sis1 does not drive $[RNQ^+]$ prion accumulation in cytosolic aggresomes or JUNK compartments (Johnston et al., 1998; Kaganovich et al., 2008). Instead, Sis1 somehow promotes $[RNQ^+]$ prion accumulation in the nucleus and this event assists in Rnq1 detoxification.

Significant pools of Sis1 are normally found in the nucleus (Luke et al., 1991), so we explored the possibility that elevating Sis1 levels changes Rnq1 localization by stimulating nuclear $[RNQ^+]$ prion assembly. To test this concept, the order of Rnq1-GFP and Sis1 expression was varied and the effect of Sis1 overexpression on the localization of $[RNQ^+]$ prions was examined (Figure 3.4). When Rnq1-GFP was expressed first, $[RNQ^+]$ prions accumulated in the cytosol, and subsequent Sis1 overexpression did not redistribute $[RNQ^+]$ prions to the nucleus (Figure 3.4*a* and *b*). However, when Rnq1-GFP was expressed first, subsequent Sis1 overexpression was still able to suppress Rnq1 toxicity (data not shown), because it stimulated $[RNQ^+]$ prion assembly (Douglas et al., 2008). In contrast, when Sis1 levels were elevated prior to Rnq1-GFP expression, the nuclear accumulation of $[RNQ^+]$ prions was evident (Figure 3.4*a* and *b*).

These data indicate that Sis1 does not drive the relocation of pre-formed, Rnq1-GFP prion aggregates from the cytosol to the nucleus. In addition, the ratio of Sis1 to $[RNQ^+]$ prion helps control whether the bulk of $[RNQ^+]$ prion assembly occurs in the cytosol or nucleus. When cytosolic levels of $[RNQ^+]$ prions are high, $[RNQ^+]$ prion assembly is favored in the cytosol. Yet, when the ratio of Sis1 to cytosolic $[RNQ^+]$ prions is elevated, Sis1 appears to promote the assembly of soluble Rnq1-GFP into nuclear $[RNQ^+]$ prions that are incapable of export back to the cytosol. Over time, this Sis1

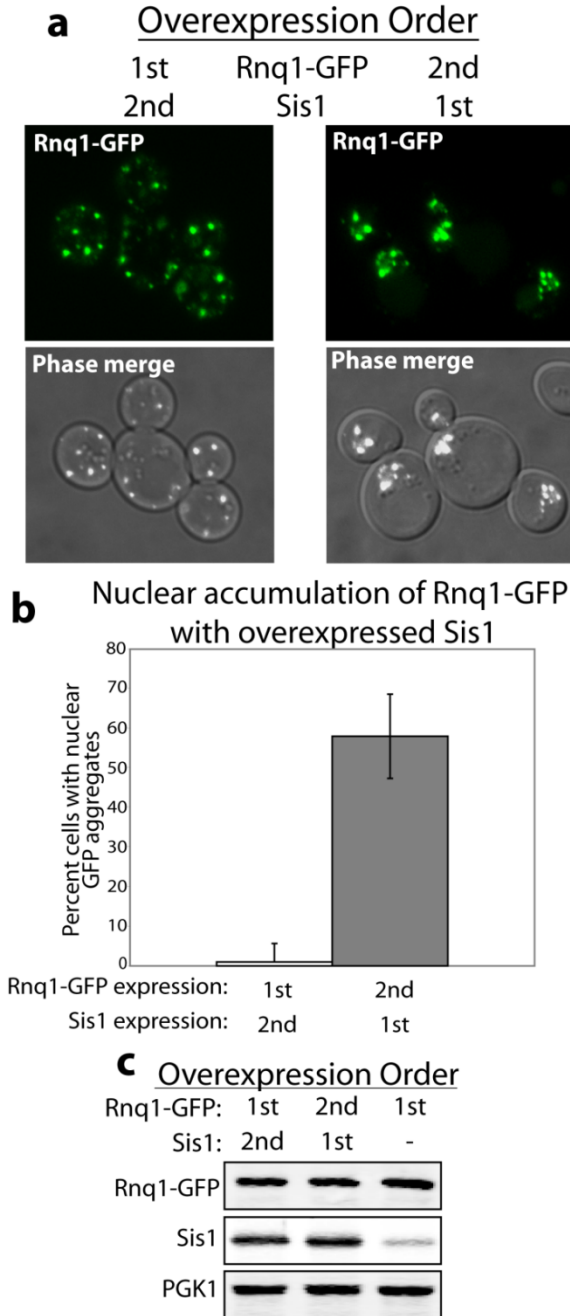


Figure 3.4 Sis1 overexpression needs to precede Rnq1-GFP expression to observe the nuclear localization of $[RNQ^+]$ prions. **(a)** Fluorescent images of the cellular distribution of Rnq1-GFP. Sis1 was expressed from the GAL1 promoter while Rnq1-GFP was under control of the CUP1 promoter. The expression order of each protein was designated as 1st or 2nd. **(b)** Quantitation of Rnq1-GFP nuclear compartmentalization populations of 200 cells from 3 separate transformations. Values are expressed in percent of total cells counted and the error bars reflect the standard deviation. The p-value was <0.0001. **(c)** Expression levels of the indicated proteins by western blot analysis.

action shifts the localization of the $[RNQ^+]$ prion assembly pathway from the cytosol to the nucleus. Thus, changes in the ratio of Rnq1 and Sis1 levels have dramatic effects on whether amyloid-like aggregate assembly occurs within the cytosol or the nucleus.

The nuclear environment favors $[RNQ^+]$ prion accumulation

To separate Sis1 action in $[RNQ^+]$ prion assembly from its impact on Rnq1 localization, we compared the toxicity of Rnq1-GFP and Rnq1-GFP L94A to that of Rnq1-GFP-NLS and Rnq1-GFP-NLS L94A. The later has the SV-40 NLS (Kalderon et al., 1984) fused to the C-terminus of the GFP moiety attached to the C-terminus of Rnq1. The Rnq1 L94A variant was employed because it contains a point mutation in the Sis1 binding site in the non-prion domain of Rnq1 (Douglas *et al.*, 2008). Rnq1 L94A is a highly toxic Rnq1 variant because its conversion into amyloid-like $[RNQ^+]$ prions is inefficient (Douglas et al., 2008). Rnq1-GFP-NLS and Rnq1-GFP-NLS L94A were expressed at levels similar to their non-NLS-tagged counterparts, but were dramatically less toxic (Figure 3.5a). Decreased toxicity of NLS-tagged Rnq1-GFP and Rnq1-GFP L94A correlated with their accumulation in the nucleus (Figure 3.5b). It should be noted that near complete nuclear accumulation of Rnq1-NLS required its conversion into its $[RNQ^+]$ prion form, as it was enriched in the nucleus, but still present in the cytosol of $[rnq^-]$ cells (Figure 3.5b). Interestingly, filter trap and SDD-AGE analysis demonstrated that SDS-resistant pools of NLS-tagged forms of Rnq1-GFP and Rnq1-GFP L94A accumulated to 1.5 fold higher levels than the non-NLS-tagged forms (Figure 3.6a-c). Analysis of similar cell extracts by size exclusion chromatography demonstrated that around 55% of total Rnq1-GFP behaved as a high molecular weight species and the other

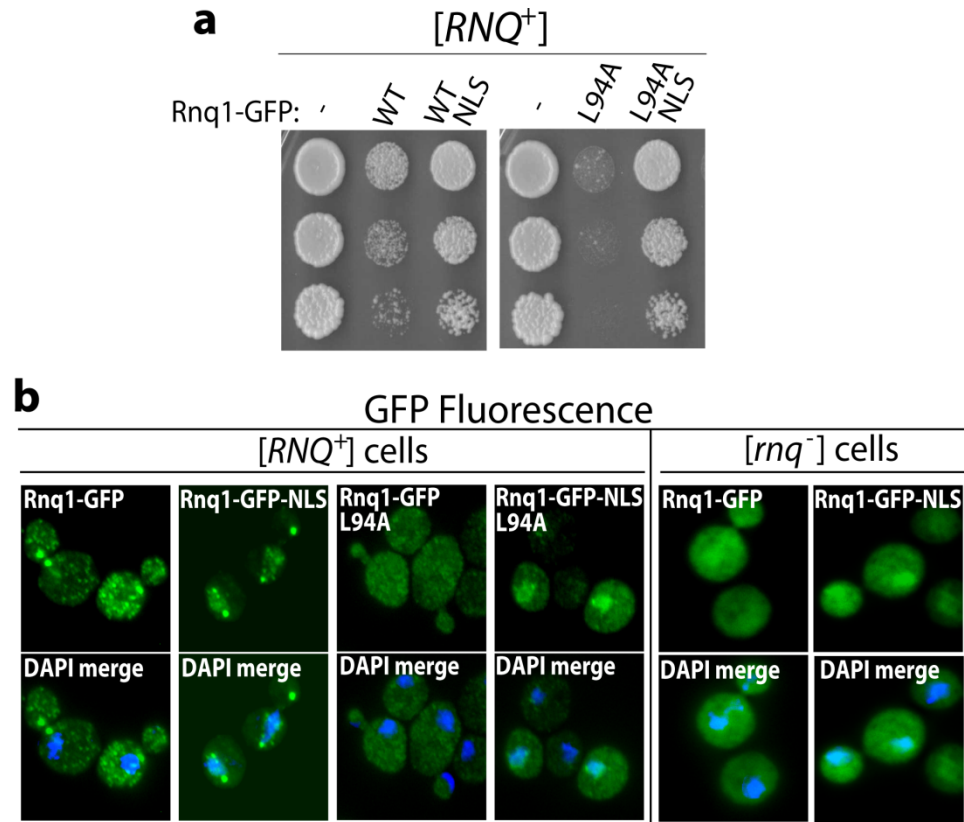


Figure 3.5 Rnq1-GFP-NLS is less toxic than Rnq1-GFP. (a) Analysis of toxicity in 5-fold dilutions of cells grown on plates supplemented with galactose to induce Rnq1 expression from the GAL1 promoter. (b) Localization of Rnq1-GFP-NLS and Rnq1-GFP via fluorescence microscopy in [RNQ⁺] and [rnq⁻] cells.

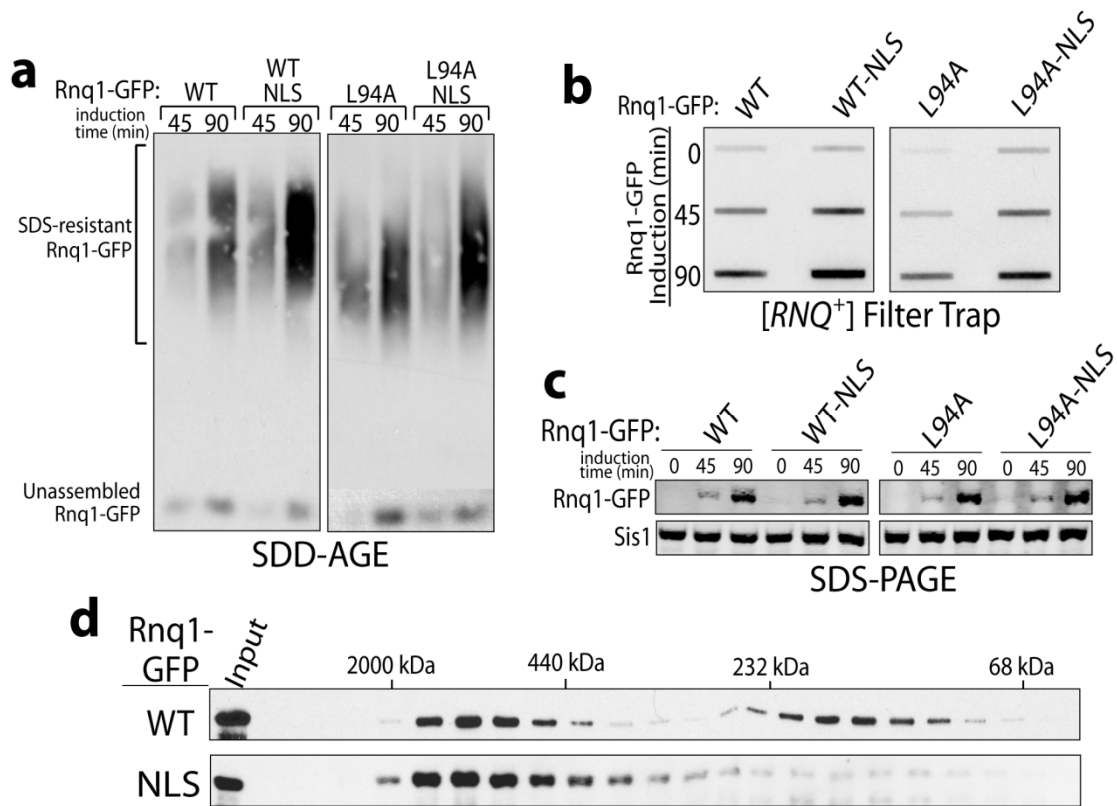


Figure 3.6 Rnq1-GFP-NLS assembles into SDS-resistant $[RNQ^+]$ prions with greater efficiency. (a) SDD-AGE analysis of the time course for the assembly of SDS-resistant $[RNQ^+]$ prions after induction of Rnq1 expression with galactose. (b) Filter trap analysis of Rnq1-GFP conversion to an SDS-resistant species at the indicated time after induced expression. Rnq1-GFP retained on the cellulose acetate filter was detected with α -GFP. (c) Time course of Rnq1-GFP expression determined by western blot. (d) Populations of Rnq1-GFP species as determined by size exclusion chromatography 4 hrs after induction of Rnq1 expression. Input corresponds to 10% of the total Rnq1-GFP protein loaded.

45% behaved as a lower molecular weight unassembled species. The nuclear environment appeared to enhance the efficiency of Rnq1 assembly into $[RNQ^+]$ prions because 85% of total Rnq1-GFP-NLS behaved as a high molecular weight species and little unassembled Rnq1-GFP-NLS was detected (Figure 3.6d). Thus, changing the cellular location of Rnq1 from the cytosol to the nucleus does not affect expression levels of Rnq1, but does decrease the pool of unassembled Rnq1 whose accumulation is associated with cell death (Douglas et al., 2008).

The dramatic decrease in unassembled Rnq1 pools observed does not appear to be related to degradation of Rnq1 because levels of total Rnq1-GFP and Rnq1-GFP-NLS are similar (Figure 3.6c). Instead, the decrease in unassembled Rnq1 observed when it accumulates in the nucleus correlates with a 1.5 fold increase in the accumulation of SDS-resistant Rnq1 aggregates (Figure 3.6a and b), which exhibit several features of amyloid (Douglas et al., 2008). These data suggest that conversion of Rnq1 into amyloid-like $[RNQ^+]$ prions is more efficient in the nucleus. This environment-dependent increase in $[RNQ^+]$ prion formation appears cytoprotective because it prevents the accumulation of unassembled Rnq1 pools that are associated with cell death.

Nuclear $[RNQ^+]$ prions act *in trans* to detoxify Rnq1 L94A

Nuclear $[RNQ^+]$ prions appear to prevent the accumulation of toxic Rnq1 conformers in the cytosol by acting as seeds that drive the ordered assembly of amyloid-like aggregates in the nucleus. If this is true then the location of pre-existing $[RNQ^+]$ prion pools should dictate the site where soluble Rnq1 is converted into its $[RNQ^+]$ prion form. To test this prediction, we asked if an NLS-tagged pool of $[RNQ^+]$ prions could act

in trans to concentrate nascent Rnq1 in the nucleus and thereby suppress Rnq1 toxicity (Figure 3.7). Rnq1-GFP-NLS or Rnq1-GFP under control of the CUP1 promoter was first expressed at low non-toxic levels, which allowed for the formation of either nuclear or cytosolic $[RNQ^+]$ prions, respectively (Figure 3.7a). After a time period that allowed for distinct compartmentalization of the GFP-tagged $[RNQ^+]$ prions, expression of Rnq1-mRFP under control of GAL1 promoter was induced for 1 hr and fluorescence of the different tagged proteins was visualized. We found that the subcellular location of Rnq1-mRFP was dependent upon the localization of preformed GFP-tagged $[RNQ^+]$ prions (Figure 3.7a). Nearly the entire pool of newly synthesized Rnq1-mRFP became co-localized with pools of nuclear $[RNQ^+]$ prions that accumulated during the prior expression of Rnq1-GFP-NLS (Figure 3.7a). Importantly, the severe growth defects caused by GAL1 dependent Rnq1-GFP L94A overexpression were suppressed through prior low-level expression of Rnq1-GFP-NLS (Figure 3.7b). Therefore, $[RNQ^+]$ prions can act *in trans* to both alter the subcellular location and toxicity of Rnq1.

To further demonstrate the concept that pools of amyloid-like assemblies can trap native amyloidogenic proteins in a specific location, we conducted cytoduction experiments (Figure 3.7c). Cytoduction refers to an experimental situation where haploid yeast initiate the mating process, fuse their plasma membranes, and mix cytosolic contents, but fail to undergo karyogamy because one of the tester strains is defective in nuclear fusion (Conde and Fink, 1976). This scenario allowed us to monitor the fate of soluble Rnq1-mRFP in the cytosol of $[rnq^-]$ cells that was introduced into $[RNQ^+]$ cells, which harbored pre-existing nuclear $[RNQ^+]$ prions formed by Rnq1-GFP-NLS (Figure 3.7c). GFP-tagged $[RNQ^+]$ prions present in the nucleus of $[RNQ^+]$ cells depleted the

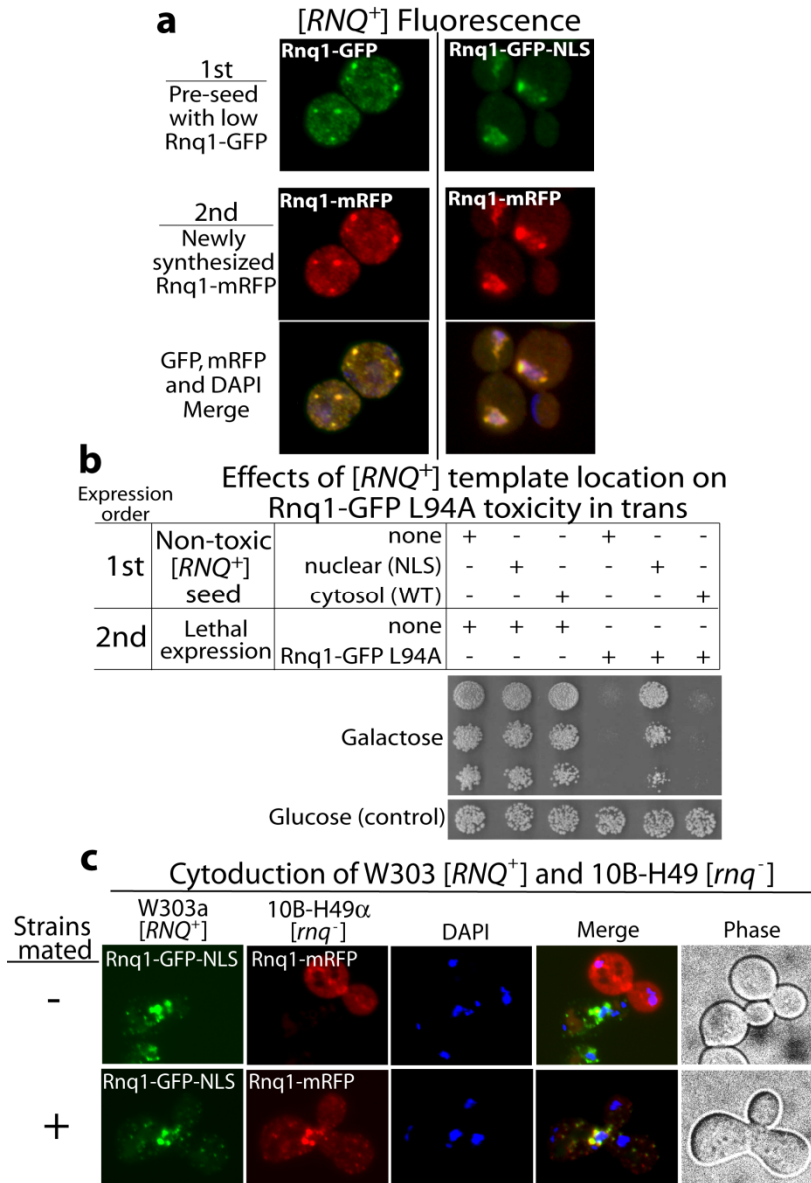


Figure 3.7 Expression of Rnq1-GFP-NLS suppresses Rnq1 L94A toxicity and promotes the nuclear accumulation of Rnq1-mRFP. (a) Prior expression of Rnq1-GFP-NLS leads to the accumulation of Rnq1-mRFP in the nucleus. Rnq1-GFP or Rnq1-GFP-NLS were expressed overnight at low, non-toxic levels from the CUP1 promoter. Subsequent expression of Rnq1-mRFP from the GAL1 promoter was induced by the addition of galactose. After 1hr, the location of the GFP and mRFP signals was determined in fixed, DAPI-stained cells by fluorescence microscopy. (b) Analysis of cell growth in 5 fold serial dilutions of [RNQ⁺] cells which harbored the indicated constructs. Cells were grown overnight in synthetic media to allow for Rnq1-GFP or Rnq1-GFP-NLS expression. Cells were then plated on agar that contained glucose (the control) or galactose to induce Rnq1-GFP L94A expression to toxic levels. (c) Rnq1-GFP-NLS in the nucleus of cytoduced [RNQ⁺] cells sequesters Rnq1-mRFP from the cytoplasm of [rnq⁻] cells. Cell fusion was analyzed 30 mins (Top row, control) and 2 hrs (bottom) after cell mixture. Merge images represent the combination of all fluorescent channels.

cytosol of [*rnq*⁻] cells of soluble Rnq1-mRFP and drove the assembly of a hybrid aggregate that contained both GFP and mRFP. Thus, nuclear [*RNQ*⁺] prions do indeed trap soluble Rnq1 in the nucleus by driving their fusion into large assemblies whose size constraints prevent export back to the cytosol. In this situation, the nuclear envelope acts as a sieve that helps suppress Rnq1 toxicity by sequestering prions in the nucleus, which, in turn, enhances [*RNQ*⁺] prion assembly.

Nuclear [*RNQ*⁺] prions concentrate Htt-103Q in the nucleus and exacerbate Htt toxicity

[*RNQ*⁺] prions promote Htt-103Q toxicity in yeast (Meriin et al., 2002) and movement of polyQ-expanded Htt protein from the cytosol to the nucleus of neurons and yeast correlates with exacerbated toxicity (DiFiglia et al., 1997; Schaffar et al., 2004). Yet, it is not clear how interaction with [*RNQ*⁺] prions or entry into the nuclear environment fosters toxicity of polyQ-expanded fragments of Htt exon-1 (Dunah et al., 2002; Schaffar et al., 2004). To address these issues, we investigated the effects that Sis1 overexpression had on the ability of the cell to tolerate Htt-103Q expression (Figure 3.8). While Sis1 expression suppressed Rnq1 toxicity (Fig. 1), the growth of yeast expressing Htt-103Q was slowed dramatically by Sis1 overexpression (Figure 3.8*a*). Interestingly, Sis1 overexpression also resulted in the nuclear accumulation of Htt-103Q-GFP aggregates in 15% of cells analyzed by fluorescent microscopy (Figure 3.8*b*). Based on these data, we explored whether [*RNQ*⁺] prions could act as environmental factors that increase Htt toxicity via attracting Htt-103Q to the nucleus (Figure 3.9 and 3.10).

To address this question we examined the effect that expression of low, non-toxic levels of Rnq1-GFP or Rnq1-GFP-NLS had on Htt-103Q toxicity. These Rnq1 variants

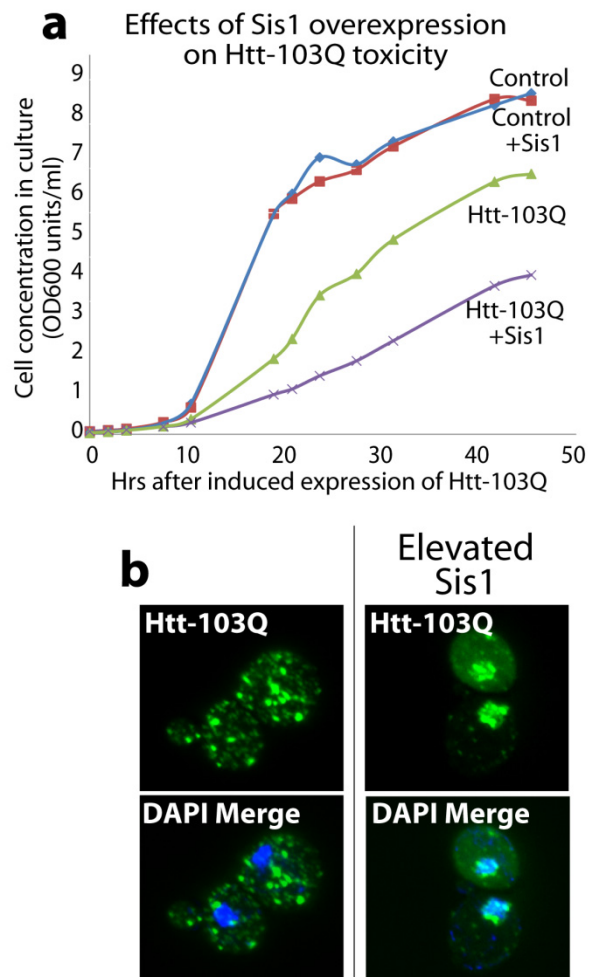


Figure 3.8 Elevation of Sis1 levels exacerbate growth defects caused by Htt-103Q overexpression. (a) Growth of $[RNQ^+]$ yeast that harbored Sis1 and/or Htt-103Q overexpression constructs as indicated. (b) Cellular localization of Htt-103Q-GFP in $[RNQ^+]$ cells with and without Sis1 overexpression as determined by fluorescence microscopy. DNA is stained with DAPI.

were expressed, then expression of Htt-103Q was induced and the influence of $[RNQ^+]$ prion cellular location on Htt toxicity was evaluated. Growth of yeast was not impacted upon expression of Htt-25Q regardless of whether $[RNQ^+]$ prions were predominantly localized in the cytosol or nucleus (Figure 3.9a). Yet, in dramatic contrast to what was observed with Rnq1 toxicity, the presence of small pools of $[RNQ^+]$ prions in the nucleus exacerbated Htt-103Q toxicity. The effect of Rnq1 localization on Htt toxicity was dependent upon the presence of the $[RNQ^+]$ prion conformer because Htt-103Q expression was not toxic in $[rnq^-]$ cells regardless of whether Rnq1-GFP or Rnq1-GFP-NLS was present (Figure 3.10).

To explain the increase in Htt toxicity observed in the presence of nuclear $[RNQ^+]$ prions, we asked if the cellular location of $[RNQ^+]$ prions controlled the location of Htt-103Q (Figure 3.9b). Rnq1-mRFP or Rnq1-mRFP-NLS were expressed at low levels from the CUP1 promoter to permit the formation of respective cytosolic and nuclear pools of mRFP-tagged $[RNQ^+]$ prions. Then, expression of Htt-25Q-GFP or Htt-103Q-GFP from the GAL1 promoter was induced for 1 hr and cells were visualized. The site of Rnq1 localization had no effect on the solubility or distribution of Htt-25Q-GFP (Figure 3.9b *left columns*). Conversely, the location of $[RNQ^+]$ prions controlled the subcellular location of Htt-103Q-GFP (Figure 3.9b *right columns*). Nuclear $[RNQ^+]$ prions relocated Htt-103Q-GFP to the nucleus through what appeared to be direct interactions as their localization was coincidental. The association between $[RNQ^+]$ prions and Htt-103Q was dependent upon the length of the expanded polyQ-region. In addition, interaction between $[RNQ^+]$ prions and Htt-103Q appeared specific, because $[RNQ^+]$ prions did not

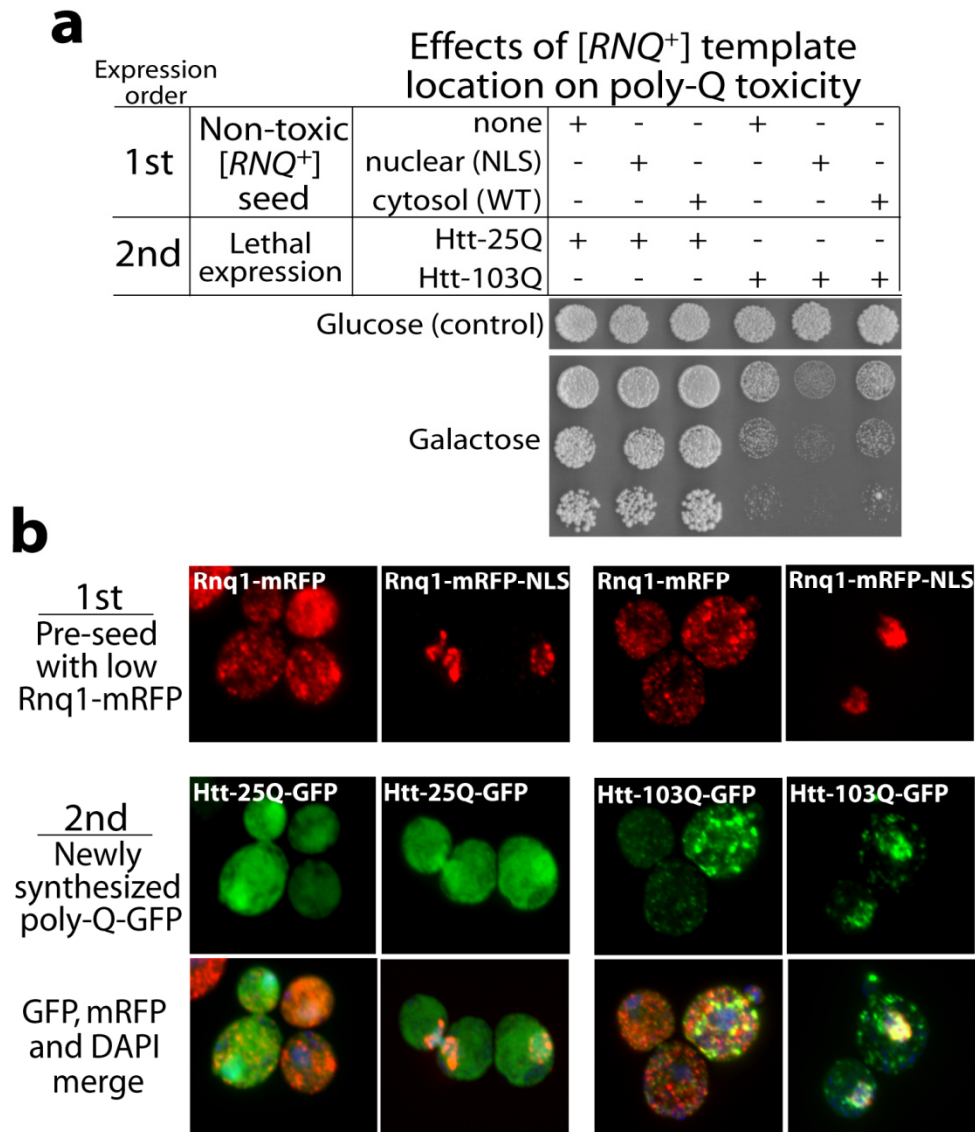


Figure 3.9 The presence of $[RNQ^+]$ prions in the nucleus exacerbates Htt-103Q toxicity. **(a)** Analysis of cell growth in 5-fold serial dilutions of $[RNQ^+]$ cells, which harbored the indicated constructs. Rnq1-GFP and Rnq1-GFP-NLS were first expressed at non-toxic levels from a CUP1 promoter in liquid media containing copper. Then, Htt-25Q-GFP and Htt-103Q-GFP were expressed at toxic levels from the GAL1 promoter on galactose plates. **(b)** The impact of Rnq1-mRFP-NLS expression on the cellular localization of Htt-25Q-GFP and Htt-103Q-GFP.

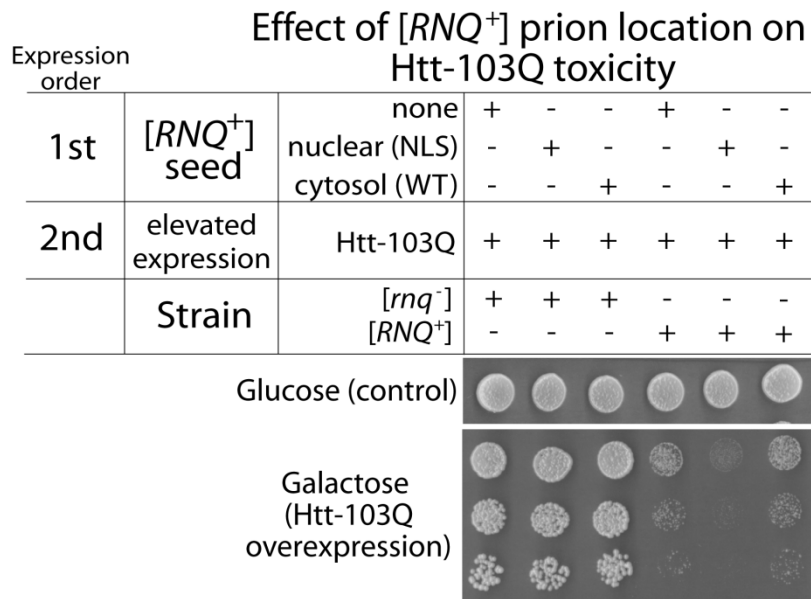


Figure 3.10 Rnq1-GFP-NLS exacerbates Htt-103Q toxicity in $[RNQ^+]$ cells but has no affect on Htt-103Q toxicity in $[rnq^-]$ cells. Analysis of cell growth in 5 fold serial dilutions of $[RNQ^+]$ and $[rnq^-]$ cells, which harbored the indicated constructs. Rnq1-GFP and Rnq1-GFP-NLS were first expressed at low non-toxic levels from a CUP1 promoter in liquid media containing copper. Then, Htt-103Q-GFP was expressed to toxic levels from the GAL1 promoter on galactose plates.

alter the location of another amyloid-like interaction partner, Het-S, that lacks polyQ expansions (Figure 3.11) (Taneja et al., 2007).

To demonstrate a physical interaction between $[RNQ^+]$ prions and Htt-103Q, we analyzed whether they could form an immunoprecipitable complex. First, endogenous Rnq1 was demonstrated to co-precipitate with Htt-103Q-GFP (Figure 3.12a). SDS-soluble forms of Htt-103Q-GFP protein that are capable of migrating into the SDS-PAGE gels showed no substantial co-precipitation with Rnq1. Yet, the SDS-insoluble Htt-103Q aggregates, which were incapable of entry into the SDS-PAGE gel, precipitated with Rnq1 and could be observed as immuno-reactive bands at the top of western blots. In addition, overexpressed Rnq1-GFP and Rnq1-GFP-NLS could also co-immunoprecipitate with SDS-resistant Htt-103Q aggregates (Figure 3.12b). Hence, nuclear $[RNQ^+]$ prions appear to trap Htt-103Q in the nucleus through direct binding to Htt-103Q.

To explore the mechanism for exacerbation of Htt-103Q toxicity, we investigated how nuclear $[RNQ^+]$ prions affected the assembly status of Htt-103Q (Figure 3.13). Accumulation of $[RNQ^+]$ prions in the cytosol had no significant effect on the assembly of Htt-103Q into an SDS-resistant species that was detected by filter-trap analysis. In addition, Htt-103Q expression had no effect on the assembly of Rnq1 into $[RNQ^+]$ prions (data not shown). Yet, when nuclear $[RNQ^+]$ prions were present, the conversion of Htt-103Q into tight SDS-resistant aggregates was reduced by 80% (Figure 3.13a).

The accumulation of a small oligomeric form of polyQ-expanded Htt in the size range of a dimer or trimer is linked to Htt toxicity in yeast (Behrends et al., 2006). Thus, we asked if decreased formation of SDS-resistant, Htt-103Q assemblies observed in the presence of nuclear $[RNQ^+]$ prions was associated with the accumulation of similar

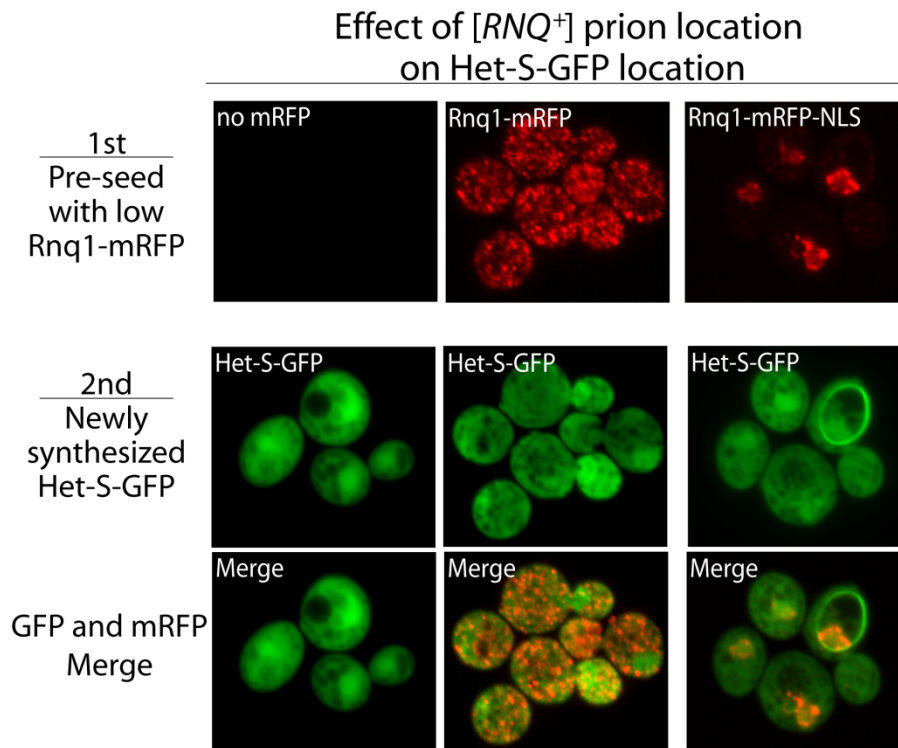


Figure 3.11 Expression of Rnq1-mRFP-NLS was unable to sequester the non-Q-rich Het-S prion to the nucleus. Rnq1-mRFP and Rnq1-mRFP-NLS were first expressed at low, non-toxic levels from a CUP1 promoter in liquid media containing copper. Then, Het-S-GFP was expressed from the GAL1 promoter by addition of galactose to the media. The localization of Het-S-GFP was monitored in the absence of exogenous Rnq1 (left column) or in the presence of exogenous Rnq1-mRFP (middle column) or Rnq1-mRFP-NLS (right column) by fluorescence microscopy.

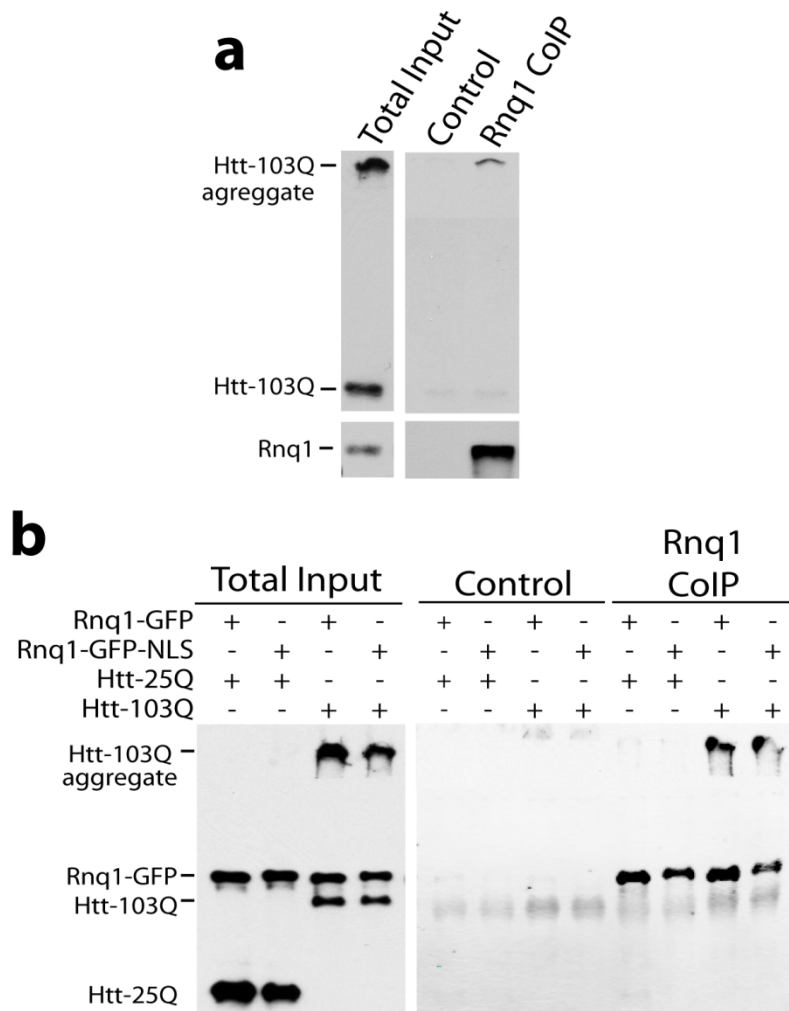


Figure 3.12 [*RNQ*⁺] prions form an immunoprecipitable complex with high molecular weight Htt-103Q. **(a)** Co-precipitation of endogenous Rnq1 and Htt-103Q in complex with each other. Extracts were generated from cells expressing Htt-103Q and endogenous Rnq1 was precipitated under native conditions with α -Rnq1. Precipitates were resolved by SDS-PAGE and western blots were probed with α -GFP to detect Htt-103Q. **(b)** Co-precipitation of Rnq1-GFP or Rnq1-GFP-NLS and Htt-103Q in complex with each other. Extracts were prepared from cells grown in liquid culture that sequentially expressed Rnq1 and Htt fusion proteins as described above. Rnq1-GFP and Rnq1-GFP-NLS were precipitated under native conditions by the addition α -Rnq1 and western blots were probed with α -GFP to detect the different forms of Rnq1 and Htt.

detergent-soluble Htt-103Q oligomers (Figure 3.13*b*). Under control conditions, 70% of Htt-103Q in cell extracts migrated on a size exclusion column as a high-molecular weight species that was SDS-resistant and could not enter into SDS-PAGE gels. The other 30% of Htt-103Q detected behaved as an SDS-sensitive form that could enter into SDS-PAGE gels and appeared as a small oligomer. Yet, the presence of nuclear $[RNQ^+]$ prions dramatically reduced the formation of high-molecular weight, Htt-103Q assemblies. This was accompanied by a corresponding increase in the accumulation of SDS-sensitive, oligomeric Htt-103Q. Therefore, increased potency of Htt toxicity observed in the presence of nuclear $[RNQ^+]$ prions is associated with a dramatic decrease in the conversion of Htt-103Q into an SDS-resistant species and the accumulation of small Htt-103Q oligomers.

We sought to evaluate whether interaction with $[RNQ^+]$ prions or the relocation of Htt-103Q to the nucleus was the major factor that decreased the cells capacity to detoxify Htt-103Q. To approach this question, an NLS was fused to the C-terminus of the GFP moiety on Htt-103Q-GFP and the ability of Htt-103Q-GFP-NLS to form SDS-resistant aggregates and kill yeast was determined (Figure 3.14). Htt-103Q-GFP-NLS accumulated in the nucleus and was more toxic to $[RNQ^+]$ cells than Htt-103Q-GFP. Yet, $[rnq^-]$ cells tolerated Htt-103Q-GFP-NLS expression (Figure 3.14*a* and *b*). When compared to Htt-103Q-GFP, the assembly of Htt-103Q-GFP-NLS into high-molecular weight, SDS-resistant aggregates was reduced by over 60% (Figure 3.14*c*). This decrease in the formation of SDS-resistant aggregates was accompanied by a significant increase in the amount of detergent-soluble, Htt-103Q oligomers that were detected by size-exclusion chromatography (Figure 3.14*d*). These data suggest that the ability of nuclear $[RNQ^+]$

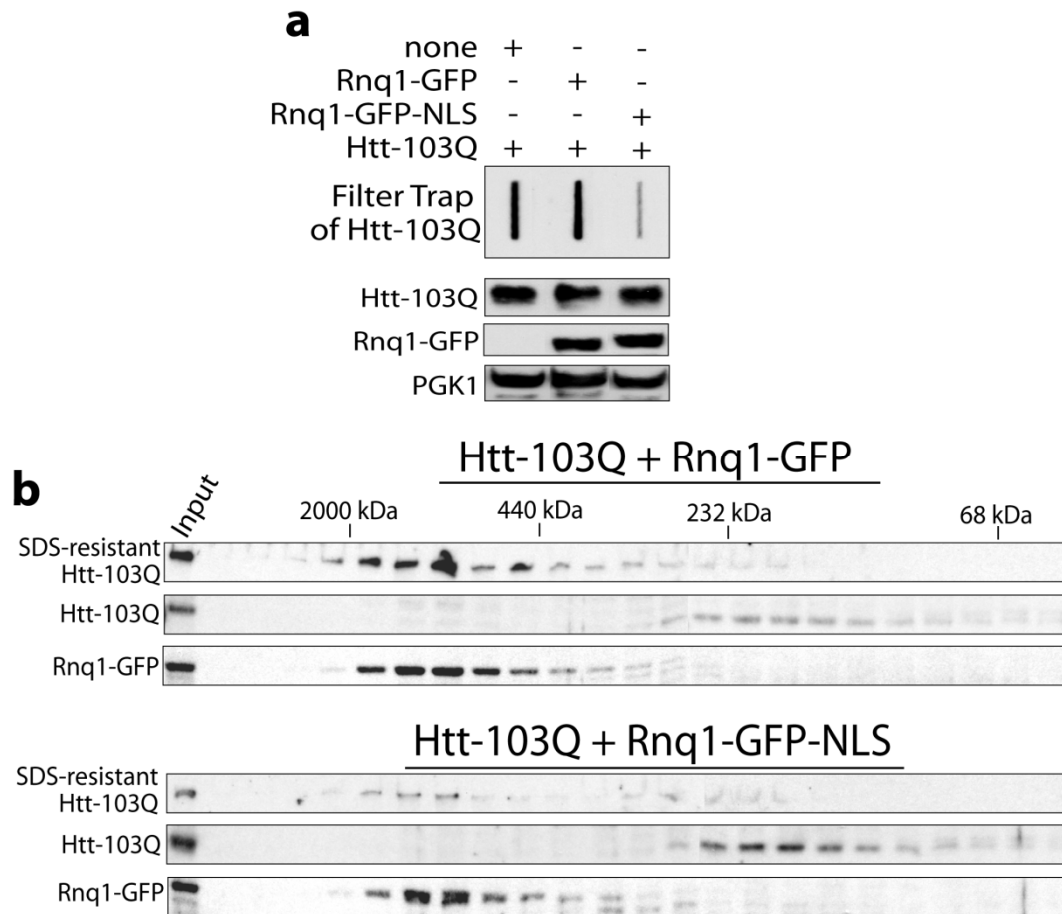


Figure 3.13 Nuclear $[RNQ^+]$ prions hinder the assembly of Htt-103Q into high molecular weight, SDS-resistant aggregates. (a) Filter trap analysis of SDS-resistant Htt-103Q aggregates. Htt-103Q retained on the cellulose acetate filter was detected with α -FLAG. Lower panels are western blots of cell extracts used in the filter trap assay. **(b)** Analysis of Htt-103Q assembly status by size exclusion chromatography. Htt-103Q was expressed for 2 hrs in cells that harbored Rnq1-GFP or Rnq1-GFP-NLS. Upper gels in each set of panels show the quantity of SDS-resistant Htt-103Q that was incapable of gel entry. Middle gels in each set of panels show the Htt-103Q which was able to migrate into gels. Lower gels in each set of panels show the mobility of either Rnq1-GFP or Rnq1-GFP-NLS. Input represents 10% of the total amount of Htt-103Q-GFP protein detected in extracts.

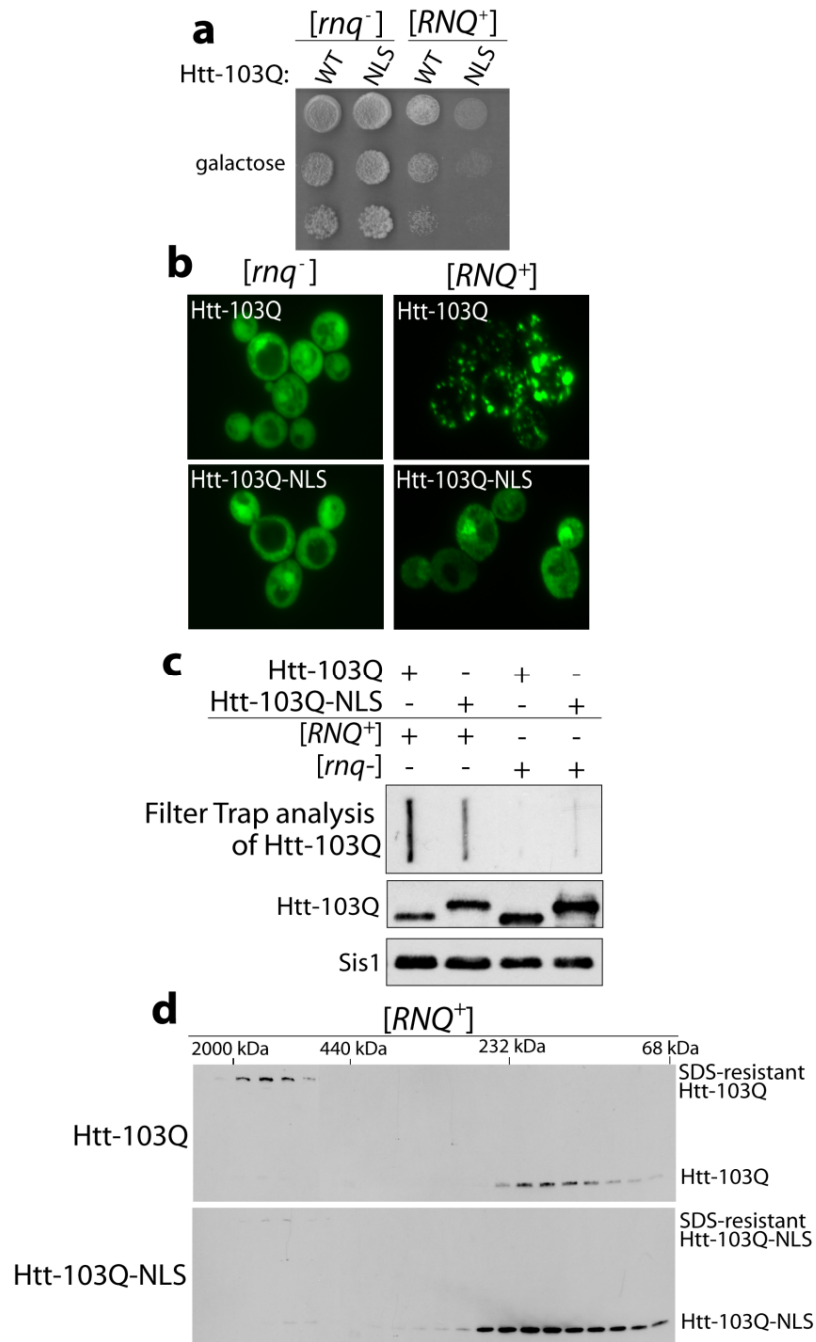


Figure 3.14 Htt-103Q-GFP-NLS forms SDS-resistant aggregates with reduced efficiency and is dramatically more toxic than Htt-103Q-GFP. (a) Analysis of cell growth in 5 fold serial dilutions of [*RNQ*⁺] and [*rnq*⁻] cells harboring the indicated forms of Htt-103Q that were expressed from the GAL1 promoter. (b) Cellular localization of Htt-103Q-GFP and Htt-103Q-GFP-NLS in [*RNQ*⁺] and [*rnq*⁻] cells as determined by fluorescence microscopy. (c) Filter trap analysis of SDS-resistant Htt-103Q and Htt-103Q-GFP-NLS aggregates. Lower panels are western blots of cell extracts used in the filter trap assay. (d) Comparison of Htt-103Q-GFP and Htt-103Q-GFP-NLS assembly status in [*RNQ*⁺] cells by size exclusion chromatography. Htt-103Q chimeras were expressed for 2 hrs in cells harboring only endogenous Rnq1.

prions to exacerbate Htt-103Q toxicity can be accounted for via their attracting Htt-103Q to an environment that has reduced capacity to convert it into an SDS-resistant species.

3.4 Discussion

Herein we demonstrate that yeast partition the model disease proteins, Rnq1 and Htt-103Q, between benign and toxic states with reciprocal efficiencies in the cytosol and nucleus. The nuclear environment favors assembly of Rnq1 into benign, amyloid-like $[RNQ^+]$ prions. Yet, Htt-103Q assembly into SDS-resistant particles is disfavored in the nucleus. An important component of the cells defense against Rnq1 and Htt-103Q toxicity is their efficient conversion to an SDS-resistant species. Yet, the cytosol and nucleus possess unique capacities to package different disease proteins into benign assemblies. These data help explain why relocation of disease proteins from the cytosol to the nucleus (Davies et al., 1997; Ross, 1997; Saudou et al., 1998) or the nucleus to the cytosol exacerbates toxicity (Neumann et al., 2006).

Data presented suggest several mechanisms by which changes in a disease protein's neighbors influence its localization and toxicity. The assembly of disease proteins into tightly aggregated species can represent a protective mechanism, but, surprisingly, is not a spontaneous process (Behrends et al., 2006; Cohen et al., 2006; Douglas et al., 2008). Different classes of molecular chaperones, whose expression is controlled in an age and stress dependent manner, prevent the accumulation of toxic detergent-soluble oligomers by facilitating conversion of disease proteins into different types of aggregated species (Behrends et al., 2006; Douglas et al., 2008). Increased activity of the Hsp40, Sis1, within physiological ranges, shifted the localization of the $[RNQ^+]$ prion assembly pathway from the cytosol to the nucleus. This relocation appeared to result from the retention of native Rnq1 in nuclear $[RNQ^+]$ prions, which is accomplished by increased prion assembly in this location and the inability of prions to

traffic out of the nucleus. Thus, the differential ability of chaperones to function in assembly events in the cytosol and nucleus can influence the intracellular location and toxicity of disease proteins.

Modest changes in chaperone activity can also influence the localization and conformation of disease protein interaction partners. This can have dramatic downstream effects on the disease protein's localization and environment. This, in turn, has profound positive or negative effects on the cell's ability to detoxify disease proteins. PolyQ proteins expose promiscuous interaction surfaces that are capable of interactions with other polyQ proteins (Duennwald et al., 2006), which can impact polyQ protein localization (Perez et al., 1998). We report that relocation of $[RNQ^+]$ prions from the cytosol to the nucleus also leads to the accumulation of Htt-103Q in the nuclear environment where it is more toxic. Thus, changes in the conformation and/or location of human polyQ interacting proteins (Duennwald et al., 2006) has the potential to impact the location and detoxification of pathogenic polyQ proteins.

Several factors may explain the apparent changes in the efficiency of $[RNQ^+]$ prion formation and Htt-103Q aggregate assembly observed when this process occurs in the nucleus instead of the cytosol. First, total Rnq1 levels are comparable when Rnq1 accumulates in the cytosol or nucleus, yet the nucleus possesses a smaller volume than the cytosol. Accumulation in the nucleus may therefore increase the local Rnq1 concentration and enhance the efficiency of $[RNQ^+]$ formation by mass action. However, the same logic does not work when Htt-103Q assembly into SDS-resistant aggregates is considered. Thus, it is more likely that the cytosol and nucleus contain different levels of proteins that either promote or hinder Rnq1 and Htt-103Q detoxification. Hsp104 is a

cytosolic shearing factor, whose levels are low in the nucleus (Tkach and Glover, 2008), which acts in conjunction with Sis1 to fragment $[RNQ^+]$ prions into smaller seeds (Aron et al., 2007; Tipton et al., 2008) that are required to promote prion propagation (Chernoff et al., 1995) as well as to nucleate formation of toxic Rnq1 species (Douglas et al., 2008). In contrast, TriC is a ringed chaperonin required for polyQ detoxification (Behrends et al., 2006; Kitamura et al., 2006; Tam et al., 2006) that is localized primarily in the cytosol (Kim et al., 1994). Thus, $[RNQ^+]$ prion assembly may benefit from the nuclear environment because Hsp104 is less active in this compartment. Yet, the absence of TriC in the nucleus could explain the enhanced toxicity and reduced aggregation efficiency of nuclear Htt-103Q.

The majority of Sis1 is normally found in the nucleus (Luke et al., 1991), which helps explain why subtle elevations in Sis1 levels increase $[RNQ^+]$ prion formation in this compartment. We surmise that pools of Rnq1 normally traffic between the cytosol and nucleus and increasing nuclear Sis1 levels helps drive the fusion of Rnq1 monomers into nuclear $[RNQ^+]$ prion seeds. However, Type II Hsp40s are known to help retain proteins in the nucleus (Cheng et al., 2008; Zhang et al., 2008), so it is also possible that Sis1 has a direct impact on the nucleocytoplasmic trafficking of Rnq1. Indeed, the non-prion domain of Rnq1 contains a hydrophobic Sis1 binding site that closely resembles a canonical nuclear export signal (Douglas et al., 2008). Sis1 binding to Rnq1 may therefore negatively regulate Rnq1 nuclear export and thereby increase nuclear Rnq1 levels. However, it was difficult to test this hypothesis because mutation of the putative NES within Rnq1 hindered Sis1 binding and altered the aggregation state of Rnq1 (data not shown). Nevertheless, it is clear that Hsp40s can directly and indirectly modulate the

cellular location where disease proteins are assembled into aggregates. This action can have protective or toxic consequences.

3.5 Materials and methods

Strains and Plasmids: Yeast strains W303, YEF473B, BY4742, and 10B-H49 were utilized to take advantage of different genetic markers, gene integrations, gene deletions and karyogomy defects. W303, *MAT α* and α , *can1-100 ade2-1, his3-11,15 leu2-3,112 ura3-1 trp1-1*; YEF473B, *MAT α* , *trp1 Δ 63, leu2 Δ , ura3-52, his3 Δ 200, lys2-8 Δ 1, NUP49-GFP::*HygB*; 10B-H49 *MAT α* , ρ° *ade2-1, lys1-1, his3-11,15, leu2-3,112, kar1-1, ura3::KANR*; BY4742 *MAT α* , *his3 Δ , leu2 Δ , lys2 Δ , ura2 Δ* . All strains harbored Rnq1 in its [RNQ⁺] form and the generation of isogenic [rnq⁻] strains was accomplished via sequential passage of cells on plates containing 3 mM guanidinium-HCl (Douglas et al., 2008). Strains were transformed with plasmids and cultured in synthetic media as previously described (Douglas et al., 2008). Individual gene deletions in the BY4742 strain background were obtained from Open Biosystems. Plasmids that express the indicated protein under control of the GAL1 promoter include pRS416-RNQ1, pRS416-RNQ1-GFP, pRS416-RNQ1-GFP L94A, pRS416-RNQ1-GFP-NLS, pRS416-RNQ1-GFP-NLS L94A, pYES3-SISI, pYES3-Flag-Htt-103Q-GFP, pYES3-Flag-Htt-25Q-GFP, pYES2-Flag-Htt-103Q-GFP, pYES2-Flag-Htt-25Q-GFP and pRS414-Het-S-GFP (Taneja et al., 2007). Plasmids that express Rnq1 under control of the CUP1 promoter include pRS316-RNQ1-GFP, pRS316-RNQ1-GFP-NLS, pRS315-RNQ1-GFP and pRS315-RNQ1-GFP-NLS. The mRFP tag (Sato et al., 2005) was subcloned in place of the GFP (between SacI and SacII restriction enzyme cut sites) in all of the CUP1 inducible Rnq1 constructs. The NLS sequence was derived from the HIV SV-40 and encodes the amino acid sequence PKKKRKV which was fused to the carboxy-terminus of the GFP or mRFP tag. The NES sequence was derived from the yeast Ssb1 chaperone and encodes the*

amino acid sequence KIEAALSDALAALQ which was fused to the C-terminus of GFP. The open reading frame of Sup35 was subcloned from genomic DNA between a 5' BamHI and 3' SacI restriction enzyme cut sites and subcloned into CUP1 inducible vector to generate pRS316-Sup35-GFP. The glyceraldehyde-3-phosphate dehydrogenase (GPD) promoter controlled expression of pRS315-*SSA1*, pRS315-*HSP104*, pRS315-*SIS1*, and pRS414-*SIS1*. The QuikChange site-directed mutagenesis kit (Stratagene) was used to create the indicated point mutations in Rnq1. pKW430 expressed a nucleocytoplasmic reporter composed of the following moieties, NLS^{SV40}-NES^{PKI}-2 x GFP (Stade et al., 1997).

Sytox dye exclusion: W303 α cells were sequentially transformed with pRS414-*SIS1* or pRS414 and then pRS416-*RNQ1* or pRS416. Transformants were grown overnight to an OD₆₀₀ of 0.2-0.4 in synthetic media containing raffinose as the carbon source. Galactose (2%) was added to the media to induce Rnq1 expression from the GAL1 promoter in pRS416-*RNQ1*. Cells were collected and sytox permeability was measured with a FluoSTAR fluorometer (Zakrzewska et al., 2007).

Fluorescence Microscopy: Rnq1-GFP or Rnq1-mRFP as well as Htt-25Q-GFP and Htt-103Q-GFP were expressed under control of the indicated inducible promoters. Images were captured from live or fixed cells in synthetic liquid media with a Nikon E600 fluorescence microscope and images were processed with Metamorph and Adobe Photoshop Software. The nuclear envelope was delineated via visualization of the nuclear pore protein, Nup49-GFP.

In the order of expression experiments, cells harbored two distinct plasmids which expressed two proteins from either the GAL1 or CUP1 promoters. Cells were grown overnight at 30°C in synthetic media containing raffinose (2%) to OD₆₀₀ of 0.5-1.5. Enough Cu⁺⁺ was present in the media to allow for the visualization of the indicated Rnq1-GFP and Rnq1-mRFP protein from the CUP1 promoter. The media was then supplemented with galactose (2%) to induce expression of the indicated protein under control of the GAL1 promoter. Following a 1-2 hr incubation, cells were collected and photographed live or fixed.

Cells were stained with DAPI to visualize nuclear DNA. Cells were first fixed with 4% formaldehyde for 30 min, washed twice with PBS and permeabilized by incubation in 0.5% PBS Triton for 10 min. Cells were then washed twice with PBS, incubated for 10 min with DAPI (1 µg/ml), and again washed twice with PBS before visualization.

Cytoduction: W303a [*RNQ*⁺] cells that harbored pRS416-GAL1-*Rnq1*-GFP-NLS were grown overnight in synthetic dropout media containing raffinose (2%). Once cells reached an OD₆₀₀ of 0.5-1.5, media was supplemented with galactose (2%) and incubated for 1-2 hr. Cells were then mated with a [*rnq*⁻] strain that is defective in karyogamy, 10B-H49α (Sondheimer and Lindquist, 2000). Prior to mating, 10B-H49α [*rnq*⁻] cells harboring pRS315-CUP-*Rnq1*-mRFP, were cultured overnight at 30°C in synthetic media. Cells with an OD₆₀₀ of 0.5-1.5 were supplemented with CuSO₄ (50 µM) and cultured for an additional 2-3 hrs before mated. Mating was conducted with 2 OD₆₀₀ units of cells from either mating type that were washed with sterile ddH₂O, mixed and

incubated on YPD plates. Incubations were performed at 30°C for either 30 mins or 2 hrs after which cells were scraped and washed with sterile PBS. Mated cells were fixed in formaldehyde and stained with DAPI before visualization.

Analysis of Rnq1 and Htt-103Q toxicity: Cell growth on agarose plates was monitored in [*RNQ*⁺] and [*rnq*-] W303α strains that harbored pRS416-*RNQ1-GFP*, pRS416-*RNQ1-GFP-NLS*, pYES2-*Flag-Htt-103Q-GFP* or pYES2-*Flag-Htt-103Q-GFP-NLS* under control of the GAL1 promoter. In the order of expression experiments, cells were transformed with two plasmids that expressed the indicated proteins under control of the GAL1 or CUP1 promoter. Cells were grown overnight in synthetic media containing raffinose (2%) to an OD₆₀₀ of 1-2 before 5-fold dilutions were spotted onto plates containing galactose (2%). Enough Cu⁺⁺ was present in the synthetic media to allow for modest, non-toxic overexpression of the indicated Rnq1 proteins off the CUP1 promoter. Plates were incubated for 3-5 days at 30°C before being photographed.

Cell growth in liquid culture was monitored in [*RNQ*⁺] W303α strains that harbored pRS315-GPD or pRS315-GPD-*SIS1* and pYES2 or pYES2-*Flag-Htt-103Q-GFP* under control of the GAL1 promoter. Cell cultures in synthetic media containing 2% raffinose were grown to an O.D. of 4-6 overnight. Cultures were then diluted to an O.D of 0.01 and allowed to grow for 4hrs before the addition of 2% galactose to induce expression of Htt-103Q. Cell concentration was determined at the indicated time points by light scattering at 600 nM.

Screen of yeast strains for nuclear trafficking factors required for suppression of Rnq1 toxicity. BY4742 strains from the yeast deletion collection that harbored the indicated deletions of non-essential genes were sequentially transformed with pRS315-GPD-*SIS1* and then pRS316-CUP1-*RNQ1-GFP*. Transformants were cultured in synthetic media overnight at 30°C to an OD₆₀₀ of 0.5-2. Enough Cu⁺⁺ was present in the media to allow for Rnq1-GFP expression and visualization. Rnq1-GFP was either distributed throughout the whole cell and scored as cytoplasmic or compartmentalized to the nucleus. The localization of Rnq1-GFP in different deletions strains was analyzed in 200 cells from 3-5 separate transformations.

Analysis of SDS-resistant Htt-103Q and Rnq1 aggregates: Monitoring the assembly of Rnq1 and Htt-103Q into SDS-resistant aggregates was performed as previously described by SDD-AGE (Douglas et al., 2008; Kryndushkin et al., 2003). For filter trap analysis, cell extracts were generated in non-denaturing lysis buffer previously described (Douglas et al., 2008). The lysate was added to a 2X slot blot sample buffer which contained a final concentration of 2% SDS, 75 mM Tris-HCl pH 6.8, 2 mM EDTA, 8% 2-mercaptoethanol, 2 mM phenylmethanesulfonyl fluoride and a protease inhibitor cocktail (Roche). 40 µl of the final sample was added to the wells of the slot blot apparatus which contained an equilibrated cellulose acetate membrane filter (Scherzinger et al., 1997). Equilibration of cellulose acetate was achieved by adding 100 µl of 1X slot blot buffer to the wells. The vacuum was never applied to the slot blot apparatus. Once samples ran through the filter and wells appeared dry, 100 µl of 0.1% SDS was added to the wells. Once dry, the membranes were washed 3 times in PBS, blocked overnight in 10% milk at

4°C and western blotted as previously described (Douglas et al., 2008). PVDF or cellulose acetate membranes were probed with α -GFP to visualize Rnq1-GFP and α -Flag to visualize Flag-Htt-103Q-GFP. Monitoring protein levels by western blot was performed as previously described (Douglas et al., 2008).

Rnq1 co-immunoprecipitation with Htt: Expression of Htt-103Q-GFP in cells harboring pYES3-*Htt-103Q-GFP* was induced by supplementation with 2% galactose. Non-denaturing cell extracts were generated 2 hrs later under the conditions described (Fan et al., 2004), and α -Rnq1 was added to lysates. Htt-103Q-GFP was immunoprecipitated with endogenous Rnq1 and detected with α -GFP by western blot. Similarly, Rnq1-GFP and Rnq1-GFP-NLS were immunoprecipitated with α -Rnq1 and probed for binding with Htt-25Q-GFP or Htt-103Q-GFP.

Size Exclusion Chromatography: Non-denaturing cell extracts were generated under the conditions described (Behrends et al., 2006) and resolved on a Sephacryl S-200 Hi-Prep column. Samples were loaded onto the column and collected as previously described (Douglas et al., 2008).

3.6 References

- Aron, R., T. Higurashi, C. Sahi, and E.A. Craig. 2007. J-protein co-chaperone Sis1 required for generation of [RNQ+] seeds necessary for prion propagation. *EMBO J.* 26:3794-803.
- Balch, W.E., R.I. Morimoto, A. Dillin, and J.W. Kelly. 2008. Adapting proteostasis for disease intervention. *Science.* 319:916-9.
- Bardwell, J.C., K. Tilly, E. Craig, J. King, M. Zylicz, and C. Georgopoulos. 1986. The nucleotide sequence of the Escherichia coli K12 dnaJ+ gene. A gene that encodes a heat shock protein. *J Biol Chem.* 261:1782-5.
- Behrends, C., C.A. Langer, R. Boteva, U.M. Bottcher, M.J. Stemp, G. Schaffar, B.V. Rao, A. Giese, H. Kretschmar, K. Siegers, and F.U. Hartl. 2006. Chaperonin TRiC promotes the assembly of polyQ expansion proteins into nontoxic oligomers. *Mol Cell.* 23:887-97.
- Bence, N.F., R.M. Sampat, and R.R. Kopito. 2001. Impairment of the ubiquitin-proteasome system by protein aggregation. *Science.* 292:1552-5.
- Burke, J.R., J.J. Enghild, M.E. Martin, Y.S. Jou, R.M. Myers, A.D. Roses, J.M. Vance, and W.J. Strittmatter. 1996. Huntingtin and DRPLA proteins selectively interact with the enzyme GAPDH. *Nat Med.* 2:347-50.
- Carrell, R.W., and D.A. Lomas. 1997. Conformational disease. *Lancet.* 350:134-8.
- Caughey, B., and P.T. Lansbury. 2003. Protofibrils, pores, fibrils, and neurodegeneration: separating the responsible protein aggregates from the innocent bystanders. *Annu Rev Neurosci.* 26:267-98.
- Cheng, I.H., K. Scarce-Levie, J. Legleiter, J.J. Palop, H. Gerstein, N. Bien-Ly, J. Puolivali, S. Lesne, K.H. Ashe, P.J. Muchowski, and L. Mucke. 2007. Accelerating amyloid-beta fibrillization reduces oligomer levels and functional deficits in Alzheimer disease mouse models. *J Biol Chem.* 282:23818-28.
- Cheng, X., M. Belshan, and L. Ratner. 2008. Hsp40 facilitates nuclear import of the human immunodeficiency virus type 2 Vpx-mediated preintegration complex. *J Virol.* 82:1229-37.

- Chernoff, Y.O., S.L. Lindquist, B. Ono, S.G. Inge-Vechtormov, and S.W. Liebman. 1995. Role of the chaperone protein Hsp104 in propagation of the yeast prion-like factor [psi+]. *Science*. 268:880-4.
- Chiti, F., and C.M. Dobson. 2006. Protein misfolding, functional amyloid, and human disease. *Annu Rev Biochem*. 75:333-66.
- Cohen, E., J. Bieschke, R.M. Perciavalle, J.W. Kelly, and A. Dillin. 2006. Opposing activities protect against age-onset proteotoxicity. *Science*. 313:1604-10.
- Conde, J., and G.R. Fink. 1976. A mutant of *Saccharomyces cerevisiae* defective for nuclear fusion. *Proc Natl Acad Sci U S A*. 73:3651-5.
- Davies, S.W., M. Turmaine, B.A. Cozens, M. DiFiglia, A.H. Sharp, C.A. Ross, E. Scherzinger, E.E. Wanker, L. Mangiarini, and G.P. Bates. 1997. Formation of neuronal intranuclear inclusions underlies the neurological dysfunction in mice transgenic for the HD mutation. *Cell*. 90:537-48.
- De Rooij, K.E., J.C. Dorsman, M.A. Smoor, J.T. Den Dunnen, and G.J. Van Ommen. 1996. Subcellular localization of the Huntington's disease gene product in cell lines by immunofluorescence and biochemical subcellular fractionation. *Hum Mol Genet*. 5:1093-9.
- Derkatch, I.L., M.E. Bradley, P. Zhou, Y.O. Chernoff, and S.W. Liebman. 1997. Genetic and environmental factors affecting the de novo appearance of the [PSI+] prion in *Saccharomyces cerevisiae*. *Genetics*. 147:507-19.
- DiFiglia, M., E. Sapp, K.O. Chase, S.W. Davies, G.P. Bates, J.P. Vonsattel, and N. Aronin. 1997. Aggregation of huntingtin in neuronal intranuclear inclusions and dystrophic neurites in brain. *Science*. 277:1990-3.
- Douglas, P.M., S. Treusch, H.Y. Ren, R. Halfmann, M.L. Duennwald, S. Lindquist, and D.M. Cyr. 2008. Chaperone-dependent amyloid assembly protects cells from prion toxicity. *Proc Natl Acad Sci U S A*. 105:7206-11.
- Duennwald, M.L., S. Jagadish, F. Giorgini, P.J. Muchowski, and S. Lindquist. 2006. A network of protein interactions determines polyglutamine toxicity. *Proc Natl Acad Sci U S A*. 103:11051-6.

- Dunah, A.W., H. Jeong, A. Griffin, Y.M. Kim, D.G. Standaert, S.M. Hersch, M.M. Mouradian, A.B. Young, N. Tanese, and D. Krainc. 2002. Sp1 and TAFII130 transcriptional activity disrupted in early Huntington's disease. *Science*. 296:2238-43.
- Fan, C.Y., S. Lee, H.Y. Ren, and D.M. Cyr. 2004. Exchangeable chaperone modules contribute to specification of type I and type II Hsp40 cellular function. *Mol Biol Cell*. 15:761-73.
- Haass, C., and D.J. Selkoe. 2007. Soluble protein oligomers in neurodegeneration: lessons from the Alzheimer's amyloid beta-peptide. *Nat Rev Mol Cell Biol*. 8:101-12.
- Johnston, J.A., C.L. Ward, and R.R. Kopito. 1998. Aggresomes: a cellular response to misfolded proteins. *J Cell Biol*. 143:1883-98.
- Kaganovich, D., R. Kopito, and J. Frydman. 2008. Misfolded proteins partition between two distinct quality control compartments. *Nature*. 454:1088-95.
- Kalderon, D., B.L. Roberts, W.D. Richardson, and A.E. Smith. 1984. A short amino acid sequence able to specify nuclear location. *Cell*. 39:499-509.
- Kayed, R., E. Head, J.L. Thompson, T.M. McIntire, S.C. Milton, C.W. Cotman, and C.G. Glabe. 2003. Common structure of soluble amyloid oligomers implies common mechanism of pathogenesis. *Science*. 300:486-9.
- Kim, S., K.R. Willison, and A.L. Horwich. 1994. Cytosolic chaperonin subunits have a conserved ATPase domain but diverged polypeptide-binding domains. *Trends Biochem Sci*. 19:543-8.
- Kitamura, A., H. Kubota, C.G. Pack, G. Matsumoto, S. Hirayama, Y. Takahashi, H. Kimura, M. Kinjo, R.I. Morimoto, and K. Nagata. 2006. Cytosolic chaperonin prevents polyglutamine toxicity with altering the aggregation state. *Nat Cell Biol*. 8:1163-70.
- Kryndushkin, D.S., I.M. Alexandrov, M.D. Ter-Avanesyan, and V.V. Kushnirov. 2003. Yeast [PSI⁺] prion aggregates are formed by small Sup35 polymers fragmented by Hsp104. *J Biol Chem*. 278:49636-43.

- Luke, M.M., A. Sutton, and K.T. Arndt. 1991. Characterization of SIS1, a *Saccharomyces cerevisiae* homologue of bacterial dnaJ proteins. *J Cell Biol.* 114:623-38.
- Meriin, A.B., X. Zhang, X. He, G.P. Newnam, Y.O. Chernoff, and M.Y. Sherman. 2002. Huntington toxicity in yeast model depends on polyglutamine aggregation mediated by a prion-like protein Rnq1. *J Cell Biol.* 157:997-1004.
- Morimoto, R.I. 2008. Proteotoxic stress and inducible chaperone networks in neurodegenerative disease and aging. *Genes Dev.* 22:1427-38.
- Muchowski, P.J., and J.L. Wacker. 2005. Modulation of neurodegeneration by molecular chaperones. *Nat Rev Neurosci.* 6:11-22.
- Neumann, M., D.M. Sampathu, L.K. Kwong, A.C. Truax, M.C. Micsenyi, T.T. Chou, J. Bruce, T. Schuck, M. Grossman, C.M. Clark, L.F. McCluskey, B.L. Miller, E. Masliah, I.R. Mackenzie, H. Feldman, W. Feiden, H.A. Kretzschmar, J.Q. Trojanowski, and V.M. Lee. 2006. Ubiquitinated TDP-43 in frontotemporal lobar degeneration and amyotrophic lateral sclerosis. *Science.* 314:130-3.
- Perez, M.K., H.L. Paulson, S.J. Pendse, S.J. Saionz, N.M. Bonini, and R.N. Pittman. 1998. Recruitment and the role of nuclear localization in polyglutamine-mediated aggregation. *J Cell Biol.* 143:1457-70.
- Ross, C.A. 1997. Intranuclear neuronal inclusions: a common pathogenic mechanism for glutamine-repeat neurodegenerative diseases? *Neuron.* 19:1147-50.
- Sato, M., S. Dhut, and T. Toda. 2005. New drug-resistant cassettes for gene disruption and epitope tagging in *Schizosaccharomyces pombe*. *Yeast.* 22:583-91.
- Saudou, F., S. Finkbeiner, D. Devys, and M.E. Greenberg. 1998. Huntingtin acts in the nucleus to induce apoptosis but death does not correlate with the formation of intranuclear inclusions. *Cell.* 95:55-66.
- Schaffar, G., P. Breuer, R. Boteva, C. Behrends, N. Tzvetkov, N. Strippel, H. Sakahira, K. Siegers, M. Hayer-Hartl, and F.U. Hartl. 2004. Cellular toxicity of polyglutamine expansion proteins: mechanism of transcription factor deactivation. *Mol Cell.* 15:95-105.

- Scherzinger, E., R. Lurz, M. Turmaine, L. Mangiarini, B. Hollenbach, R. Hasenbank, G.P. Bates, S.W. Davies, H. Lehrach, and E.E. Wanker. 1997. Huntingtin-encoded polyglutamine expansions form amyloid-like protein aggregates in vitro and in vivo. *Cell*. 90:549-58.
- Schwimmer, C., and D.C. Masison. 2002. Antagonistic interactions between yeast [PSI(+)] and [URE3] prions and curing of [URE3] by Hsp70 protein chaperone Ssa1p but not by Ssa2p. *Mol Cell Biol*. 22:3590-8.
- Sondheimer, N., and S. Lindquist. 2000. Rnq1: an epigenetic modifier of protein function in yeast. *Mol Cell*. 5:163-72.
- Stade, K., C.S. Ford, C. Guthrie, and K. Weis. 1997. Exportin 1 (Crm1p) is an essential nuclear export factor. *Cell*. 90:1041-50.
- Steffan, J.S., A. Kazantsev, O. Spasic-Boskovic, M. Greenwald, Y.Z. Zhu, H. Gohler, E.E. Wanker, G.P. Bates, D.E. Housman, and L.M. Thompson. 2000. The Huntington's disease protein interacts with p53 and CREB-binding protein and represses transcription. *Proc Natl Acad Sci U S A*. 97:6763-8.
- Tam, S., R. Geller, C. Spiess, and J. Frydman. 2006. The chaperonin TRiC controls polyglutamine aggregation and toxicity through subunit-specific interactions. *Nat Cell Biol*. 8:1155-62.
- Taneja, V., M.L. Maddelein, N. Talarek, S.J. Saupe, and S.W. Liebman. 2007. A non-Q/N-rich prion domain of a foreign prion, [Het-s], can propagate as a prion in yeast. *Mol Cell*. 27:67-77.
- Taylor, J.P., J. Hardy, and K.H. Fischbeck. 2002. Toxic proteins in neurodegenerative disease. *Science*. 296:1991-5.
- Tipton, K.A., K.J. Verges, and J.S. Weissman. 2008. In vivo monitoring of the prion replication cycle reveals a critical role for Sis1 in delivering substrates to Hsp104. *Mol Cell*. 32:584-91.
- Tkach, J.M., and J.R. Glover. 2008. Nucleocytoplasmic trafficking of the molecular chaperone Hsp104 in unstressed and heat-shocked cells. *Traffic*. 9:39-56.

- Zakrzewska, A., A. Boorsma, D. Delneri, S. Brul, S.G. Oliver, and F.M. Klis. 2007. Cellular processes and pathways that protect *Saccharomyces cerevisiae* cells against the plasma membrane-perturbing compound chitosan. *Eukaryot Cell*. 6:600-8.
- Zhang, Y., Z. Yang, Y. Cao, S. Zhang, H. Li, Y. Huang, Y.Q. Ding, and X. Liu. 2008. The Hsp40 family chaperone protein DnaJB6 enhances Schlafen1 nuclear localization which is critical for promotion of cell-cycle arrest in T-cells. *Biochem J*. 413:239-50.